universität wien

MASTERARBEIT / MASTER'S THESIS

Titel der Masterarbeit / Title of the Master's Thesis

‘Microbial Activity and Biochemical Particle Composition Along a Fine Particle Size Continuum in Mountain vs Agricultural Streams’

verfasst von / submitted by

Leonie Theresa Haferkemper, B.Sc.

angestrebter akademischer Grad / in partial fulfilment of the requirements for the degree of

Master of Science (MSc)

Wien, 2023 / Vienna, 2023

Studienkennzahl lt. Studienblatt / degree programme code as it appears on the student record sheet:	UA 066 833
Studienrichtung lt. Studienblatt / degree programme as it appears on the student record sheet:	Masterstudium Ecology and Ecosystems
Betreut von / Supervisor:	Univ.-Prof. Mag. Dr. Christian Griebler
Mitbetreut von / Co-Supervisor:	Dr. Katrin Attermeyer

Acknowledgements

This work would not have been possible without the help and support of numerous people. Firstly, I would like to thank my supervisor Katrin for guiding me through the entire project. No matter how busy you were, you took so much time to develop ideas, discuss questions, problems, and results, and give feedback. Thank you for sharing your enthusiasm and encouragement, whenever I got lost in too many details you made me take a step back and see the bigger picture. Thanks also to Christian for supporting the whole project from Vienna. Gerti, thank you for your help in the field and for sweetening my day with a coffee break during busy sampling days. Thank you for all the technical support in the lab, for your endless patience in explaining and discussing the methodological details of the elemental analysis, and for not completely losing your hope and humour in the face of endless problems with the EA-IRMS. Thanks to Mia and Hanna for your help in the field during your internships at the WCL. Thank you, Theresa, for your help in the lab and for suggesting mountain streams. Thanks to Gabi for suggesting agricultural streams. Hermann, thank you for building the particle sampling equipment. Thank you, Sam, for your help with the fatty acid analysis. Thank you for all the explanations and for always finding the time when I had difficulties or questions. Martin, thank you for giving me the opportunity to include fatty acid analysis in my project. Len, thank you for all your advice about life and science. Your entertaining and educational stories from all over the world during the very comfortable car journeys to Lunz have opened up new perspectives for me. Thanks to the Carbocrobe group and so many other people working at or visiting the WasserCluster, you gave me a social life while working and made me feel at home in Lunz. Thanks to Karla, Isa, and Jakob for taking the time to proofread the thesis in detail. Isa, you have become so much more than a competent lab and presentation partner, thank you for being the best friend I could have imagined during our studies. You broadened my horizons in many ways, made life in Lunz and Vienna so much more liveable, and were always there to share thoughts and experiences. A big thank you to my flatmates in Vienna and my friends for giving me a life outside of my thesis. Thank you to my parents and my family, who supported me throughout my studies and always trusted that I would find my way. And finally, thank you, Simon, for your patience and optimism, and for believing in me more than I sometimes did myself. You always had an open ear for me, without complaining that you had already listened to the same worries and thoughts a few times.

Table of Contents

Abstract

The processing of organic matter (OM) in stream ecosystems is a key component of the fluvial carbon cycle and affects carbon transport, mineralisation, and burial. Research to date has focused on the cycling of dissolved OM (DOM) although suspended particles are increasingly recognised as active sites of OM cycling. Nevertheless, the properties and processing of fine particles < 1000 µm size remain poorly understood and especially the finest size fractions < 100 µm are commonly not included. This study investigated the microbial activity and biochemical particle composition along a fine particle size continuum in five mountain streams characterised by forested catchment areas and five agricultural lowland streams. Suspended particles were separated into five size classes from 500 µm to 0.7 µm size. Bacterial production rates measured in agricultural streams were 20 times higher than in mountain streams, resulting in carbon turnover times of 25 and 227 days, respectively. The particle composition did not generally differ between stream types, implying that environmental characteristics are relevant for controlling the fine particle turnover. Comparing the size classes, bacterial production rates were highest on the finest particles < 15 µm, > 98.8% of the total microbial activity occurred on these particles in both stream types. Additionally, measured fatty acid composition and C/N ratios indicated an increased microbial biomass on the finest particles. Thus, fine particles < 15 µm are overlooked hotspots of microbial OM turnover in streams and understanding the drivers and mechanisms of their processing is essential to improve our understanding of fluvial carbon cycling.

Keywords: suspended particles, FPOM, seston, microbial activity, particle size, particle composition, fatty acids, carbon turnover, streams, land use

1) Introduction

Despite making up only 2.5% of the global water resources (Oki & Kanae, 2006), inland waters are a fundamental part of the Earth's carbon (C) cycle, receiving as much as 5.1 Pg C per year from the terrestrial environment according to most recent estimates (Drake et al., 2018). Only about 0.9 Pg C is exported to the marine environment via the aquatic continuum since inland waters are active sites for C transformation, mineralisation, and burial (Cole et al., 2007). The composition of terrestrial C inputs to freshwater systems varies greatly between different catchment conditions (Tranvik et al., 2009). In addition, human activity, such as deforestation or land use change, has been shown to alter the inputs, processing, and export of C in inland waters (Regnier et al., 2013).

Studies on the effects of land use alterations on aquatic ecosystems revealed impacts in terms of primary productivity, respiration, and microbial processing of C. It has been shown that organic matter (OM) inputs to headwater streams differ depending on the predominant land use type in the catchment, suggesting implications on C cycling in these streams (Lu, Canuel, et al., 2014). Headwater streams (stream order 1-3) are increasingly recognized as an especially important interface between the terrestrial and aquatic biosphere as they globally account for almost 90% of the total length of perennial rivers and streams (Argerich et al., 2016; Downing et al., 2012). It is therefore essential to consider headwater streams when investigating C cycling in inland waters.

The composition and complex processing of OM strongly shape the biogeochemical cycles in stream ecosystems (Mena-Rivera, 2022). OM and the organic carbon (OC) associated with it are typically divided into two fractions, which are defined arbitrarily and not uniformly based on the pore size of a filter through which the material passes. Dissolved organic matter (DOM) and dissolved organic carbon (DOC) describe the fraction passing a pore size of 0.2 µm to 0.7 µm, whereas particulate organic matter (POM) and particulate organic carbon (POC) refer to the fraction retained on that filter (Derrien et al., 2019). Compared to DOM, much less is known about the composition and cycling of POM during transport in river networks although the global fluxes of DOC and POC show a comparable magnitude (Meybeck, 1982; Yang et al., 2016). The reactivity and microbial turnover of POC were found to be significantly higher compared to DOC along a continuum of boreal inland waters (Attermeyer et al., 2018). Moreover, DOM aggregation processes or modifications of the DOM pool in the presence of particles suggest highly interlinked processing of DOM and POM (Lau, 2021), highlighting the importance of the particulate fraction for C cycling in aquatic systems.

POM can be further divided into a coarse (CPOM) and a fine (FPOM) fraction. Conventionally, particles > 1000 µm are considered as CPOM (Wotton, 1994). However, there is no consistent definition of CPOM and FPOM size ranges, e.g. Akamatsu et al. (2011) describe POM with a size of 1000 µm to 250 µm as CPOM. CPOM primarily consists of terrestrially derived material including leaves, branches, and pieces of wood (Marshall et al., 2021) while FPOM comprises material from various sources (Tant et al., 2013). Suspended particles in streams are also referred to as seston or suspended particulate matter (SPM) as they contain both OM as well as inorganic materials (e.g. clay and silt minerals) and microbial communities associated with it (Atkinson et al., 2009; Mena-Rivera, 2022; Peters et al., 1989).

The processing of organic particles is linked to the microbial community associated with it (Bižić-Ionescu et al., 2018). Studies on the microbial colonisation of particles in marine and freshwater (lake) environments found large variability among individual particles, which can be due to their high heterogeneity (Bižić-Ionescu et al., 2015). One approach to categorise OM is the division into size classes since size is linked to the reactivity and turnover time in aquatic systems (Amon & Benner, 1996).

According to the size-reactivity continuum model, larger particles are of more recent origin and thus more bioavailable to microbes that sequentially break up the material into smaller and less reactive particles during decomposition (Amon & Benner, 1996). Although the model was developed by studying DOM decomposition, Amon & Benner (1996) suggested its applicability to POM based on investigating the composition of different POM size classes in the Amazon. Benner & Amon (2015) extended the scope of the model to marine POM, which mainly originates from photoautotrophic primary production. The heterogeneous composition of fine particles in streams which include algal material, inputs from soils, aggregated DOM, and particles generated by the decomposition of terrestrial CPOM, could explain deviations from the model predictions for POM in streams (Tant et al., 2013; Wurzbacher et al., 2016). However, studies investigating particle-associated microbial activities across different particle size classes in streams indicate that the predictions of the size-reactivity continuum model apply to particles in streams as well. Peters et al. (1989) assessed the microbial activity of seston from North American headwater streams in a size range from 500 µm to 10 µm and detected a decreasing microbial biomass and production per unit surface area with decreasing particle size. Wurzbacher et al. (2016) found that the microbial respiration rate decreased with decreasing particle size on size-fractionated shredded leaf litter in a 2000 µm to 20 µm size range. It was furthermore concluded that smaller particles result from a sequential breakdown of CPOM and decrease in quality with decreasing size. Finer particles contained more refractory components such as lignin since labile, organic compounds are preferably used during decomposition (Peters et al., 1989). Labile components generally have higher ^{13}C values than refractory components, at least in terrestrial ecosystems (Potapov et al., 2019), that provide leaf CPOM to streams mainly as leaf litter (Wallace et al., 1995).

However, this may not apply to all types of streams since the quantity and quality of POM and the relative proportion of terrestrially derived (allochthonous) and in-stream produced (autochthonous) OM present in streams vary depending on the predominant land use type in the catchment (Lu, Canuel, et al., 2014; Wild et al., 2019). As the source of OM affects its composition, it also determines its reactivity and microbial processing according to a study on DOM not considering POM (Strauss & Lamberti, 2002). In contrast to forested streams that are dominated by allochthonous inputs of OM, a significant proportion of POM in streams with agricultural land use in their catchment may originate from in-stream primary production. This has been attributed to higher nutrient concentrations (Delong & Brusven, 1992), increased light availability due to the clearing of the riparian vegetation, warmer temperatures (Hagen et al., 2010; Lu, Canuel, et al., 2014), and reduced flow velocities (Ghosh & Gaur, 1998). Agricultural land use thus promotes a shift from plant- and soil-derived to microbial- and algal-derived OM in streams. In addition, higher microbial respiration rates were measured on algal- compared to terrestrially derived particles (Yoshimura et al., 2010). Therefore, distinguishing between streams characterised by different catchment land use is of high importance when studying properties and turnover of POM related to C cycling in streams.

In summary, there are several knowledge gaps regarding the sources, properties, and processing of fine particles in streams despite their importance for organic C cycling (Attermeyer et al., 2018) and the need to understand the effects of anthropogenic influences on C cycling in inland waters (Regnier et al., 2013). Research on different categories of fine particles is generally scarce although high heterogeneity among particles has been found. Studies investigating differences in OM composition of streams along gradients of different land uses commonly do not include measurements of microbial activities (Hagen et al., 2010; Lambert et al., 2017; Lu, Canuel, et al., 2014). Therefore, it is largely

unknown how the differences in OM composition affect its microbial turnover and thus the C cycling in different stream types. Furthermore, size-specific studies simultaneously assessing particle composition and associated microbial activity in streams are rare, and especially the finest size fractions < 100 µm are typically not included. The few studies considering fine particle size fractions revealed effects of particle size, composition, and quality on the particle-attached microbial activity (Peters et al., 1989; Wurzbacher et al., 2016), however, it remains unclear how these can be generalised across different stream types.

To address these gaps and limitations, this study aimed at comparing the microbial activity and biochemical composition of different size classes of fine particles < 500 µm, hereafter referred to as fine particulate matter (FPM), in two different headwater stream types: in mountain streams characterised by forested catchments and agricultural lowland streams. The FPM-attached microbial activity was evaluated by measuring bacterial protein production (BPP) using a ^{3}H-labelled leucine incorporation approach. Furthermore, analyses of POC and particulate nitrogen (PN) contents, C/N ratios, bulk stable isotope ratios of C and N, and fatty acid composition were conducted to examine the sources, quality, and composition of the fine particles.

Several hypotheses were tested to compare the two stream types and the different size classes of fine particles. Comparing the two stream types, a higher abundance of autotrophic algae in agricultural streams was hypothesised, indicated by the presence of algal-specific fatty acids and more depleted $\delta^{13}C$ values reflecting a rather autochthonous source of fine particles. Furthermore, a higher FPM-attached prokaryotic productivity and a higher prokaryotic abundance in agricultural streams compared to mountain streams were hypothesised, indicated by a higher BPP and a larger proportion of bacterial fatty acids.
Comparing the different size classes of fine particles, a higher FPM-attached prokaryotic production with increasing particle size was hypothesised, according to the size-reactivity continuum model (Amon & Benner, 1996). This includes the expectation of increasing microbial biomass with increasing particle size, indicated by a higher proportion of bacterial fatty acids. An increasing particle quality with increasing particle size was hypothesised, indicated by a decreasing C/N ratio and more enriched $\delta^{13}C$ values.

2) Methods

2.1) Study sites

Field samplings were carried out on ten streams in two Austrian federal states over a period of seven weeks in the summer 2022. From 26 July to 5 September, five mountain streams in Lower Austria and Styria (Hinterwildalpenbach, Oberer Seebach, Ois, Salza, Steinbach) and five agricultural streams in Lower Austria (Feichsen, Ofenbach, Sierning, Schweinzbach, Zettelbach) were sampled once each (Figure 1). The mountain streams are situated in the Northern Limestone Alps, with the bedrock mainly consisting of limestone, dolomite, and marl (Brüggemann-Ledolter et al., 2015). They furthermore belong to the fluvial bioregion of the Northern Prealps (Kalkalpen). The fluvial bioregions for Austrian streams are defined based on their abiotic characteristics as well as biological indicators (Bundesministerium für Landwirtschaft, Regionen und Tourismus, 2020). The agricultural streams are located between the Austroalpine Nappes and the North Alpine Foreland Basin. The bedrock in this geological boundary zone contains clay, marl, malm rock, sandstone, limestone, sand, and gravel stone (Brüggemann-Ledolter et al., 2015). According to their heterogeneous geology, the agricultural streams are assigned to different fluvial bioregions. The stream Feichsen and the headwaters of Zettelbach (11.53 km^2 catchment size) and Sierning (3.25 km^2 catchment size) are part of the bioregion Flysch while the stream Schweinzbach and the downstream areas of Zettelbach and Sierning are classified into the bioregion Bavarian-Austrian Alpine Foreland (Bayrisch-Österreichisches Alpenvorland) (Bundesministerium für Landwirtschaft, Regionen und Tourismus, 2020).

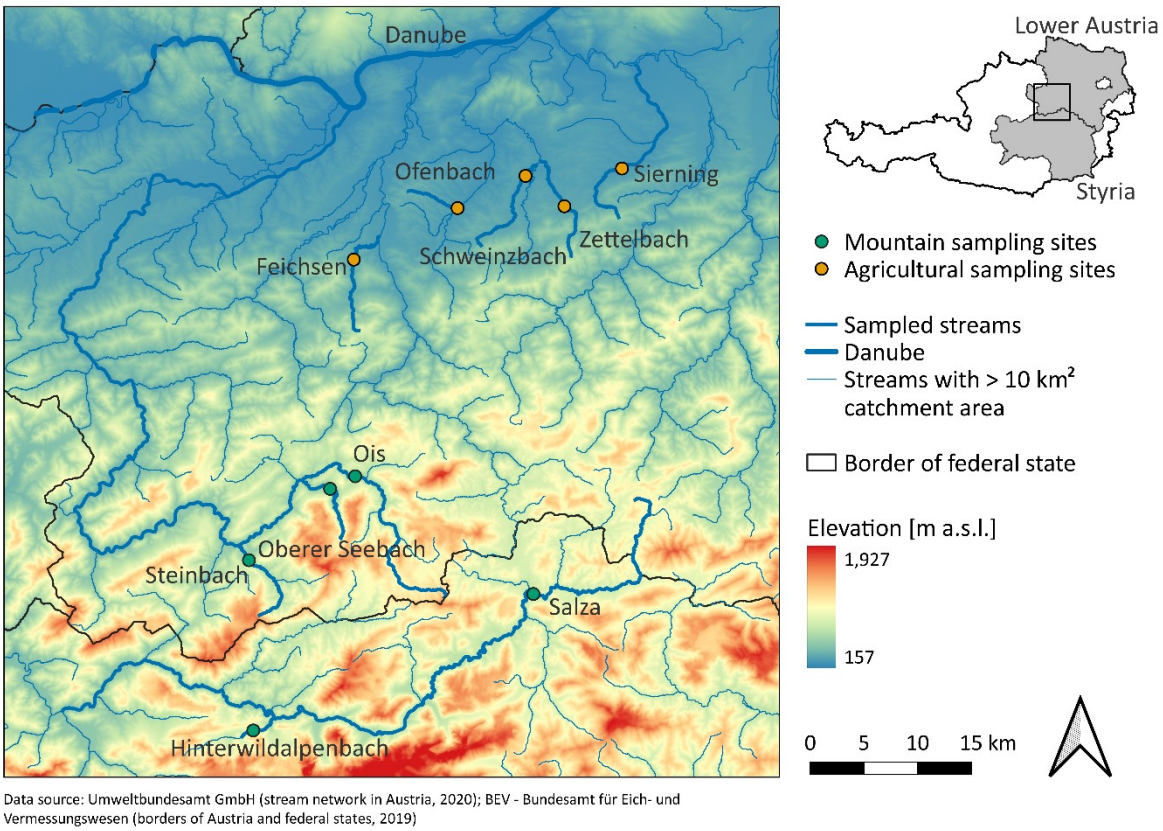

Figure 1: Map of the sampling area in Lower Austria and Styria showing the sampled streams, the sampling sites, and all surrounding rivers with a catchment area > 10 km^2. For geographical orientation, the Danube is highlighted with a thicker line at the top of the map.

The climate in which all the streams are located is temperate. The annual precipitation at the sampling sites (Table 1) ranged from 1115 kg/m^2 to 1532 kg/m^2 for the mountain streams (mean 2010-2022) and from 749 kg/m^2 to 972 kg/m^2 for the agricultural streams (mean 2010-2022). Mean air temperatures (Table 1) of the mountain streams ranged from 7.9 °C to 8.9 °C while they ranged from 10.6 °C to 11.1 °C for the agricultural streams (mean 2010-2022, GeoSphere Austria, 2023).

Table 1: Annual precipitation and mean air temperature at all study sites. Values for the year 2022 are displayed as well as the arithmetic mean from 2010 to 2022. The data was obtained from the SPARTACUS Spatial Dataset for Climate in Austria which interpolates measured meteorological data on a spatial resolution of 1 km x 1 km (GeoSphere Austria, 2023).

Stream type	**Stream name**	**Annual precipitation, mean 2010-2022 [kg/m^2]**	**Annual precipitation 2022 [kg/m^2]**	**Mean air temperature, mean 2010-2022 [°C]**	**Mean air temperature 2022 [°C]**
Mountain	Hinterwildalpenbach	1506	1391	8.3	8.8
	Ois	1597	1527	8.5	9.1
	Oberer Seebach	1560	1498	8.6	9.2
	Salza	1115	1005	7.9	8.4
	Steinbach	1532	1462	8.9	9.5
Agricultural	Feichsen	972	952	10.6	11.2
	Ofenbach	769	731	11.1	11.6
	Schweinzbach	749	713	11.0	11.5
	Sierning	807	742	11.1	11.6
	Zettelbach	862	792	10.7	11.3

2.2) Catchment delineation and catchment land use

The proportion of different land use types in the catchment areas upstream of the sampling locations was calculated using geospatial analyses performed in the software QGIS (version 3.22.11; QGIS.org, 2022). First, catchments were delineated based on a digital terrain model (DTM, spatial resolution 10 m x 10 m; Geoland.at, 2015) using the GRASS toolbox (version 7). The *r.fill.dir* function was applied to correct the DTM and fill artificial depressions. Based on the corrected DTM, the flow accumulation and flow direction were calculated using the tool *r.watershed* with the minimum size of exterior watershed set to 100 and enabling single flow direction. Subsequently, absolute values of the flow direction were computed since the encoding represents flow direction using numbers and sets negative values for the direction if the surface runoff leaves the current geographic region. The flow accumulation for each raster cell is defined as the number of upstream raster cells draining through this cell, thus, it represents the water accumulation. A threshold value of how many raster cells need to drain through a cell to consider it as part of a stream was determined by testing different threshold values and comparing the results to a map of the streams in Lower Austria and Styria (Umweltbundesamt GmbH, 2020). This procedure yielded a threshold value of 1000, so streams were delineated using the tool *r.stream.extract* with a minimum flow accumulation set to 1000. Based on these defined streams, catchments of the sampled streams were delineated until the location of the sampling site by applying the *r.water.outlet* tool. The resulting catchments in raster data format were converted into polygons in the vector format with the tool *r.to.vect* and the function *smooth corners of features* enabled. All catchments were merged to one layer and the geometry of this layer was checked and fixed if errors occurred using the functions *Check validity* and *Fix geometries* in the Vector geometry toolbox. In addition, the attribute table was checked if there was only one polygon created per catchment and catchments separated into two polygons were merged manually. Finally, the catchment area was calculated using the field calculator.

Land cover data was obtained as a vector data set from the CORINE Land Cover (CLC) inventory in the framework of the Copernicus programme (European Environmental Agency (EEA), 2019). The detailed land use categories were first summarised into the five major groups Artificial surfaces (1), Agricultural areas (2), Forests and semi-natural areas (3), Wetlands (4) and Water bodies (5) using the field calculator to generate a new field with these groups in the attribute table. Then, features of the same major group were summarised using the *Dissolve* tool.
Finally, the prepared layers for catchment area and land cover were intersected. In the attribute table, the field calculator was used to compute the area of the different land cover categories in each catchment and this area was divided by the whole catchment area upstream of the sampling site to obtain proportions of each land cover class in the catchment.

Total catchment areas of the sampled streams were delineated additionally to the catchment areas upstream of the sampling site to review the accuracy of the catchment delineation done in QGIS. The total catchment area was calculated and cross-checked with the catchment areas provided in the stream's data sheets of the third national water management plan (NGP 2021; Bundesministerium für Landwirtschaft, Regionen und Tourismus, 2020), accessed via Wasser Informationssystem Austria (WISA).

2.3) Stream characterisation: morphological and chemical analyses

Discharge and cross-sectional area as well as physical, chemical, and biological water parameters were measured at the sampling sites to characterise the stream's morphology and water quality. Furthermore, water samples for nutrient and DOC analysis were taken.

The cross-sectional area and the flow velocity were recorded in the field to assess riverbed morphology, flow rates and discharge at each stream sampling site. For the cross-sectional area (A), the total stream width (W) from the left to the right bank (in flow direction) was measured using a measuring rope. In addition, the local water depth (d) and distance to the left bank (w) were measured at five characteristic points of the cross-section with a folding ruler (Figure 2A). The total length of the contact line between water and riverbed (wetted perimeter, U) and the mean depth were calculated from those measurements.

Along a cross section, the stream was divided into regular intervals (W/5) to measure flow velocity at five evenly distributed points at 20% and 80% of the local water depth. If the depth was < 0.2 m, only one flow velocity measurement at 60% of the local depth was performed (Figure 2B). In total, 11 measurements of total depth were conducted along the cross section, starting at 0.2 m distance from the left bank, continuing at a regular interval and ending at 0.2 m distance from the right bank (Figure 2B). At five of these depth measurement points, the flow velocity was measured using the handheld electromagnetic water flow meter OTT MF Pro (OTT HydroMet GmbH, Kempten, Germany). The magnetic-inductive measurement method examines flow velocity in a range of 0 m/s to 6 m/s with an accuracy of ± 2% of the measured value ± 0.015 m/s (from 0 m/s to 3 m/s) and an accuracy of ± 4% of the measured value ± 0.015 m/s (from 3 m/s to 5 m/s). It measures depth in a range from 0 m to 3.05 m with an accuracy of the larger of ± 2% of the measured value or ± 0.015 m using an absolute pressure sensor with a single point calibration (OTT HydroMet GmbH, 2023). The total discharge (Q) was calculated based on the flow velocity measurements.

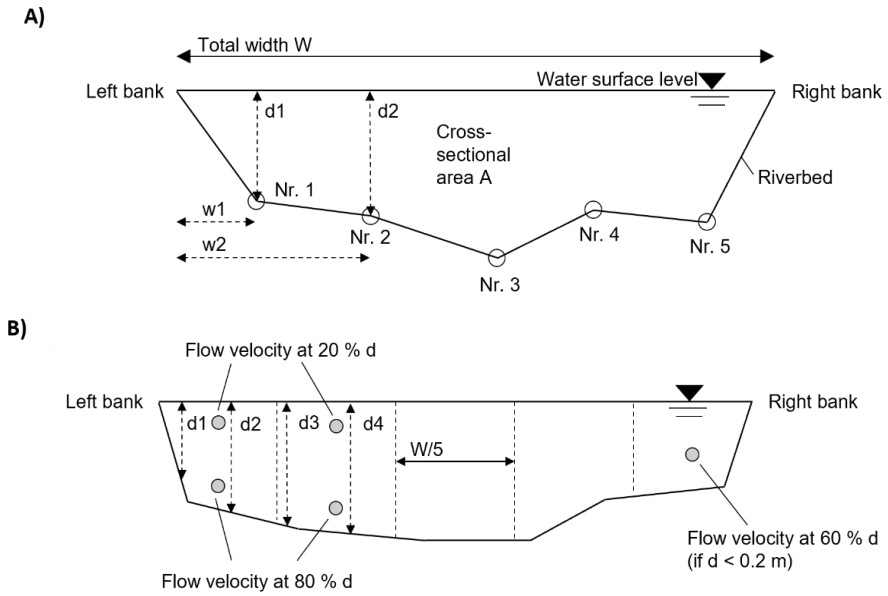

Figure 2: Sketches explaining measurements of the cross-sectional area (A) and the discharge (B). Total stream width (W), local depth (d) and distance to left bank (w) were measured at five characteristic points of the riverbed for calculating the cross-sectional area (A). Flow velocities were measured at 20% and 80% of the local water depth (d) at evenly distributed sampling points along a cross section if the water depth was > 0.2 m to calculate the discharge (Q). Flow velocity was measured once at 60% of the local water depth (d) if the depth was < 0.2 m.

Additionally, parameters to characterise water chemistry, physics, and biology were measured in the field. The pH was measured using the pH meter WTW pH 3310 connected to a SenTix 41 electrode (Xylem Analytics, Weilheim, Germany). The conductivity meter WTW Cond 3310 connected to a TetraCon 325 electrode (Xylem Analytics, Weilheim, Germany) was used to measure electrical conductivity. Water temperature, dissolved oxygen, chlorophyll *a*, and total dissolved solid (TDS) concentrations were measured using the multi-parameter probe HYDROLAB HL4 (OTT HydroMet GmbH, Kempten, Germany).

Triplicate water samples filtered through a pre-combusted GF/F filter (pore size 0.7 µm, Whatman™, Global Life Sciences Solutions USA LLC, Marlborough, MA, USA) were taken in acid-washed glass tubes for analysing DOC concentrations and in plastic tubes for analysing dissolved nutrient concentrations. The water samples were stored on ice and in the dark during transport to the laboratory and in the fridge until analysis.

The concentrations of dissolved nutrients (ammonium, NH_4-N; nitrate, NO_3-N, and soluble reactive phosphorus, SRP) were measured using a continuous flow nutrient analyser (CFA, Alliance Instruments, Salzburg, Austria). The CFA consisted of several analytic consoles for the different analyses. The samples were aspired by an autosampler, split, and added to the individual consoles via tubing. The continuous flowing reaction stream in the tubing also included the chemicals needed for the reaction and is segmented via gas bubbles (Alliance Instruments GmbH, 2007). Different wet-chemical methods with subsequent photometric determination of the reaction products were applied to measure the dissolved nutrient concentrations: the indophenol blue method was used for NH_4-N (Ivančič & Degobbis, 1984), an automated hydrazine reduction method for NO_3-N (Kempers & Luft, 1988), and an automatic ascorbic acid reduction method for SRP (Eberlein & Kattner, 1987). Detection limits of the CFA were 2 µg/L for NH_4-N, 100 µg/L for NO_3-N, and 0.5 µg/L for SRP.

The DOC concentrations were analysed on a total organic carbon (TOC) analyser (TOC-L CSH, Shimadzu, Kyoto, Japan). DOC was measured as non-purgeable organic carbon (NPOC), assuming that the samples did not contain significant amounts of purgeable or volatile organic compounds. For the analysis, the samples were first acidified to convert all inorganic carbon (carbonates and hydrogen carbonates) into carbon dioxide (CO_2) which was then removed from the sample by bubbling. The organic carbon was subsequently oxidized to CO_2, which was transferred to and measured by a nondispersive infrared (NDIR) detector (Shimadzu Europa GmbH, 2023). Each sample was analysed in four technical replicates and as a result, the mean and standard deviation of these replicates were calculated.

2.4) Particle sampling scheme

Particle samples of five different size classes, ranging from 500 µm to 0.7 µm size, were collected for measuring bacterial protein production (BPP) via incorporation of ^{3}H-labelled leucine into protein to determine the heterotrophic microbial activity. Furthermore, samples were taken for analysing POC and PN contents, C/N ratios, bulk stable isotopes of C and N (these parameters will be summarised as elemental analysis hereafter) and fatty acid (FA) composition to assess the biochemical particle composition. At each site, stream water was collected and pre-filtered over a 500 µm sieve to exclude larger particles. Subsequently, the fine particles were separated into five different size classes by filtration on nets and filters (Figure 3). The five size classes covered particle sizes ranging from 1) 500 µm - 100 µm, 2) 100 µm - 50 µm, 3) 50 µm - 15 µm, 4) 15 µm - 2.7 µm, and 5) 2.7 µm - 0.7 µm. The fine particle samples of the three larger size classes were collected directly on site by sequentially filtering water through nets of different mesh sizes and collecting the particles retained on the nets (Figure 3A). The filtered water containing particles < 15 µm was transported to the laboratory to obtain particle samples of the two smaller size classes by filtration (Figure 3B). The filtration process for each analysis will be described in more detail in the following sections.

2.5) Particle sampling in the field

Triplicate samples were taken at each sampling site for measuring the BPP, for elemental analysis, and for analysing the fatty acid composition. For each of these samples, stream water was collected from the water surface with caution not to disturb bottom sediments and pre-filtered over a 500 µm sieve. The 500 µm-pre-filtered water was subsequently filtered through mesh nets with 100 µm, 50 µm, and 15 µm pore size to collect particles in the three large size classes (Figure 3A). In total, 50 L were filtered for elemental and fatty acid analysis. The particles collected on each of the three nets were rinsed into separate 50 mL tubes using MilliQ water. 10 L of the filtered water were taken to the laboratory to obtain samples of the two smaller size classes for elemental analysis; 20 L (in agricultural streams) or 24 L (in mountain streams) were taken for fatty acid analysis.

For measuring the bacterial protein production, 7 L (in agricultural streams) or 10 L (in mountain streams) of the 500 µm-pre-filtered water were subsequently filtered over the nets to obtain particles of the three larger size classes. The particles collected on the nets were rinsed into separate scintillation vials using 10 mL GF/F-filtered stream water. A 0.5 L glass bottle was filled with the filtered water and taken to the laboratory to be sampled for the two small size classes.

Additionally, 30 L of 500 µm-pre-filtered stream water were filtered over a 15 µm mesh net to characterise the size distribution of the larger particles (500 µm - 15 µm). The particles collected on the net were rinsed into a 50 mL tube using MilliQ water.

All particle samples were stored on ice and in the dark during transport to the laboratory and all stream water samples containing particles < 15 µm were stored in the shade or in the stream to avoid warming.

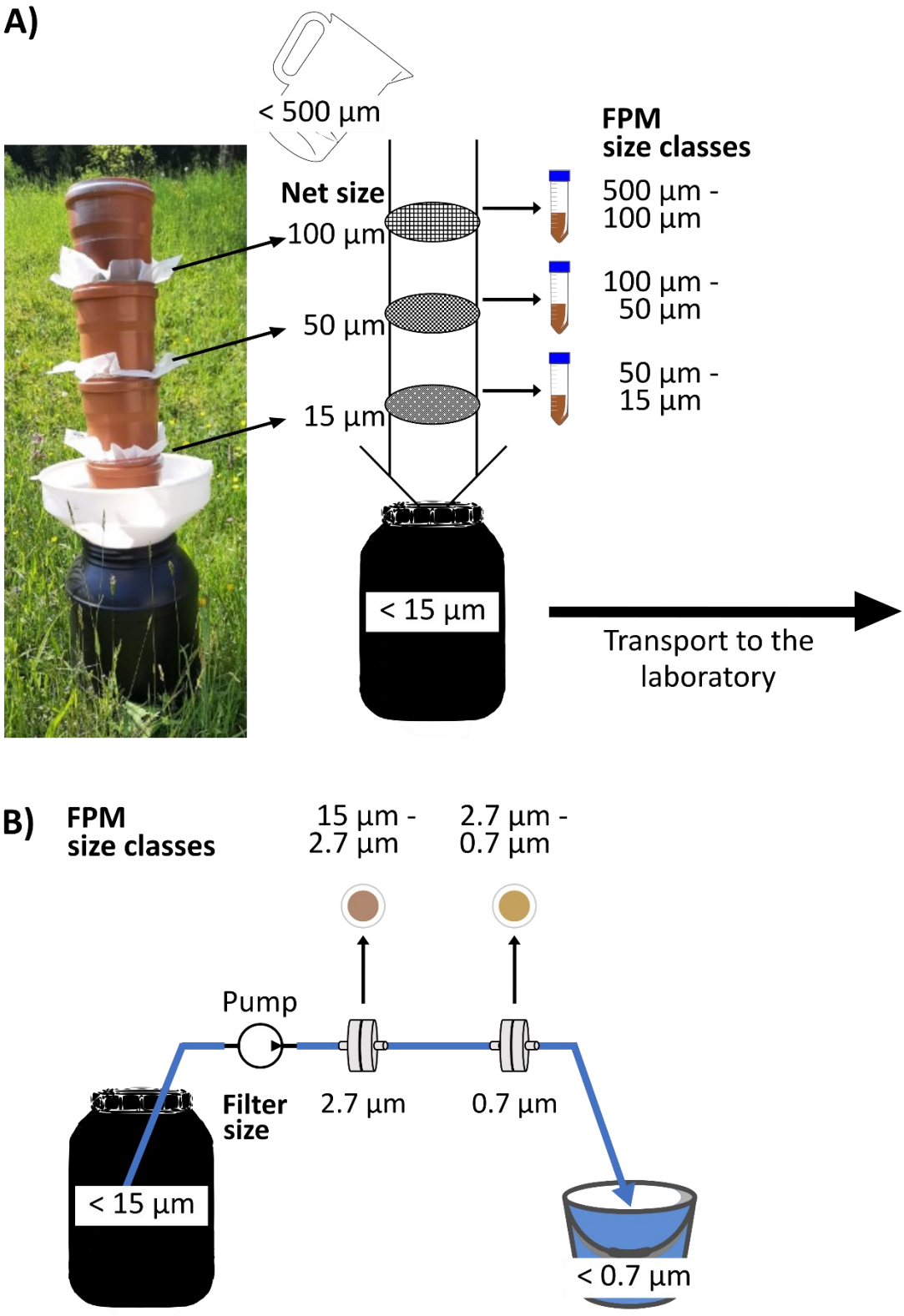

Figure 3: Schematic representation of the set-up for sequential filtering of the five particle size classes in the field (A) and in the laboratory for element and fatty acid analyses (B). In the field, the stream water was pre-filtered through a 500 µm sieve and subsequently filtered through nets with increasingly smaller mesh sizes. The water that passed through the finest mesh (15 µm) was collected in a barrel (A). The barrel was taken to the laboratory, where the two finest particle size classes were obtained by filtration with a peristaltic pump. The water that passed through the finest filter (0.7 µm pore size) was disposed of and not used for analyses (B).

2.6) Bacterial protein production

After return to the laboratory, BPP samples were incubated immediately. First, samples for the two smaller particle size classes were taken from the water samples containing particles < 15 µm. Due to varying available pore sizes depending on the filter type needed for the different analyses, the size classes 4) 15 µm - 3 µm and 5) 3 µm - 0.8 µm were used for measuring BPP instead of 4) 15 µm - 2.7 µm and 5) 2.7 µm - 0.7 µm.

10 mL of the 15 µm-pre-filtered water was pipetted into scintillation vials to obtain samples for the size class 15 µm - 3 µm for each of the three replicate samples. Blanks were prepared in six additional scintillation vials with 10 mL pre-filtered water of the same replicate. To collect samples for the size class 3 µm - 0.8 µm for each of the three replicates, the 15 µm-pre-filtered water was first filtered through a cellulose nitrate filter of 3 µm pore size (Sartorius Stedim Biotech GmbH, Göttingen, Germany) attached to a syringe, then 10 mL of this water was pipetted into a scintillation vial for the incubation.

The samples for the two smaller size classes and the collected particles of the three larger particle size classes suspended in 10 mL stream water were incubated with ^{3}H-labelled leucine at a final concentration of 80 nmol/L ([4.5-^{3}H]-L-Leucine, Lot # 152-064-140, Hartmann Analytic GmbH, Braunschweig, Germany). Samples were incubated close to in situ temperatures in a water bath for 1 h in the dark. The temperature was measured at the beginning and the end of the incubation and deviated from the temperature measured in the stream by a maximum of ± 4 °C. A 50% solution of trichloroacetic acid (TCA, final concentration in the samples: 5% TCA) was used for killing the blanks prior to the incubation and to terminate the incubation of samples afterwards.

The next day, samples of the four larger size classes and three of the blanks were filtered through cellulose nitrate filters of 25 mm diameter and 3 µm pore size (Sartorius Stedim Biotech GmbH, Göttingen, Germany). Samples for the finest size class (3 µm - 0.8 µm) and the three remaining blanks were filtered through cellulose nitrate filters of 0.8 µm pore size instead (Sartorius Stedim Biotech GmbH, Göttingen, Germany). All filters were washed twice with cold 5% TCA solution, once with cold 50% ethanol and once with MilliQ water, placed into scintillation vials and incubated with ethyl acetate for 15 minutes to dissolve the filters. Finally, 5 mL of liquid scintillation cocktail (LSC, Ultima Gold, PerkinElmer, Inc., Waltham, MA, USA) were added and the samples were stored in the dark overnight. The next day, the amount of leucine incorporated was measured on a liquid scintillation counter (LS 6500, Beckman Coulter, Brea, CA, USA).

There were two streams where samples were treated differently than described above: For Oberer Seebach only the samples of the size class 15 µm - 3 µm and three blanks were filtered through cellulose nitrate filters of 3 µm pore size, all other samples were filtered through cellulose nitrate filters of 0.8 µm pore size. For the stream Feichsen, the filtration and preparation for the measurement was done two days after the sampling and incubation.

Bacterial protein production (BPP) and bacterial carbon production (BCP) were calculated using incorporation rates of the labelled leucine into protein, which are estimated from the appearance of radioactivity in the samples, following the calculations described by Kirchman (2001). The radioactivity was measured as disintegrations per minute (DPM) on the scintillation counter. The DPM, the specific activity (SA), and the isotope dilution (ID) were used to calculate the amount of incorporated leucine (Leu_{inc}) by the equation:

$$Leu_{inc}\,[nmol] = \left(DPM_{sample} - DPM_{blank}\right) / \left(SA \cdot 2.22 \cdot 10^{6}\right) \cdot ID \qquad (1)$$

First, the DPM value of the blank is subtracted from the DPM value of the sample. For the blank value, the mean of the three replicate blanks per filter size was calculated. Depending on the filter used for filtration of the sample, the blank value was chosen accordingly: for the four larger size classes, the blank value measured in water samples filtered through the 3 µm filter was used. For the size class 3 µm - 0.8 µm, the blank value measured in water samples filtered through the 0.8 µm filter was used. An exception is Oberer Seebach, where the 3 µm-blank was only used for the size class 15 µm - 3 µm, for all other size classes the blank value measured in water samples filtered through the 0.8 µm filter was used as this represents the filter used for the other samples of this stream.
SA is the specific activity of the labelled leucine [Ci/mmol or µCi/nmol] multiplied by a factor to convert the unit DPM to µCi. Since the activity decreases over time due to radioactive decay, the current specific activity and not the specific activity given in the product data sheet of the labelled leucine was used for the calculation. The current specific activity was calculated by measuring the activity of 2.5 µL pure labelled leucine on the scintillation counter.
ID is the abbreviation for isotope dilution that corrects for diluting the labelled ('hot') leucine with not labelled ('cold') leucine. The isotope dilution is calculated by:

$$ID = \frac{\left(V_{hot\ Leu} \cdot c_{hot\ Leu}\right) \cdot \left(V_{cold\ Leu} \cdot c_{cold\ Leu}\right)}{\left(V_{hot\ Leu} \cdot c_{hot\ Leu}\right)} \qquad (2)$$

where V is the volume and c the concentration of the hot and cold leucine, respectively.

With the amount of incorporated leucine, the rate of leucine incorporation was calculated using the equation:

$$rate\ Leu_{inc}\,[nmol/(L \cdot h)] = 60 \cdot Leu_{inc} / \left(V \cdot t\right) \qquad (3)$$

with the sample volume V [L], the incubation time t [minutes] and the factor 60 to convert minutes to hours.

Following, the BPP was calculated using:

$$BPP\,[ng/(L \cdot h)] = rate\ \mathrm{Leu}_{inc} \cdot \left(\frac{100}{7.3}\right) \cdot 131.2 \cdot ID_{intracellular} \qquad (4)$$

where the factor 100/7.3 accounts for the constant proportion of 7.3% of leucine in protein (Kirchman et al., 1985) and 131.2 is the molecular weight of leucine [g/mol]. $ID_{intracellular}$ corrects for an intracellular isotope dilution resulting from the presence of leucine produced by intracellular leucine biosynthesis. This may continue to an unknown extent despite the high availability of extracellular leucine added for the incubation. Here, two was used as a factor for $ID_{intracellular}$ which is a commonly used factor (Kirchman, 2001; Simon & Azam, 1989).

With the carbon to protein ratio of 0.86 in average bacterial protein (Simon & Azam, 1989), the BCP was calculated from the BPP:

$$BCP\,[ng\ C/(L \cdot h)] = BPP \cdot 0.86 \qquad (5)$$

In addition, the BPP and BCP in ng/(mg·h) were calculated based on the median particle concentration to relate the volumetric bacterial production rates to the amount of particles. The median was computed for each size class in each stream. The available sample dry weights used for calculating the particle concentration were the three replicate samples for elemental and fatty acid analysis, ideally resulting in a total of six samples for calculating the median dry weight. In some cases, fewer samples could be taken for the median calculation because filters for the elemental analysis were damaged or the amount of particles was not sufficient to be weighed. As the sample dry weights were based on the filtration of different volumes, the dry weights were divided by the respective filtered water volume to yield particle concentrations in mg/L before calculating the medians.

Furthermore, the total bacterial production rates per L and per mg were calculated by adding up the production rates of all five particle size classes per sequentially filtered replicate sample, resulting in three replicate values per stream. In case a negative value was calculated for the production rate of a sample because the DPM value of the sample was lower than the mean blank DPM value, it was assumed that the bacterial production was too low to be measured. Therefore, all negative values were set to 0 for calculating total production rates.

2.7) Elemental analysis

In the laboratory, water samples for determining POC and PN contents, C/N ratios, and bulk stable isotope ratios of C and N were subsequently filtered through a GF/D filter (2.7 µm pore size) and a GF/F filter (0.7 µm pore size; Whatman™, Global Life Sciences Solutions USA LLC, Marlborough, MA, USA) both with a diameter of 25 mm using a peristaltic pump at a constant speed of 200 rpm. For the Oberer Seebach, the first stream sampled, the speed was set to 400 rpm because only one pump was used at that time to simultaneously filter water for the samples for elemental and fatty acid analyses. Realising that this caused high pressure and therefore leaking of the filter holders of 25 mm diameter, the filtration speed was reduced to 200 rpm for the following samplings. The filtration was stopped when the GF/D filters clogged or after all water was filtered. The amount of water remaining in the canisters was measured to determine the volume of the water used for the filtration. This volume was needed to calculate volumetric particle concentrations. The filters and the particles collected in tubes in the field were stored at -80 °C until further processing. All samples were freeze-dried and stored in the dark at room temperature afterwards.

The filters were stored in a desiccator, weighed using a micro balance (Sartorius CPA2P, Sartorius Lab Instruments GmbH & Co. KG, Göttingen, Germany), and fumigated with 37% (w/w) HCl for removal of carbonates. They were weighed again to be able to calculate the amount of material needed for the analysis. The filters were grinded using an agate mortar and pestle to obtain a homogenous sample. Based on analyses of test samples to determine the required amount of homogenised material needed for the analysis, it was aimed for a weight of 1 mg sample on GF/D filters of agricultural streams and 1.5 mg for mountain streams. For the samples on GF/F filters, a maximum of 0.7 mg of sample and, for most of the samples, the whole filter was used. The respective sample amount was weighed into tin boats (10 mm x 10 mm x 20 mm; IVA Analysentechnik GmbH & Co. KG, Meerbusch, Germany) that were compressed and again stored in a desiccator until analysis.

The particle samples in tubes were first weighed into Eppendorf tubes to achieve total weights of the collected material using a micro balance (Sartorius CPA2P, Sartorius Lab Instruments GmbH & Co. KG, Göttingen, Germany). By analysing test samples from one mountain stream and one agricultural stream, it was determined that 1.25 mg of sample were required for the analysis. Samples of the three replicates were pooled for the two largest size classes in some streams (particles 500 µm - 100 µm and 100 µm - 50 µm for Ois, Oberer Seebach, Steinbach, Feichsen, Schweinzbach and Zettelbach and particles 500 µm - 100 µm for Ofenbach) to approximate this amount. The samples were weighed into silver capsules (diameter 3.5 mm x 9 mm, 0.07 mL; IVA Analysentechnik GmbH & Co. KG, Meerbusch, Germany) that were transported to a heating plate on a metal tray and acidified to remove all inorganic carbon by successive addition of liquid 20% HCl (v/v). In total, 100 µL of HCl were used per sample and after adding the last portion of acid, the samples were left to dry on the heating plate at 70 °C for at least 3 h. The samples were then compressed and wrapped into tin capsules (5 mm x 9 mm; IVA Analysentechnik GmbH & Co. KG, Meerbusch, Germany) to improve the combustion of silver capsules in the elemental analyser by a momentary exothermic flash combustion of the tin capsules (Brodie et al., 2011). They were stored in a desiccator until analysis. For some samples, the analysis was repeated with a larger amount of sample if the nitrogen peak amplitude detected by the elemental analyser was low (< 1000) and sufficient sample material was available.

The POC and PN content of all prepared samples was measured on a Flash HT Plus CHNS/O elemental analyser (Thermo Fisher Scientific, Bremen, Germany). The elemental analyser was coupled to an isotope ratio mass spectrometer (IRMS, Delta V Advantage, Thermo Fisher Scientific, Bremen, Germany) that analysed stable isotope ratios of POC and PN.

As blanks for the elemental analysis, grinded empty GF/D and GF/F filters, compressed into tin boats, and empty silver capsules wrapped in tin capsules were used, respectively. Algae (Bladderwrack; 1.25% ± 0.02% N and 33.67% ± 0.29% C) and high organic sediment (0.52% ± 0.02% N and 7.45% ± 0.14% C; both supplied by IVA Analysentechnik GmbH & Co. KG, Meerbusch, Germany) were used as standards for determining the POC and PN content of the samples. For the filter samples, the available standards and amounts were 0.3 mg and 1 mg for algae and sediment. For the particle samples, standards were selected from 1.25 mg, 0.8 mg, or 0.3 mg of algae and sediment.
As isotopic working standards, urea standards with two different known values for $\delta^{15}N$ (Urea#3: 40.61‰ ± 0.03‰ and Urea#1: 0.26‰ ± 0.03‰) and $\delta^{13}C$ (Urea#3: 11.71‰ ± 0.03‰ and Urea#1: -34.13‰ ± 0.03‰) were used (Arndt Schimmelmann, Biogeochemical Laboratories, Indiana University, Bloomington, IN, USA).
In each analytical run, another urea standard (Urea#2a: $\delta^{15}N$ = 20.73‰ ± 0.04‰, $\delta^{13}C$ = -9.14‰ ± 0.02‰, Arndt Schimmelmann, Biogeochemical Laboratories, Indiana University, Bloomington, IN, USA) was included as a long-term control material and confirmed the stability and precision of measured values over time. This standard was also included in analytical runs of previous studies conducted in the laboratory and during the last five years, $\delta^{13}C$ values of 9.15‰ ± 0.58‰ and $\delta^{15}N$ values of 20.42‰ ± 0.65‰ (mean ± standard deviation, N = 77) were measured, resulting in an uncertainty of 6.3% for $\delta^{13}C$ values and 3.2% for $\delta^{15}N$ values, respectively.

For the filter samples that were only analysed as test samples beforehand in another run (all GF/F filters and two replicates of the GF/D filters from the agricultural stream Feichsen), glycine (USGS64; 18.6% N and 32.0% C, $\delta^{15}N$ = 1.76‰ ± 0.06‰ and $\delta^{13}C$ = -40.81‰ ± 0.04‰) and L-valine (USGS74; 12.0% N and 51.2% C, $\delta^{15}N$ = 30.19‰ ± 0.07‰ and $\delta^{13}C$ = -9.30‰ ± 0.04‰; both obtained from the Reston Stable Isotope Laboratory (RSIL) of the United States Geological Survey (USGS) Reston, VA, USA) were used as elemental and isotopic standards.

The POC and PN content of the samples was determined for all samples for which a correct weight was available, i.e. for all particle samples and the filter samples for which the filter was not damaged during filtration (nine of 60 filters were damaged). First, the constant k was calculated for each of the standards and each element using the equations:

$$k_C = \%\, C \cdot mean\ weight \cdot mean\ peak\ area \qquad (6)$$

and

$$k_N = \%\, N \cdot mean\ weight \cdot mean\ peak\ area \qquad (7)$$

with the known C and N content of the standards (% C and % N), the mean of the weights of a certain amount of standard weighed in and the mean of the measured peak areas of these standards. The constant was used to calculate the POC (% C_{sample}) and PN (% N_{sample}) content of samples by multiplication with the sample's peak area and weight:

$$\%\, C_{sample} = k_C \cdot peak\ area \cdot sample\ weight \qquad (8)$$

$$\%\, N_{sample} = k_N \cdot peak\ area \cdot sample\ weight \qquad (9)$$

For C, the peak area of the corresponding blank was subtracted from the peak area of samples and standards beforehand to correct for any C present in the filters, the tin boats, or the silver and tin capsules. The standard used for the calculation of POC and PN contents was selected first according to

its weight to match the sample weight and second according to its elemental C and N content matching the sample elemental content best. For all three replicate samples per size class and stream, the same standard was selected to avoid introducing errors regarding the variability within streams. However, different standards for the POC and the PN content were used in some cases within the same size class and stream. The relative POC and PN contents [%] were divided by 100 to achieve concentrations related to sample dry weight [mg/mg]. These were multiplied by the median particle concentration per size class in each stream to obtain volumetric concentrations.

The measured stable isotope ratios ($\delta^{13}C$ and $\delta^{15}N$) were converted to the international stable isotope reference scales (Vienna Pee Dee Belemnite, VPDB, for $\delta^{13}C$ and atmospheric nitrogen, Air-N_2, for $\delta^{15}N$) using a two-point linear normalisation to the urea standards (Paul et al., 2007). The isotopic composition of samples is expressed in the δ-notation, describing the relative difference between the isotope ratio of the sample and the standard in ‰:

$$\delta X_{sample} = \left(\frac{R_{sample}}{R_{standard}} - 1\right) \cdot 1000\ [‰] \qquad (10)$$

X represents the heavier isotope of an element (^{13}C or ^{15}N), and R is the concentration ratio of the heavier to the lighter isotope ($^{13}C/^{12}C$ and $^{15}N/^{14}N$) in the sample and standard, respectively.

Prior to the normalisation, the $\delta^{13}C$ values were blank corrected. The relative intensity (rel. intensity, in %) of the measurement was calculated from the automatic sample dilution (dil.) using an internal, experimentally determined formula:

$$rel.intensity = 0.004 \cdot (100 - dil.)^2 + 0.6225 \cdot (100 - dil.) - 2.5389 \qquad (11)$$

Then the measured peak area was multiplied by the relative intensity to obtain the theoretical undiluted peak area which was used to calculate the blank-corrected $\delta^{13}C$ value of samples and standards:

$$\delta^{13}C_{blank\ corr} = \frac{\delta^{13}C_{meas} \cdot area_{meas} - \delta^{13}C_{blank} \cdot area_{blank}}{area_{meas} - area_{blank}} \qquad (12)$$

No blank correction was done for $\delta^{15}N$ values and for the filter samples that were analysed as test samples in another run using glycine and valine as isotopic working standards. For two analytical runs, a high blank was measured, and the correction caused a higher deviation of the normalised $\delta^{13}C$ values of the standards from their certified $\delta^{13}C$ values compared to non-corrected, normalised $\delta^{13}C$ values. Therefore, no blank correction was applied to the measured $\delta^{13}C$ values in these runs.

Finally, the two-point linear normalisation was conducted, which is a linear regression of measured and true δ values of two certified reference standards. The true δ value of samples is estimated using the linear relationship:

$$\delta_{true} = m \cdot \delta_{meas} + b \qquad (13)$$

with the slope (or expansion factor) m and the intercept (or additive correction factor) b and the blank-corrected, measured δ value for C and the raw, measured δ value for N.

2.8) Fatty acid analysis

In the laboratory, water samples for analysing fatty acid composition were subsequently filtered through a GF/D filter (2.7 µm pore size) and a GF/F filter (0.7 µm pore size; Whatman™, Global Life Sciences Solutions USA LLC, Marlborough, MA, USA) both with a diameter of 47 mm using a peristaltic pump at a constant speed of 400 rpm. As already described for the collection of samples for the elemental analysis, the filtration was terminated when the GF/D filter was clogged before filtering the whole water sample and the volume remaining in the canisters was measured. The filter samples as well as the particles collected in tubes were stored at -80 °C until further processing.

All samples were freeze-dried and stored at -20 °C afterwards. The particle samples were weighed into Eppendorf tubes using a micro balance (Sartorius CPA2P, Sartorius Lab Instruments GmbH & Co. KG, Göttingen, Germany) to determine the amount of sample. Based on the results of analysing test samples, all samples of one size class in one stream with a weight < 1 mg were pooled to ensure that sufficient lipid material was available for the extraction. This applied to the same samples as for the elemental analysis. The two largest size classes 500 µm - 100 µm and 100 µm - 50 µm in the streams Ois, Oberer Seebach, Steinbach, Feichsen, Schweinzbach and Zettelbach and the size class 500 µm - 100 µm for the stream Ofenbach were pooled.

The FA analysis was conducted according to Guo et al. (2016) as a three-step process consisting of lipid extraction, derivatisation to fatty acid methyl esters (FAMEs), and quantification of FAMEs using gas chromatography (GC). All samples were weighed prior to the FA analysis on a micro balance (Sartorius CPA2P, Sartorius Lab Instruments GmbH & Co. KG, Göttingen, Germany). The whole filters were used and folded to fit into a glass centrifuge tube. The particle samples were weighed into tin capsules which were then transferred to centrifuge tubes. Following, 2 mL chloroform was added, ensuring that the whole sample was immersed. The samples were stored under an N_2 atmosphere at -80 °C for at least one night to secure that the chloroform freezes.
The lipid extraction and derivatisation were performed under an N_2 atmosphere, and the samples were stored on ice in between the steps. The lipids were extracted by adding 1 mL methanol and 1 mL chloroform-methanol (2:1 v/v) to the samples plus 0.8 mL sodium chloride solution (NaCl, 0.9%) to separate the lipid and non-lipid phases. The samples were sonicated for ten minutes in an ice water bath, vortexed for one minute, and centrifuged for five minutes at 4 °C and 3000 rpm. Following, the double pipetting technique with two glass Pasteur pipettes was used to collect the extracted lipids from the bottom phase in the centrifuge tube and to transfer them to a new vial. 1.5 mL chloroform was added to the sample and the extraction process was repeated two more times. The extracted lipids were evaporated to a final volume of around 1.5 mL using a stream of N_2 gas and the extracts were stored at -20 °C until further processing.
For a gravimetric assessment of the total lipid content, duplicate 100 µL aliquots of the lipid extracts were transferred into pre-weighed tin capsules, dried, and reweighed. The remaining extract was stored at -20 °C until the derivatisation to FAMEs. The gravimetry was repeated if the two values for the lipid content showed more than 25% deviation from each other. Prior to the derivatisation, the exact volume of the extracted lipids was determined. The entire lipid extracts were used to obtain FAMEs. 2 mL sulfuric acid-methanol mix (1:100 v/v) as a methylation reagent as well as 1 mL toluene were added under an N_2 atmosphere, the samples were then shaken manually and incubated for 16 h at 50 °C in a water bath. Subsequently, 2 mL potassium hydrogen carbonate ($KHCO_3$) and 5 mL hexane were added, the samples were shaken, CO_2 released, and the samples were centrifuged for three minutes at 4 °C and 1500 rpm. The upper organic layer containing FAMEs was transferred into a new

vial. The addition of 5 mL hexane to the samples, shaking, release of CO_2, and centrifugation were repeated one more time. All collected upper organic layers of a sample were evaporated until dryness under a stream of N_2 gas. Hexane was used to redissolve and collect the FAMEs and to transfer them to 1.5 mL GC vials in two replicates. In the GC vials, the solution was again concentrated under N_2 gas to the volume required for GC (1.5 mL, 1 mL, or 0.5 mL, depending on the lipid content of the sample). The methylated extracts were stored at -80 °C until analysis.

FAMEs were quantitatively analysed using a gas chromatograph connected to a flame ionisation detector (GC-FID: Trace GC with TriPlus RHS Autosampler, Thermo Fisher Scientific, Waltham, MA, USA). Samples were injected in the splitless mode. Helium was employed as a carrier gas at a flow rate of 1.6 mL/min and hydrogen (H_2, 40 mL/min), nitrogen (N_2, 45 mL/min), and air (450 mL/min) were used as detector gases. FAMEs were separated by an HP-88 column (length: 100 m, inner diameter: 0.25 mm, film thickness: 0.2 µm, format: 7 inch; Agilent Technologies, Inc., Santa Clara, CA, USA). The total run time for each sample lasted 96 minutes. The temperature was programmed to start at 70 °C (1 min hold), to ramp up to 160 °C (3 min hold) by 60 °C/min, then ramp up to 176 °C (9 min hold) by 2.4 °C/min, followed by a ramp of 1 °C/min up to 186 °C (6 min hold), then increasing by 0.5 °C/ min to 202 °C (6 min hold), by 1.8 °C/min up to 212 °C (4 min hold) and ultimately by 4.5 °C/min to 245 °C (4 min hold).
FAMEs were identified by comparing their retention time with known reference standards (Supelco 37 Component FAME Mix, CRM47885; and Bacterial Acid Methyl Ester (BAME) Mix, 47080-U; both obtained from Sigma-Aldrich, Merck KGaA, Darmstadt, Germany) and two in-house standards for stearidonic acid (18:4n-3) and eicosatetraenoic acid (20:4n-3). In total, these standards allowed to identify 47 single FAs. Peaks were integrated and, if necessary, manual peak adjustment was performed using the software Chromeleon™ 7 (Thermo Fisher Scientific, Waltham, MA, USA). FAME concentrations were quantified using 7-point calibration curves based on known concentrations of their standards and reported as mass fractions [µg FAME/mg dry mass] and additionally as mass percentage of total FAME [%]. The mass fractions were converted to volumetric concentrations [µg/L] by multiplying them with the median of the particle concentration in each particle size class in each stream.

Fatty acids were categorised into groups according to their degree of saturation: saturated fatty acids (SFA), monounsaturated fatty acids (MUFA), and polyunsaturated fatty acids (PUFA). The latter were further divided into omega-3 and omega-6 PUFA (n-3 PUFA and n-6 PUFA). Another group of interest were fatty acids that can be used as bacterial biomarkers since this can be related to the microbial activity measurements. Bacterial fatty acids (BFA) comprised the fatty acids anteiso-15:0, iso-15:0, 15:0, iso-16:0, iso-17:0, 16Δ9,10, 17:0, 17:1n-7, 18Δ9,10, 18:1n-6, and 18:1n-7 (Guo et al., 2016). Further single FAs were considered as biomarkers: n-3 PUFA (eicosapentaenoic acid/ EPA, 20:5n-3; α-linolenic acid/ ALA, 18:3n-3; stearidonic acid, 18:4n-3; and docosahexaenoic acid/ DHA, 22:6:n-3) are biomarkers of algae and palmitoleic acid (16:1n-7) of diatoms in particular (Torres-Ruiz et al., 2007). Fungi of terrestrial and marine environments are characterised by palmitic acid (16:0), stearic acid (18:0), oleic acid (18:1n-9), and linoleic acid (LIN, 18:2n-6) (Cooney et al., 1993; Stahl & Klug, 1996), so these fatty acids are also used as fungal biomarkers in this study. Single FAs with a mean concentration of > 0.05 µg/L were defined as major components (according to Mills et al., 2003) and FAs with a maximum proportion of $\geq 5\%$ (percentage of total FAME) were considered to be the most abundant FAs.

2.9) Particle size distribution

The samples for characterising the size distribution of particles from 500 µm to 15 µm size were stored at room temperature and ambient light conditions until analysis. Excess water in the tubes was removed by pipetting to a volume of 4 mL to 5 mL to concentrate the particles. Samples were carefully shaken and ultrasonicated in an ultrasonication bath for ten minutes to disperse larger particle aggregations. In some samples, larger aggregations were still visible after ultrasonication. It was avoided to add these large aggregations to the particle size analyser since the largest size of sampled particles was 500 µm.

A laser diffractometer (LS 13 320 XR Laser Diffraction Particle Size Analyzer, Beckman Coulter, Brea, CA, USA) connected to the control and analysis software ADAPT (version 1.3.337, Beckman Coulter, Brea, CA, USA) was used for analysing the samples. The instrument determines the particle size distribution by measuring the pattern of light scattered by particles in a sample using two complementary optical systems. It includes a laser diffraction optical system and the company's PIDS system (Polarization Intensity Differential Scattering), each consisting of an illumination source, a sample chamber where the light beam passes and interacts with the suspended particles, a lens system to focus the scattered light, and photodetectors to record the scattered light intensity patterns (Beckman Coulter, Inc., 2019). The resulting pattern represents the sum of patterns scattered by each particle in the sample. Following each analytical run, various statistical parameters are automatically computed by the ADAPT software and can be used to draw conclusions about the particle size distribution.

An adaptation of the Default ULM (Universal Liquid Module) method was applied for characterising particle size distribution: Before each measurement, there were two rinse cycles of 8 s. Debubbling was enabled, and the circulation pump speed was set to 45%. The target range for sample loading was set to 8% ± 6%, and the PIDS technology was enabled. Three consecutive runs for each sample were completed, each with a run time of 60 s. The analysis of test samples beforehand showed only low variation between consecutive runs and no effect of 60 s vs 90 s run time on the results. Therefore, a run time of 60 s was chosen, and the number of runs was not increased. Also, comparable results were already achieved with a sample loading of at least 1%.

A sample volume of 1 mL to 2 mL was added to the instrument depending on the concentration of particles in the sample. The analysis was started with a sample loading ranging from 1.0% to 4.4% and the PIDS loading ranging from 6.9% to 37.6%. Due to small amounts of sample, the pre-set sample loading of at least 2% could not be reached for all samples, nevertheless, based on the preliminary tests, the analysis was started, and results were used. The mean particle size and its standard deviation were assessed which were calculated by the software based on the arithmetic mean and standard deviation of the particle size distribution of each run.

2.10) Data analysis

All statistical analyses were conducted and plots were created using the software R (version 4.2.2; R Core Team, 2022) and the ggplot2 package (version 3.4.0; Wickham, 2016). The data used for the statistical analyses included:

1) Data on the FPM concentration [mg/L] in each particle size class in each stream. As explained above, the median of all available sample dry weights divided by the volume filtered for the respective sample was computed based on the particle samples for elemental and fatty acid analysis (see Appendix 1 for median FPM concentrations and samples sizes used for the calculation).
2) Data on the heterotrophic microbial activity, measured as bacterial protein production rates and reported per unit volume [ng/(L·h)] as well as in relation to particle dry weight [ng/(mg·h)].
3) Data on biochemical particle composition and particle quality, obtained from elemental and fatty acid analyses. POC and PN contents relative to water volume [µg/L] and to particle dry weight [mg/mg], C/N ratios and $\delta^{13}C$ and $\delta^{15}N$ values were calculated from the elemental analysis as described above. Concentrations [µg/L] of total lipids, bacterial fatty acids, and single FAs as well as relative proportions [%FAME] of fatty acid groups and single FAs were determined from the fatty acid analysis.

For each analysed parameter, the median of the three replicate samples per size class and stream was calculated and used for the data analyses, resulting in five data points per size class and stream type. This was performed to avoid dependencies within the data and to harmonise the number of samples available per size class since some samples were pooled and therefore no replicates were available anymore.

2.10.1) Comparison of stream types

General differences in microbial activity and particle composition between agricultural and mountain streams were assessed using total bacterial production rates and total POC, PN, total lipid, and BFA concentrations. These were obtained by summing the production rates and concentrations of all size classes for each replicate per stream and then calculating the median value for each stream, resulting in five data points per stream type. Furthermore, differences in the amount of particles were examined by comparing total FPM concentrations, i.e. the sum of median FPM concentrations across all size classes, between the stream types. When comparing the two stream types, non-parametric Mann-Whitney U tests were conducted and considered significant at $p < 0.05$. To test the hypothesis that there is a higher bacterial production and biomass in agricultural than in mountain streams, one-sided Mann-Whitney U tests were calculated with the total bacterial production rates and total BFA concentrations. Two-sided Mann-Whitney U tests were applied to compare total FPM, POC, PN, and total lipid concentrations to examine differences in particle quality and amount between stream types.

In more detail, all available parameters were compared between the two stream types within each size class. Again, Mann-Whitney U tests were utilised for the statistical comparison and the significance level was adjusted by a Bonferroni-correction to account for repeated testing in all five size classes. The tests were thus considered significant at $p < 0.01$. One-sided tests were applied to test if bacterial production rates and BFA concentrations were higher in agricultural compared to mountain streams. Two-sided tests were used to compare particle amount, indicated by the FPM concentration, and biochemical particle composition between stream types, assessed by total lipid, POC, and PN concentrations as well as the C/N ratio and $\delta^{13}C$ and $\delta^{15}N$ values. When examining bacterial production

rates per size class, negative values were treated as NAs instead of setting them to 0 to not artificially increase differences. For $\delta^{15}N$, only values for the three larger size classes were considered due analytical problems with the filter samples for the two finest size classes (15 µm - 2.7 µm and 2.7 µm - 0.7 µm).

Compositional differences in the fatty acid profiles between particles of agricultural and mountain streams were visualised by Principal Component Analyses (PCAs). Relative proportions [%FAME] in each stream and size class of the most abundant single FAs (≥ 5% of total FAME) and the FA groups (SFA, MUFA, n-3 PUFA, n-6 PUFA, and BFA) were used to compare particle quality as this provides more information on the particle composition than their concentrations. After scaling the variables, the *prcomp()* function from the stats package (version 4.2.2; R Core Team, 2022) was applied to calculate the PCA. The *autoplot()* function included in the ggplot2 package (version 3.4.0; Wickham, 2016) was used to create visualisations of the PCAs.

2.10.2) Comparison of size classes

Statistical analyses to examine differences in microbial activity and particle amount, quality, and composition between the particle size classes were conducted separately for the two smaller size classes and the three larger size classes due to the methodological differences in sample collection. Median values per size class and stream of bacterial production rates, C/N ratios, $\delta^{13}C$ and $\delta^{15}N$ values and FPM, POC, PN, total lipid, and BFA concentrations were compared among the size classes. Again, for $\delta^{15}N$ values only results from the large size classes were included.

For comparing the two smaller size classes (15 µm - 2.7 µm and 2.7 µm - 0.7 µm; obtained by filtration in the lab), non-parametric Wilcoxon signed-rank tests (two-sided) were applied and considered significant if $p < 0.05$. Negative values for the bacterial production rates were excluded by setting them as NAs. The three larger size classes (500 µm - 100 µm, 100 µm - 50 µm, and 50 µm - 15 µm; collected on nets in the field) were compared using the Friedman test, if significant ($p < 0.05$) followed by the Conover's test of multiple comparisons with Bonferroni-correction to adjust *p*-values as post hoc test, which is included in the PMCMRplus package (version 1.9.6; Pohlert, 2022). Negative values for the bacterial production rates were set to 0 for the Friedman test since it requires a data table without NAs.

All statistical analyses were calculated within stream types, i.e. separately for mountain and agricultural streams. In addition, they were conducted including all streams regardless of stream type if no significant difference was found in the previous comparison of the stream types in each size class. Differences in the fatty acid composition of differently sized particles were examined based on the PCAs already applied for detecting compositional differences between stream types.

3) Results

3.1) Stream characterisation

The selected streams were different regarding their catchments and morphological and physical characteristics according to the stream type (Table 2). The elevation above sea level was higher for the sampling sites at mountain streams, ranging from 551 m to 770 m, compared to a range from 268 m to 330 m for the sampling sites at agricultural streams.

The catchment areas of the mountain streams upstream of the sampling sites ranged from 19 km^2 to 133 km^2 size. The streams Ois and Salza had considerably larger catchment areas than the other mountain streams. However, all catchments were dominated by forests and semi-natural areas (> 90%). The catchment area was smaller for the agricultural streams with sizes from 4 km^2 to 22 km^2. The land use in these catchments was less homogeneous than in the mountain catchments but all streams showed a lower proportion of forests and semi-natural areas (11.6% - 50.5%) and a higher proportion of agricultural areas (47.7% - 88.4%) compared to the mountain streams. The streams Feichsen and Zettelbach had lower proportions of agricultural areas in their catchment compared to the other agricultural streams and for the Zettelbach, the proportion of agricultural land use was 3% less than the percentage of forests and semi-natural areas. All other agricultural streams were dominated by agricultural land use in their catchment area.

Morphologically, the mountain streams were characterised by larger cross-sectional areas (1.15 m^2 - 4.49 m^2) and deeper mean depths (0.20 m - 0.68 m) than the agricultural streams (0.11 m^2 - 0.86 m^2 and 0.10 m - 0.22 m, respectively). The flow regime of mountain streams showed higher flow velocities from 0.28 m/s to 0.68 m/s and accordingly a higher discharge of 0.74 m^3/s to 1.70 m^3/s compared to agricultural streams, except for Oberer Seebach. In this stream, a low mean flow velocity of 0.02 m/s was measured, and a discharge of 0.05 m^3/s was calculated. This velocity is lower than the flow velocities measured in agricultural streams (ranging from 0.04 m/s to 0.15 m/s), the discharge is still higher than in four of the agricultural streams.

Mean particle sizes of FPM, pre-filtered over a 500 µm sieve and collected on a 15 µm net, revealed that larger particles were transported in mountain streams (median ± IQR: 68.4 µm ± 21.0 µm) compared to agricultural streams (median ± IQR: 46.8 µm ± 12.7 µm).

The parameters characterising water chemistry, physics, and nutrient loading of the streams also showed differences between stream types (Table 3). The water temperature was lower in mountain streams than in agricultural streams, ranging from 8.7 °C to 14.9 °C and from 14.9 °C to 18.8 °C, respectively. The pH across all streams was less variable with values from 8.0 to 8.6 and without pronounced differences between stream types. Dissolved oxygen concentrations were > 10 mg/L in mountain streams and slightly higher than in agricultural streams, however all streams except for the agricultural streams Ofenbach and Schweinzbach (88.6% and 86.4%) and the mountain stream Oberer Seebach (98.1%) were oversaturated with oxygen. The specific electrical conductivity varied among the streams, but the values and their range were lower in mountain than in agricultural streams (269 µS/cm - 376 µS/cm compared to 462 µS/cm - 721 µS/cm). Within the agricultural streams, a lower conductivity was measured in the streams Feichsen and Zettelbach (< 480 µS/cm) while it was > 660 µS/cm in the remaining agricultural streams. Chlorophyll *a* concentrations were generally lower in mountain streams and ranged from 0.80 µg/L to 2.02 µg/L, with the highest concentration measured in the Steinbach. All other mountain streams showed chlorophyll *a* concentrations < 1.05 µg/L. In agricultural streams, chlorophyll *a* concentrations ranged from 1.75 µg/L to 4.88 µg/L. The concentrations of total dissolved solids were again lower in mountain streams (0.15 g/L - 0.23 g/L) than

in agricultural streams (0.29 g/L in Feichsen and Zettelbach and 0.42 g/L - 0.45 g/L in the remaining streams).

DOC concentrations are presented as median values since in three streams one of the three replicates showed a large deviation from the usually consistent values of the replicate samples. The concentrations were lower in mountain streams with values ranging from 1.19 mg/L to 1.80 mg/L, except for the Steinbach which showed the highest DOC concentration of all sampled streams (3.46 mg/L). The DOC concentrations ranged from 2.18 mg/L to 3.41 mg/L in the agricultural streams. Dissolved nutrient concentrations were generally lower in mountain compared to agricultural streams. Ammonium concentrations ranged from below the detection limit of 2 µg/L to 7.1 µg/L in mountain streams and from 4.7 µg/L to 15.7 µg/L in agricultural streams. Only the mountain stream Oberer Seebach showed a higher ammonium concentration than the agricultural streams. The nitrate concentrations varied between 454 µg/L and 705 µg/L in mountain streams and ranged from 373 µg/L to 2737 µg/L in agricultural streams. Zettelbach was the stream with the lowest nitrate concentration, in all other agricultural stream concentrations of > 1000 µg/L were measured. The SRP concentrations were lower in all mountain streams than in the agricultural streams, ranging from below the detection limit of 0.5 µg/L to 3.5 µg/L, whereas they varied between 28.4 µg/L and 90.7 µg/L in the agricultural streams.

Table 2: Parameters characterising the catchments, morphology, and water flow of the sampled streams: elevation, catchment area upstream of the sampling site, proportion of forests and semi-natural areas as well as agricultural area in the catchment, cross-sectional area, mean depth, mean velocity, discharge, and mean particle size (± standard deviation, SD).

Stream type	Stream name	Sampling date	Elevation [m a.s.l.]	Catchment area [km^2]	Forests and semi-natural areas [%]	Agri-cultural area [%]	Cross-sectional area [m^2]	Mean depth [m]	Mean velocity [m/s]	Discharge [m^3/s]	Mean particle size [µm] ± SD [µm]
Mountain	Hinterwildalpenbach	25.08.2022	688	26	93.0	6.9	1.15	0.20	0.60	0.74	84.6 ± 98.4
	Oberer Seebach	26.07.2022	610	19	96.1	2.2	2.94	0.27	0.02	0.05	68.4 ± 37.2
	Ois	05.08.2022	640	96	93.6	3.2	4.49	0.36	0.25	0.99	81.0 ± 82.8
	Salza	01.08.2022	760	133	90.7	8.8	4.20	0.38	0.28	1.31	59.5 ± 63.3
	Steinbach	29.08.2022	551	36	100.0	0.0	2.12	0.23	0.68	1.70	56.2 ± 48.6
Agricultural	Feichsen	26.08.2022	330	22	42.6	57.4	0.86	0.19	0.15	0.13	46.8 ± 46.1
	Ofenbach	05.09.2022	268	4	11.6	88.4	0.11	0.17	0.07	0.02	49.7 ± 45.5
	Schweinzbach	29.07.2022	289	18	16.5	83.5	0.27	0.12	0.08	0.02	37.0 ± 37.8
	Sierning	03.08.2022	270	19	19.8	74.2	0.61	0.22	0.06	0.04	33.5 ± 39.7
	Zettelbach	08.08.2022	322	16	50.5	47.7	0.39	0.10	0.04	0.02	53.0 ± 64.3

Table 3: Chemical, physical, and biological characteristics of the sampled streams: water temperature (T), pH, dissolved oxygen (dO), specific electrical conductivity (Cond.), concentration of chlorophyll *a* (Chl *a*), total dissolved solids (TDS), and dissolved organic carbon (DOC, median ± IQR is shown). Dissolved nutrient concentrations (ammonium, N-NH_4, nitrate, N-NO_3, and soluble reactive phosphorus, SRP) are shown as mean values ± standard deviation (SD).

Stream type	Stream name	T [°C]	pH	dO [mg/L]	dO [%]	Cond. [µS/cm]	Chl *a* [µg/L]	TDS [g/L]	DOC [mg/L] ± IQR [mg/L]	N-NH_4 [µg/L] ± SD [µg/L]	N-NO_3 [µg/L] ± SD [µg/L]	SRP [µg/L] ± SD [µg/L]
Mountain	Hinterwildalpenbach	8.7	8.6	11.2	102.4	269	0.93	0.16	1.32 ± 0.036	< 2	639 ± 22	0.6 ± 0.1
	Oberer Seebach	10.7	8.2	10.3	98.1	242	0.80	0.15	1.36 ± 0.006	7.1 ± 0.1	672 ± 1	2.2 ± 0.1
	Ois	11.5	8.3	10.6	102.8	311	0.55	0.19	1.19 ± 0.539	3.2 ± 1.2	583 ± 49	3.5 ± 1.5
	Salza	14.9	8.6	10.3	108	376	1.05	0.23	1.80 ± 0.021	3.4 ± 0.3	454 ± 13	< 0.5
	Steinbach	13.3	8.5	10.0	101.2	279	2.02	0.17	3.46 ± 0.095	< 2	705 ± 60	< 0.5
Agricultural	Feichsen	16.6	8.4	9.3	101.5	476	2.07	0.29	3.41 ± 0.038	5.0 ± 0.7	1125 ± 37	28.4 ± 0.3
	Ofenbach	14.9	8.0	8.4	88.6	721	4.88	0.45	2.79 ± 0.048	8.7 ± 0.8	2737 ± 92	61.3 ± 5.0
	Schweinzbach	17.7	8.0	7.7	86.4	664	1.75	0.42	2.48 ± 0.051	12.3 ± 2.6	1120 ± 101	90.7 ± 6.6
	Sierning	18.8	8.2	9.0	102.7	690	2.21	0.44	2.18 ± 1.734	15.7 ± 0.4	1826 ± 104	63.7 ± 0.5
	Zettelbach	16.7	8.4	10.1	110	462	1.80	0.29	2.45 ± 4.324	4.7 ± 0.1	373 ± 140	35.9 ± 0.2

3.2) Particle quantity

The **total FPM concentration** was on average 3.9 times higher in **agricultural compared to mountain streams** (Mann-Whitney U test, $p = 0.007937$, $W = 0$) and ranged from 0.20 mg/L to 0.92 mg/L and from 1.86 mg/L to 5.01 mg/L, respectively (Figure 4A, Table 4). **Divided by size class**, the FPM concentrations were again higher in agricultural streams in the two finest size classes, on average by more than 6 times in the size class 15 µm - 2.7 µm and by more than 5 times in the finest size class (for both size classes: Mann-Whitney U tests, $p = 0.007937$, $W = 0$; Figure 4B, Table 4). The FPM concentration in the size class 50 µm - 15 µm was on average 3 times higher in agricultural than in mountain streams, this difference was however not significant. For the two largest size classes, very low particle FPM were measured, and these did not differ between stream types (Mann-Whitney U tests, see Table 4 for *p*- and *W*-values and sample sizes).

Table 4: Total FPM concentration (size class 'all') and FPM concentration per size class, divided by stream type. Medians, means, interquartile ranges (IQR), and sample sizes (N) are presented. Additionally, *p*-values and *W*-values from comparisons of the total FPM concentration or the FPM concentration in each size class between the stream types using two-sided Mann-Whitney U tests are given in the rows of the mountain streams and printed in bold if a significant difference was detected with $p < 0.05$ or $p < 0.01$ after Bonferroni correction. The size class refers to the lowest size of each particle size class (e.g. 100 stands for the size class 500 µm - 100 µm).

Stream type	Size class	Median [mg/L]	Mean [mg/L]	IQR [mg/L]	N	*p*	*W*
Mountain	all	0.71	0.62	0.27	5	**0.007937**	**0**
Agricultural	all	2.78	3.19	1.70	5		
Mountain	100	0.01	0.05	0.03	5	0.4206	17
	50	0.01	0.05	0.03	5	0.8413	11
	15	0.09	0.11	0.05	5	0.03175	2
	2.7	0.36	0.35	0.17	5	**0.007939**	**0**
	0.7	0.04	0.06	0.05	5	**0.007939**	**0**
Agricultural	100	0.02	0.02	0.01	5		
	50	0.03	0.02	0.03	5		
	15	0.29	0.35	0.14	5		
	2.7	2.19	2.56	1.67	5		
	0.7	0.21	0.23	0.01	5		

The majority of particles were present in the size class 15 µm - 2.7 µm, except for the Hinterwildalpenbach where the larger size classes also accounted for considerable proportions of the total FPM amount (Figure 5). Here, the size class 15 µm - 2.7 µm accounted for only 29% of the total FPM amount while it made up 61% to 90% for the other streams. The finest size class accounted for 5% to 14% of the total FPM amount and the two largest size classes comprised the lowest amount of FPM in all streams except for the Hinterwildalpenbach. **Differences in FPM concentration among the size classes** were assessed for all streams together only for the three large size classes since the concentrations in the two smaller size classes differed between stream types and within stream types (Appendix 2). A larger amount of FPM was found in the size class from 50 µm - 15 µm compared to the two larger size classes when assessing all streams together ($p = 0.0005531$, *Friedman* $Chi^2 = 15$, $df = 2$). This difference was not confirmed when testing the stream types separately, although the Friedman test revealed a significant difference between some of the size classes, it was not detected by the post hoc tests (see Appendix 2 for *p*- and *Friedman* Chi^2-values and sample sizes). The amount of FPM was

on average 9 times and 10 times higher in the size class 15 µm - 2.7 µm than in the finest size class in mountain and agricultural streams, respectively, but these differences were not significant (Wilcoxon signed-rank tests, $p = 0.0625$, $V = 15$ for both stream types).

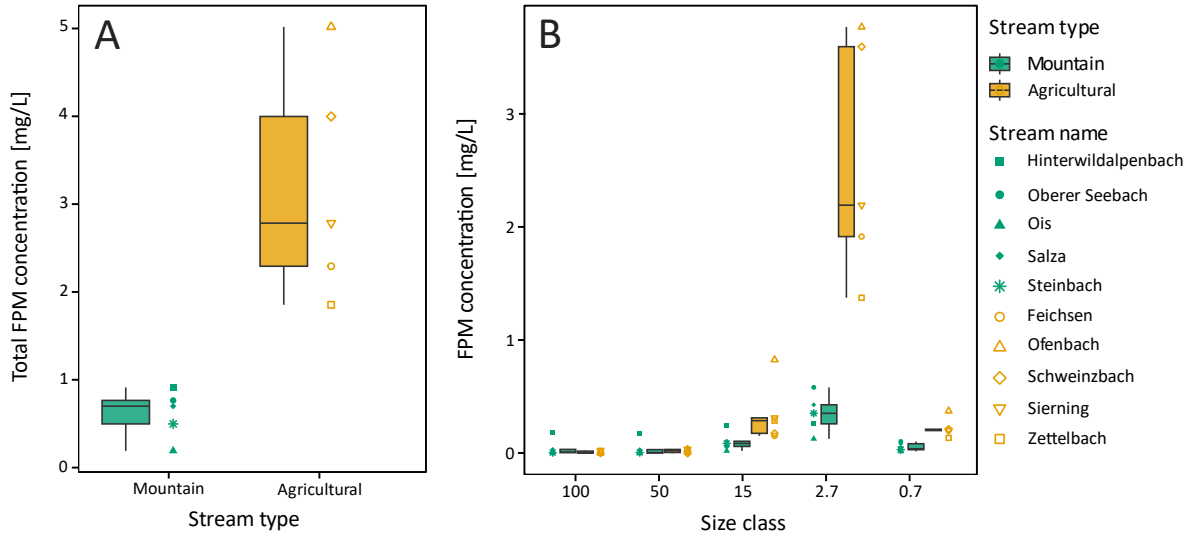

Figure 4: Total (A) and size-class specific (B) median FPM concentration of each stream divided by stream type. The boxplots visualise the median of the FPM concentration by stream type or by stream type and size class (horizontal line), the boxes encompass the first to third quartile and the whiskers extend to a maximum of 1.5 times the interquartile range. Outliers are only shown with the individual data points. The x-axis labels refer to the lowest size of each particle size class (e.g. 100 stands for the size class 500 µm - 100 µm).

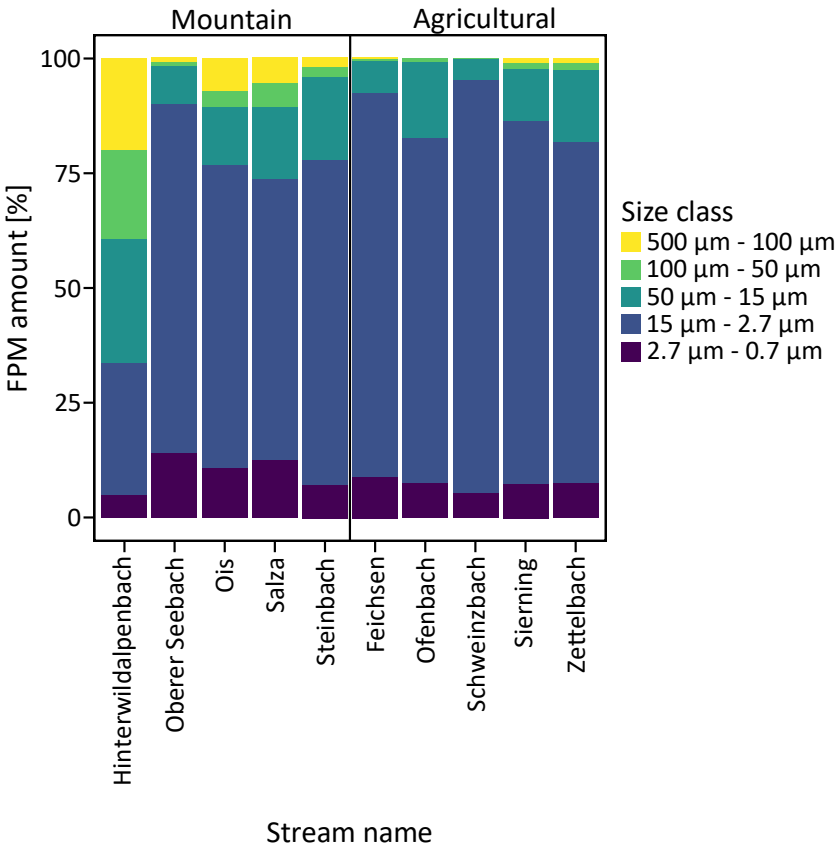

Figure 5: Median proportion of FPM in each size class of the total FPM amount in all sampled streams.

3.3) Heterotrophic microbial activity

The **total BPP between the two stream types** was different, however, the magnitude of the difference depended on the relation to volume or particle dry weight. The total BPP related to volume was on average 20 times higher in agricultural streams than in mountain streams (one-sided Mann-Whitney U test, $p = 0.007937$, $W = 1$), with median values ranging from 11.06 ng/(L·h) to 168.00 ng/(L·h) in mountain streams compared to 105.60 ng/(L·h) to 3078.60 ng/(L·h) in agricultural streams (Figure 6A, Table 5). Contrastingly, the total BPP related to particle dry weight did not differ significantly between stream types (one-sided Mann-Whitney U test, $p = 0.1548$, $W = 7$). However, production rates in agricultural streams were on average two times higher than in mountain streams and ranged from 71 ng/(mg·h) to 785 ng/(mg·h) and from 86 ng/(mg·h) to 2405 ng/(mg·h), respectively (Figure 6B, Table 5).

Furthermore, the **BPP in each of the size classes** showed higher median rates in agricultural than in mountain streams across all size classes when looking at volumetric rates (Figure 6C). However, no significant difference was found between the stream types (one-sided Mann-Whitney U tests with Bonferroni-corrected significance level, see Table 5 for *p*- and *W*-values and sample sizes). Considering the medians (Table 5), the activity in agricultural streams was 2.5 times higher in the size class 500 µm - 100 µm, 3.1 times higher in the size class 100 µm - 50 µm, 4.9 times higher in the size class 50 µm - 15 µm, 13.5 times higher in the size class 15 µm - 3 µm and 6.1 times higher in the size class 3 µm - 0.8 µm. The absolute difference between stream types is hardly noticeable in the three larger size classes due to very low production rates which only accounted for < 1.2% of the total BPP. The difference is more pronounced in the two smaller size classes (> 100 ng/(L·h) for the size class 3 µm - 0.8 µm and > 400 ng/(L·h) for the size class 15 µm - 3 µm). The BPP related to particle dry weight showed a larger overlap within the size classes between agricultural and mountain streams compared to the volumetric BPP and again higher median production rates in agricultural streams, except for the finest size class (Figure 6D). No significant difference was found between the stream types in any of the size classes (one-sided Mann-Whitney U tests with Bonferroni-corrected significance level, see Table 5 for *p*- and *W*-values and sample sizes).

Detailed results of comparing the **BPP between the particle size classes** are presented in Appendix 3. The median BPP related to volume was considerably higher in the two small size classes compared to the three larger size classes in both stream types (Figure 6C): the median activity in the size class 3 µm - 0.8 µm was more than 500 times higher than the activity in the three large size classes in mountain and more than 600 times higher in agricultural streams. In the size class 15 µm - 3 µm, the median activity in mountain streams was more than 800 times higher than the activity in the three large size classes and in agricultural streams it was more than 2400 times higher. All activities in the larger size classes > 15 µm were < 0.5 ng/(L·h).

Comparing the BPP in the two small size classes, it was 1.6 times higher in the size class 15 µm - 3 µm compared to the finest size class 3 µm - 0.8 µm in mountain streams and 3.5 times higher in the size class 15 µm - 3 µm in agricultural streams (Wilcoxon signed-rank test, see Appendix 3 for *p*- and *V*-values and sample sizes). The Friedman test comparing the BPP in the three large size classes indicated significant differences between size classes when testing all streams ($p = 0.001148$, *Friedman* $Chi^2 = 6.2$, $df = 2$) and when testing the agricultural streams only ($p = 0.02237$, *Friedman* $Chi^2 = 7.2$, $df = 2$) but the post hoc tests did not confirm significant differences between any of the size classes (Appendix 3). The BPP related to particle dry weight was also noticeably higher in the two small size classes compared to the three larger size classes (Figure 6D). The relative differences were, however, lower compared to

the BPP related to volume. The BPP in the finest size class 3 µm - 0.8 µm was at least 290 times higher in mountain and at least 110 times higher in agricultural streams compared to the three large size classes 500 µm - 100 µm, 100 µm - 50 µm, and 50 µm - 15 µm. Similarly, the BPP in the size class 15 µm - 3 µm was more than 70 times higher than in the three large size classes in mountain and more than 50 times higher in agricultural streams.

In contrast to the BPP related to volume where no significant differences between the two finest size classes were found, the size class 3 µm - 0.8 µm showed 2 to 3.5 times higher activities than the size class 15 µm - 3 µm in relation to particle dry weight. This difference was statistically significant only when including all streams, irrespective of the stream type (Wilcoxon signed-rank test, $p = 0.01563$, $W = 0$; Appendix 3).

Among the three larger size classes, the Friedman test revealed significant differences in BPP related to particle dry weight when considering all streams and only agricultural streams. Across all streams, the activity in the size class 500 µm - 100 µm and 100 µm - 50 µm was higher than in the size class 50 µm - 15 µm but although overall significant, no significant differences between size classes were detected when only considering the agricultural streams (see Appendix 3 for *p*- and *Friedman Chi*^{2}-values and sample sizes).

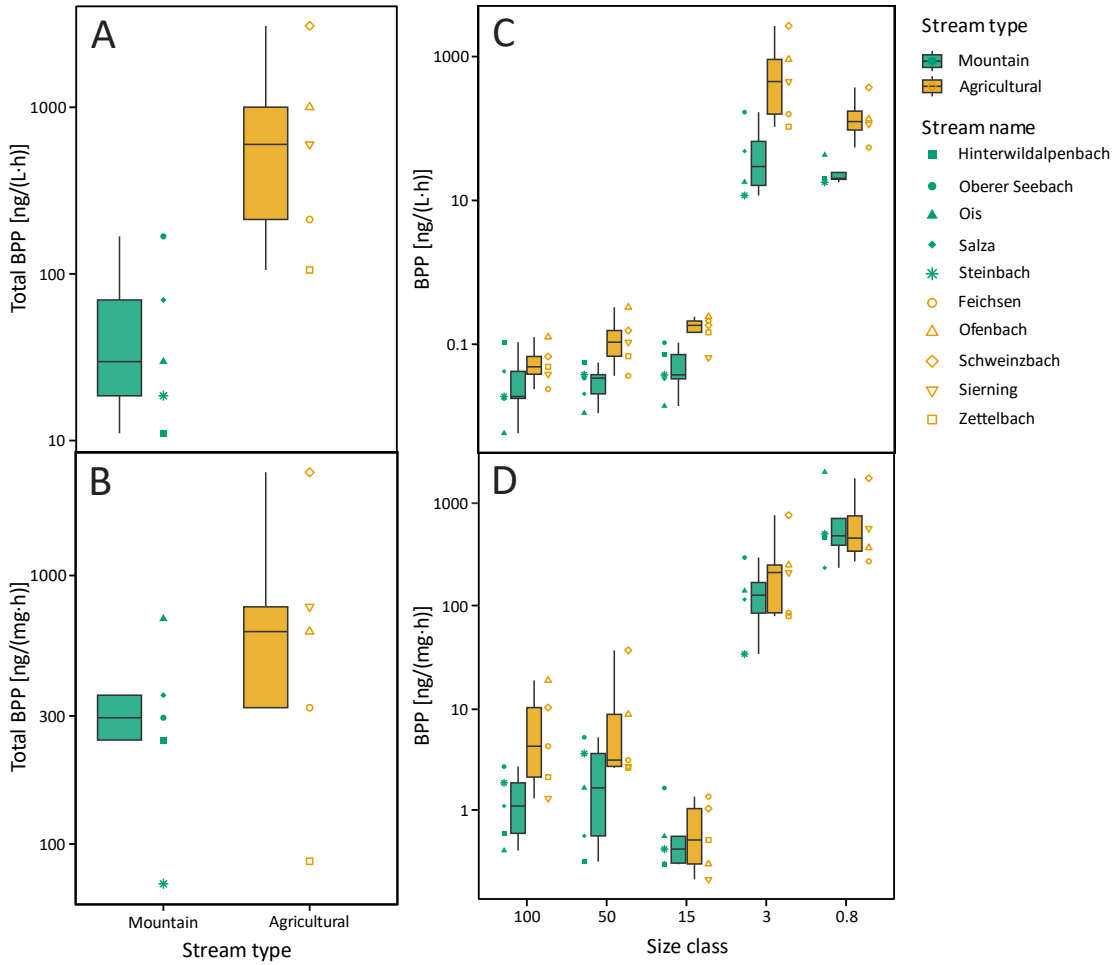

Figure 6: Total (A, B) and size-class specific (C, D) median bacterial protein production rate (BPP) of each stream divided by stream type in relation to water volume (A, C) and particle dry weight (B, D). The boxplots visualise the median of the BPP by stream type or by stream type and size class (horizontal line), the boxes encompass the first to third quartile and the whiskers extend to a maximum of 1.5 times the interquartile range. Outliers are only shown with the individual data points. The x-axis labels refer to the lowest size of each particle size class (e.g. 100 stands for the size class 500 µm - 100 µm) and the y-axis is logarithmically scaled.

Table 5: Total BPP (size class 'all') and BPP in each particle size class, divided by stream type. Median, mean, interquartile range (IQR), and sample size (N) are shown for BPP related to water volume [ng/(L·h)] and BPP related to particle dry weight [ng/(mg·h)]. Additionally, *p*- and *W*-values from comparisons of the total BPP or BPP in each size class between the stream types using one-sided Mann-Whitney U tests are given in the rows of the mountain streams and printed in bold if a significant difference was detected with $p < 0.05$ or $p < 0.01$ after Bonferroni correction. The size class refers to the lowest size of each particle size class (e.g. 100 stands for the size class 500 µm - 100 µm).

Stream type	**Size class**	**Median [ng/(L·h)]**	**Mean [ng/(L·h)]**	**IQR [ng/(L·h)]**	**N**	***p***	***W***
Mountain	all	29.75	59.42	51.19	5	**0.007937**	**1**
Agricultural	all	598.60	999.30	789.50	5		
Mountain	100	0.02	0.04	0.02	5	0.1111	6
	50	0.03	0.03	0.02	5	0.01587	2
	15	0.04	0.05	0.04	5	0.01587	2
	3	33.01	61.38	61.75	4	0.03175	2
	0.8	20.15	25.16	6.23	4	0.01429	0
Agricultural	100	0.05	0.06	0.03	5		
	50	0.11	0.14	0.09	5		
	15	0.18	0.17	0.06	5		
	3	448.08	858.11	752.90	5		
	0.8	124.65	168.49	94.59	4		
Stream type	**Size class**	**Median [ng/(mg·h)]**	**Mean [ng/(mg·h)]**	**IQR [ng/(mg·h)]**	**N**	***p***	***W***
Mountain	all	293.12	329.23	113.43	5	0.1548	7
Agricultural	all	613.50	836.50	439.30	5		
Mountain	100	1.06	1.28	1.22	5	0.02778	3
	50	1.60	2.18	2.93	5	0.1111	6
	15	0.40	0.62	0.24	5	0.5794	13
	3	123.54	141.70	81.63	4	0.3651	8
	0.8	468.44	783.01	465.15	4	0.5571	8
Agricultural	100	4.09	7.04	7.73	5		
	50	2.99	10.39	5.79	5		
	15	0.49	0.66	0.71	5		
	3	204.68	270.13	159.82	5		
	0.8	455.09	721.03	508.24	4		

3.4) Biochemical particle composition and particle quality

3.4.1) POC and PN contents and C/N ratios

First, **agricultural and mountain streams** were compared. The **total POC and PN** content related to water volume (Figure 7A and B) could not be calculated for the mountain stream Steinbach since there were no filter weights available and therefore no POC and PN content could be determined in the size classes 15 µm - 2.7 µm and 2.7 µm - 0.7 µm. Agricultural streams showed on average 2.2 times higher total POC and 2.8 times higher PN contents than mountain streams (Mann-Whitney U test, $p = 0.01587$, $W = 0$, Table 6) with values ranging from 117.5 µg/L POC to 237.5 µg/L in mountain and from 251.5 µg/L POC to 683.7 µg/L in agricultural streams. For PN, the values ranged between 12.18 µg/L and 27.35 µg/L and from 33.31 µg/L to 86.33 µg/L, respectively.

When comparing the two stream types in each of the particle size classes (Figure 7C and D), median **POC and PN** contents related to volume were noticeably higher in agricultural compared to mountain streams in the three smaller size classes, at least two times in the size classes 50 µm - 15 µm and 2.7 µm - 0.7 µm and at least 3 times in the size class 15 µm - 2.7 µm. However, pairwise comparisons between stream types revealed no significant difference in any of the size classes (Mann-Whitney U tests, see Table 6 for *p*- and *W*-values and sample sizes).

In contrast, median POC and PN contents related to particle dry weight [mg/mg] were higher in mountain streams compared to agricultural streams in most size classes with the clearest difference of on average two times higher values in the size class 15 µm - 2.7 µm (Figure 8). Again, pairwise comparisons between stream types detected no significant difference in any size class (Mann-Whitney U tests, see Table 7 for *p*- and *W*-values and sample sizes).

The median **C/N ratio** was higher in mountain streams than in agricultural streams in the four smaller size classes and higher in agricultural streams in the size class 500 µm - 100 µm (Figure 9). It increased continuously with particle size from 7.8 to 20.8 in the agricultural streams while it increased from 8.3 to 19.7 until the size class 100 µm - 50 µm and decreased again to 15.5 in the largest size class in mountain streams. No significant differences between stream types in any of the size classes were detected (Mann-Whitney U tests, *p*- and *W*-values, and sample sizes given in Table 7).

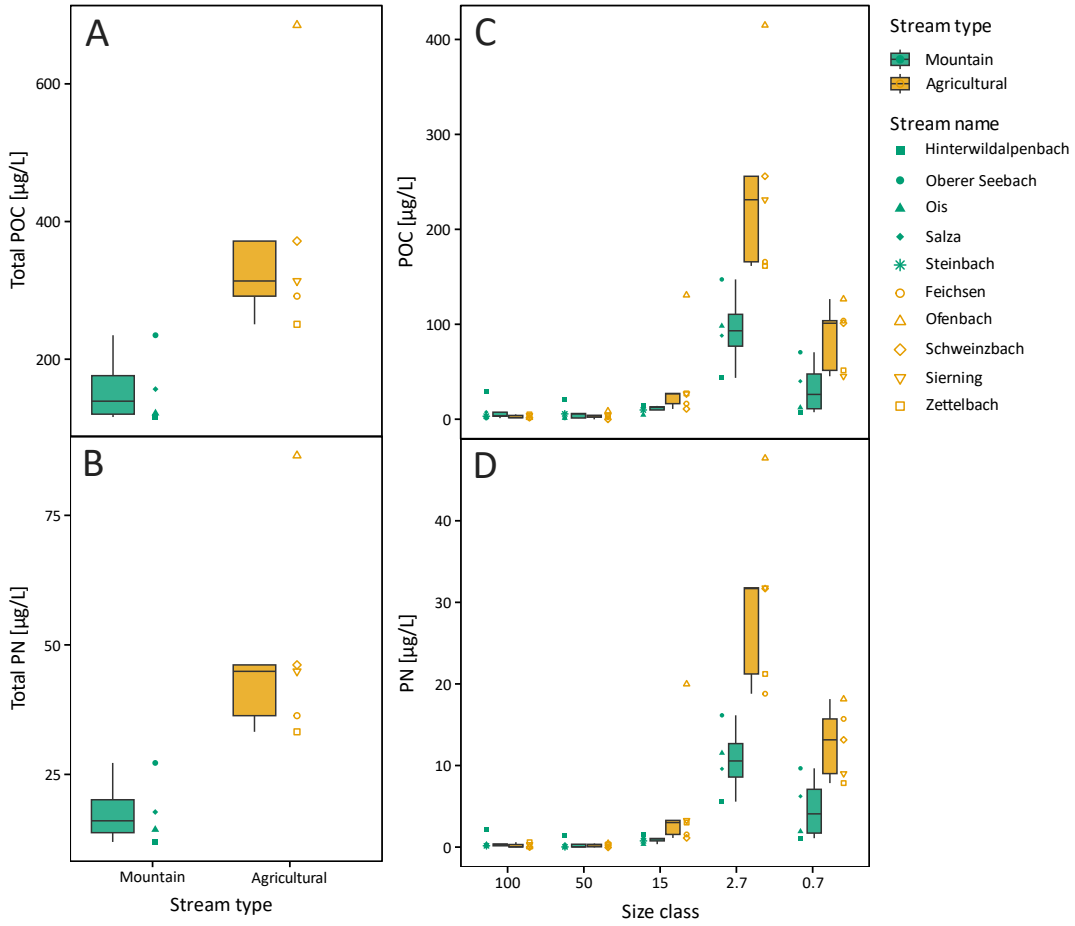

Figure 7: Total (A, B) and size-class specific (C, D) median POC (A, C) and PN (B, D) content of each stream divided by stream type. The boxplots visualise the median POC or PN content by stream type or by stream type and size class (horizontal line), the boxes encompass the first to third quartile and the whiskers extend to a maximum of 1.5 times the interquartile range. Outliers are only shown with the individual data points. The x-axis labels refer to the lowest size of each particle size class (e.g. 100 stands for the size class 500 µm - 100 µm).

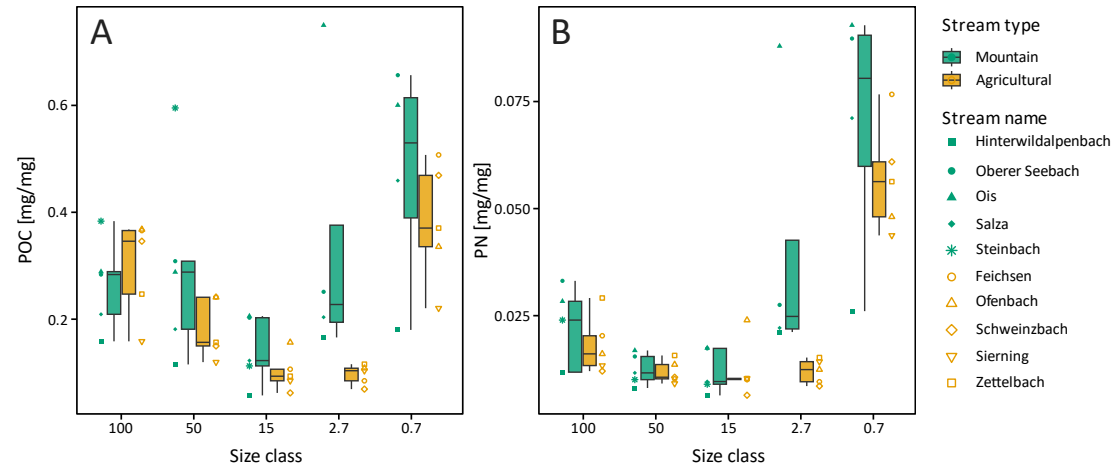

Figure 8: Median POC (A) and PN (B) content related to particle dry weight of each stream divided by size class and stream type. The boxplots visualise the median of the POC or PN content by stream type and size class (horizontal line), the boxes encompass the first to third quartile and the whiskers extend to a maximum of 1.5 times the interquartile range. Outliers are only shown with the individual data points. The x-axis labels refer to the lowest size of each particle size class (e.g. 100 stands for the size class 500 µm - 100 µm).

Table 6: Total POC and PN contents (size class 'all') and POC and PN contents in each particle size class related to water volume, divided by stream type. Median, mean, interquartile range (IQR), and sample size (N) are shown. Additionally, *p*- and *W*-values from comparisons of the total elemental contents or the POC and PN content in each size class between the stream types using two-sided Mann-Whitney U tests are given in the rows of the mountain streams and printed in bold if a significant difference was detected with $p < 0.05$ or $p < 0.01$ after Bonferroni correction. The size class refers to the lowest size of each particle size class (e.g. 100 stands for the size class 500 µm - 100 µm).

Parameter	Stream type	Size class	Median [µg/L]	Mean [µg/L]	IQR [µg/L]	N	*p*	*W*
POC	Mountain	all	140.4	158.5	55.6	4	**0.01587**	**0**
	Agricultural	all	314.1	382.7	79.6	5		
	Mountain	100	4.2	9.5	4.2	5	0.5476	16
		50	6.4	7.6	4.7	5	0.6905	15
		15	13.3	11.5	3.3	5	0.05556	3
		2.7	93.6	94.7	33.4	4	0.01587	0
		0.7	26.8	33.2	36.5	4	0.06349	2
	Agricultural	100	2.5	3.5	2.4	5		
		50	4.2	4.4	2.0	5		
		15	27.5	43.0	10.7	5		
		2.7	231.0	245.7	89.7	5		
		0.7	101.5	86.1	52.1	5		
PN	Mountain	all	16.24	18.00	6.32	4	**0.01587**	**0**
	Agricultural	all	44.92	49.43	9.75	5		
	Mountain	100	0.42	0.71	0.22	5	0.2222	19
		50	0.12	0.46	0.33	5	1	12
		15	1.09	1.04	0.29	5	0.03175	2
		2.7	10.60	10.75	4.08	4	0.01587	0
		0.7	4.15	4.79	5.35	4	0.06349	2
	Agricultural	100	0.12	0.28	0.29	5		
		50	0.38	0.30	0.30	5		
		15	3.09	5.85	1.71	5		
		2.7	31.64	30.19	10.51	5		
		0.7	13.18	12.80	6.67	5		

Table 7: POC and PN contents in each particle size class related to particle dry weight and C/N ratios, divided by stream type. Median, mean, interquartile range (IQR), and sample size (N) are shown. Additionally, *p*- and *W*-values from comparisons of the elemental contents and the C/N ratios between the stream types using two-sided Mann-Whitney U tests are given in the rows of the mountain streams and printed in bold if a significant difference was detected with $p < 0.01$ after Bonferroni correction. The size class refers to the lowest size of each particle size class (e.g. 100 stands for the size class 500 µm - 100 µm).

Parameter	**Stream type**	**Size class**	**Median [mg/mg]**	**Mean [mg/mg]**	**IQR [mg/mg]**	**N**	***p***	***W***
POC	Mountain	100	0.284	0.266	0.079	5	0.8413	11
		50	0.289	0.298	0.126	5	0.3095	18
		15	0.124	0.142	0.090	5	0.3095	18
		2.7	0.229	0.343	0.180	4	0.01587	20
		0.7	0.529	0.474	0.223	4	0.5556	13
	Agricultural	100	0.346	0.298	0.118	5		
		50	0.158	0.183	0.091	5		
		15	0.095	0.103	0.022	5		
		2.7	0.106	0.098	0.023	5		
		0.7	0.371	0.381	0.133	5		
PN	Mountain	100	0.024	0.022	0.016	5	1	13
		50	0.012	0.013	0.005	5	1	13
		15	0.010	0.012	0.008	5	0.6905	10
		2.7	0.025	0.040	0.021	4	0.01587	20
		0.7	0.080	0.070	0.030	4	0.4127	14
	Agricultural	100	0.016	0.018	0.007	5		
		50	0.011	0.012	0.003	5		
		15	0.011	0.012	0.000	5		
		2.7	0.013	0.012	0.005	5		
		0.7	0.056	0.057	0.013	5		
C/N	**Stream type**	**Size class**	**Median**	**Mean**	**IQR**	**N**	***p***	***W***
	Mountain	100	15.5	14.6	5.5	5	0.4206	8
		50	19.7	28.6	6.0	5	0.3095	18
		15	14.2	13.8	1.1	5	0.01587	24
		2.7	9.9	9.8	0.3	4	0.7302	12
		0.7	8.3	8.4	0.7	4	0.5556	13
	Agricultural	100	20.8	21.0	11.4	5		
		50	16.2	17.8	6.5	5		
		15	10.5	10.3	1.7	5		
		2.7	9.4	9.5	1.3	5		
		0.7	7.8	7.8	0.8	5		

The particle quality in terms of POC and PN content and C/N ratio was also compared **between the particle size classes**. Medians, sample sizes, and results of all statistical comparisons are shown in Appendix 4. The **volumetric POC and PN** contents increased from the finest size class to the size class 15 µm - 2.7 µm and were noticeably lower in the three larger size classes. The POC content (Figure 7C) was highest in the size class 15 µm - 2.7 µm in both stream types with maximum values of 147.5 µg/L in mountain and 414.1 µg/L in agricultural streams. Across all streams, it was on average more than three times higher compared to the size class 2.7 µm - 0.7 µm (Wilcoxon signed-rank test, $p = 0.003906$, $V = 45$). POC contents in the size class 15 µm - 2.7 µm compared to 2.7 µm - 0.7 µm were on average more than three times higher in mountain streams and more than two times higher in agricultural streams, however, these differences were not statistically significant. The three larger size classes showed lower POC contents, especially the size classes 500 µm - 100 µm and 100 µm - 50 µm with < 10 µg/L in most streams. In addition, median values for the size class 50 µm - 15 µm were at least two times lower compared to the two finest size classes. Among the three larger size classes, the POC content was on average more than three times higher in the size class 50 µm - 15 µm when considering all streams (Friedman test, $p = 0.00823$, *Friedman Chi*$^2 = 9.6$, $df = 2$). A significant difference was also indicated when only testing the agricultural streams but not confirmed with the post hoc tests (see Appendix 4 for sample sizes and *p*- and *Friedman Chi*^{2}-values).

Similar to the POC content, the volumetric PN content was highest in the size class 2.7 µm - 0.7 µm in both stream types (Figure 7D). When considering all streams, PN was on average two times higher in the size class 15 µm - 2.7 µm than in the size class 2.7 µm - 0.7 µm (Wilcoxon signed-rank test, $p = 0.003906$, $V = 45$). In both stream types, PN contents were on average more than two times higher in the size class 15 µm - 2.7 µm compared to the size class 2.7 µm - 0.7 µm but these differences were not statistically significant. Again, the two largest size classes showed the lowest PN concentrations with median values of < 1 µg/L while it was slightly higher in the size class 50 µm - 15 µm. A significantly higher PN content in the size class 50 µm - 15 µm than in the size class 100 µm - 50 µm was detected when considering all streams. This was not found when mountain and agricultural streams were tested separately although the Friedman test indicated significant differences between some size classes, even when testing only within each stream type (see Appendix 4 for sample sizes and *p*- and *Friedman Chi*^{2}-values).

The **POC and PN contents related to particle dry weight** [mg/mg] also showed similar patterns along the size continuum but these differed from the pattern of the volumetric POC and PN concentrations. The highest POC and PN contents [mg/mg] were found in the size class 2.7 µm - 0.7 µm, they decreased with increasing size until the size class 50 µm - 15 µm and then increased again in mountain streams (Figure 8). In agricultural streams, the size classes 15 µm - 2.7 µm and 50 µm - 15 µm both showed the lowest POC and PN contents. Overall, POC contents ranged from 0.06 mg/mg to 0.75 mg/mg and PN contents from 0.007 mg/mg to 0.093 mg/mg.

When considering all streams, the POC content in the size class 2.7 µm - 0.7 µm was more than three times higher than in the size class 15 µm - 2.7 µm (Wilcoxon signed-rank test, $p = 0.01953$, $V = 3$). The median POC content in the size class 2.7 µm - 0.7 was more than two and three times higher than in the size class 15 µm - 2.7 µm in mountain and agricultural streams, respectively (Wilcoxon signed-rank test, $p = 0.125$, $V = 2$ and $p = 0.0625$, $V = 0$). Among the three larger size classes, the POC content was lower in the size class 50 µm - 15 µm compared to the two largest size classes when testing across all streams (Friedman test, $p = 0.0002249$, *Friedman Chi*$^2 = 16.8$, $df = 2$). No significant differences were detected in mountain streams while the POC content was more than three times lower in the size class 50 µm - 15 µm compared to the size class 500 µm - 100 µm in agricultural streams (see Appendix 4 for sample sizes and *p*- and *Friedman Chi*^{2}-values).

The PN content was highest in the size class 2.7 µm - 0.7 µm in both stream types with values ranging from 0.026 mg/mg to 0.093 mg/mg. The median PN content in this size class was more than four times higher compared to the size class 15 µm - 2.7 µm when including all streams (Wilcoxon signed-rank test, $p = 0.003906$, $V = 0$) and only agricultural streams while it was more than three times higher in mountain streams (see Appendix 4 for sample sizes and *p*- and *V*-values). The lowest PN contents of on average 0.010 mg/mg to 0.013 mg/mg were measured in the size classes 100 µm - 50 µm, 50 µm - 15 µm, and 15 µm - 2.7 µm in agricultural and in the size classes 100 µm - 50 µm and 50 µm - 15 µm in mountain streams. When testing all streams, a higher PN content in the size class 500 µm - 100 µm compared to the size classes 100 µm - 50 µm and 50 µm - 15 µm was revealed (see Appendix 4 for sample sizes and *p*- and *Friedman Chi*^{2}-values).

The **C/N ratio** (Figure 9) increased with size from around 8 in the finest size class to a median value of 19.7 in the size class 100 µm - 50 µm and decreased towards a median value of 15.5 in the largest particle size class in mountain streams. In agricultural streams, a continuous increase with size from around 8 to around 20 was observed. However, no significant differences between size classes were detected in each stream type (see Appendix 4 for sample sizes and test statistics). When analysing all streams, the C/N ratio increased on average by 1.8 from the finest size class to the size class 15 µm - 2.7 µm (Wilcoxon signed-rank test, $p = 0.03906$, $V = 45$). In addition, the C/N ratio increased on average by 5.8 from the size class 100 µm - 50 µm to the size class 50 µm - 15 µm (see Appendix 4 for sample sizes and *p*- and *Friedman Chi*^{2}-values).

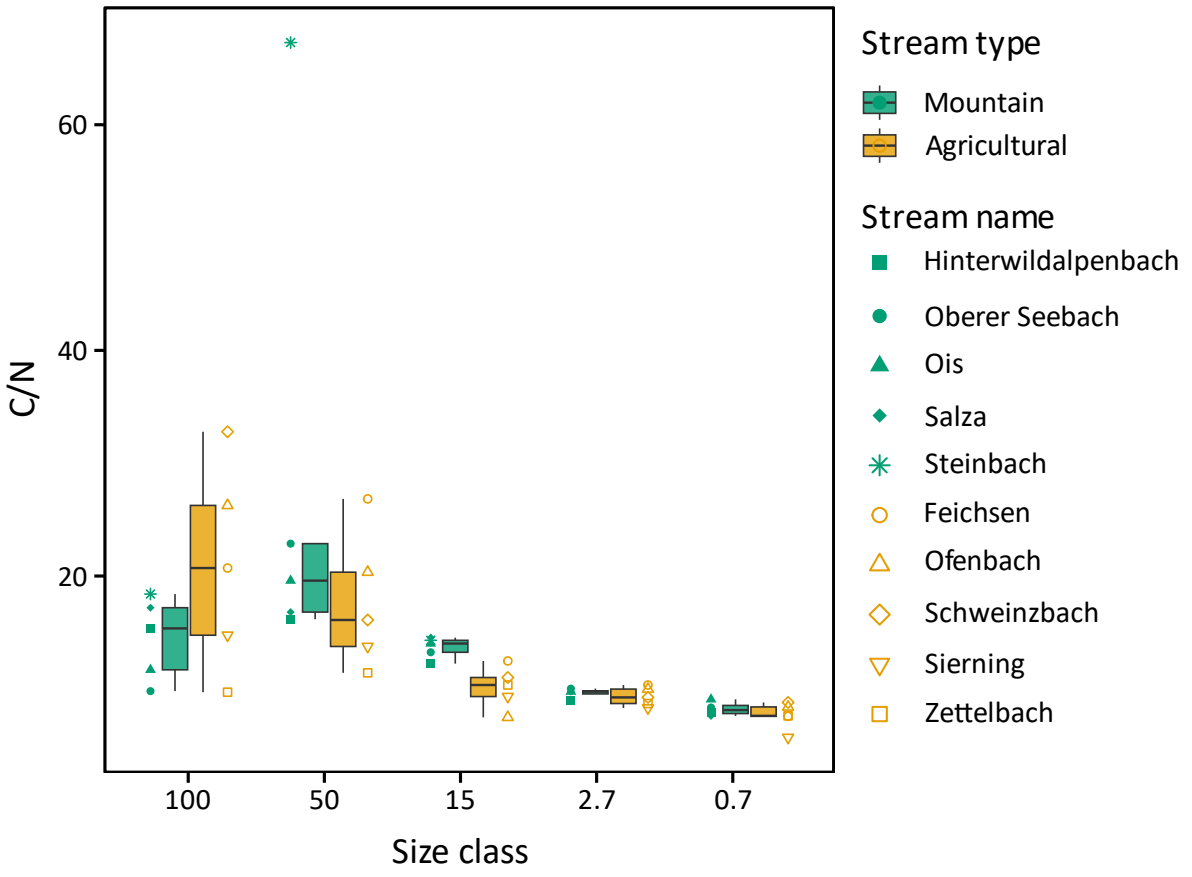

Figure 9: Median molar C/N ratio of each stream divided by size class and stream type. The boxplots visualise the median C/N ratio by stream type and size class (horizontal line), the boxes encompass the first to third quartile and the whiskers extend to a maximum of 1.5 times the interquartile range. Outliers are only shown with the individual data points. The x-axis labels refer to the lowest size of each particle size class (e.g. 100 stands for the size class 500 µm - 100 µm).

3.4.2) $\delta^{13}C$ and $\delta^{15}N$ stable isotope ratios

The isotopic composition of fine particles was analysed to gain information on their origin and source. For $\delta^{15}N$, only values for the three larger size classes were considered due to analytical problems with implausibly high values distributed along a wide range (5‰ to 67‰) in the two smaller size classes. Comparing the stable isotope ratios **between stream types**, $\delta^{13}C$ values ranged from -31.1‰ to -27.2‰ in mountain and from -33.0‰ to -27.7‰ in agricultural streams (Figure 10A, Table 8). The variability was higher in mountain streams in all size classes (IQR ≥ 1.8‰, compared to ≤ 1.7‰ in agricultural streams), especially in the finest size class there was a low variability of 0.2‰ in agricultural streams. Pairwise comparisons in each size class did not reveal any significant differences between the stream types (Table 8).

Contrastingly, $\delta^{15}N$ values differed between stream types (Figure 10B, Table 8) with negative medians of all size classes in mountain streams while they were positive in agricultural streams. The most pronounced differences between stream types were found in the size class 50 µm - 15 µm, where the median $\delta^{15}N$ values in agricultural streams exceeded the ones in mountain streams by 4.7‰ (Mann-Whitney U test, $p = 0.007937$, $W = 0$). They were higher by 5.7‰ and 3‰ in the size classes 100 µm - 50 µm and 500 µm - 100 µm, respectively, in agricultural streams (see Table 8 for *p*- and *W*-values).

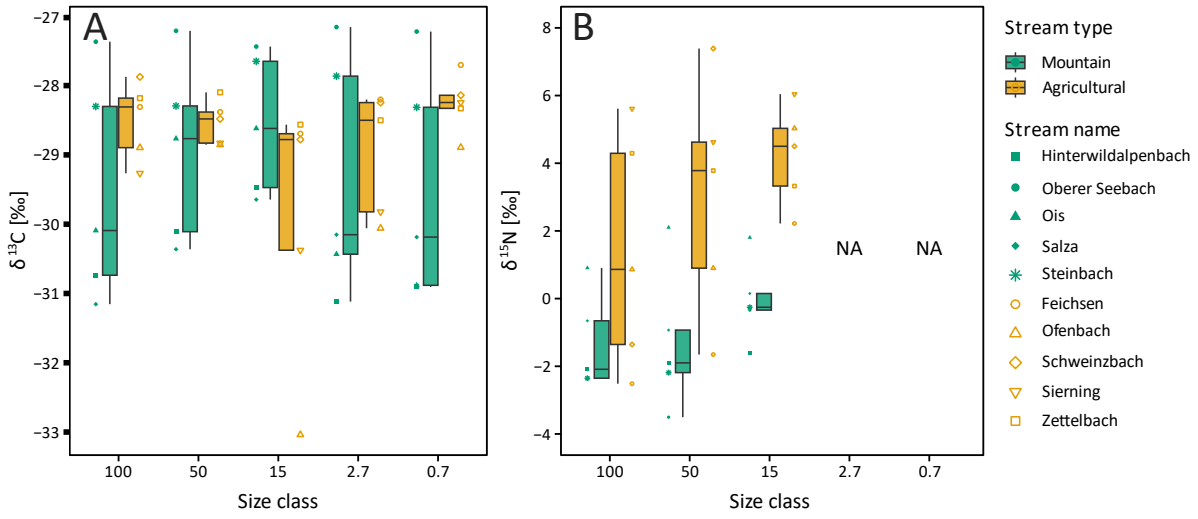

Figure 10: Median $\delta^{13}C$ (A) and $\delta^{15}N$ value (B) of each stream divided by size class and stream type. For $\delta^{15}N$, the data for the size classes 15 µm - 2.7 µm and 2.7 µm - 0.7 µm were not available (NA) due to analytical problems. The boxplots visualise the median δ values by stream type and size class (horizontal line), the boxes encompass the first to third quartile and the whiskers extend to a maximum of 1.5 times the interquartile range. Outliers are only shown with the individual data points. The x-axis labels refer to the lowest size of each particle size class (e.g. 100 stands for the size class 500 µm - 100 µm).

Table 8: $\delta^{13}C$ and $\delta^{15}N$ values in each particle size class divided by stream type. For $\delta^{15}N$, the data for the size classes 15 µm - 2.7 µm and 2.7 µm - 0.7 µm were not available due to analytical problems. Median, mean, interquartile range (IQR), and sample size (N) are shown. Additionally, *p*- and *W*-values from comparisons between the stream types using two-sided Mann-Whitney U tests are given in the rows of the mountain streams and printed in bold if a significant difference was detected with $p < 0.01$ after Bonferroni correction. The size class refers to the lowest size of each particle size class (e.g. 100 stands for the size class 500 µm - 100 µm).

Parameter	Stream type	Size class	Median [‰]	Mean [‰]	IQR [‰]	N	*p*	*W*
$\delta^{13}C$	Mountain	100	-30.1	-29.5	2.4	5	0.4206	8
		50	-28.8	-29.0	1.8	5	0.8413	11
		15	-28.6	-28.6	1.8	5	0.3095	18
		2.7	-30.2	-29.3	2.6	5	0.6905	10
		0.7	-30.2	-29.5	2.6	5	0.3095	7
	Agricultural	100	-28.3	-28.5	0.7	5		
		50	-28.5	-28.5	0.4	5		
		15	-28.8	-29.9	1.7	5		
		2.7	-28.5	-29.0	1.6	5		
		0.7	-28.3	-28.3	0.2	5		
$\delta^{15}N$	Mountain	100	-2.1	-1.3	1.7	5	0.4206	8
		50	-1.9	-1.3	1.3	5	0.05556	3
		15	-0.2	0.0	0.5	5	**0.007937**	**0**
	Agricultural	100	0.9	1.4	5.6	5		
		50	3.8	3.0	3.7	5		
		15	4.5	4.2	1.7	5		

The stable isotope ratios were subsequently compared **between size classes**. Because of significant differences in $\delta^{15}N$ values between mountain and agricultural streams, the size classes were only compared within stream types while they were analysed for all streams and separately for each stream type for the $\delta^{13}C$ values. The $\delta^{13}C$ values showed a large variability and overlap between size classes in mountain streams, no significant differences were detected between any of the size classes in this stream type and when considering all streams (Appendix 5). When analysing agricultural streams, the variability was noticeably lower in the size classes 2.7 µm - 0.7 µm, 100 µm - 50 µm and 500 µm - 100 µm although all median $\delta^{13}C$ values ranged around -28‰ (Figure 10A). The Friedman test indicated a significant difference among the three large size classes in agricultural streams which was not confirmed by post hoc tests (Appendix 5). For $\delta^{15}N$, there seems to be a decrease with increasing size, especially in agricultural streams (Figure 10B). However, no significant differences between size classes were observed in both stream types (Appendix 5).

The median $\delta^{13}C$ values were plotted against the corresponding median C/N ratio for all streams and size classes where a correct sample weight was available (N = 48) to obtain additional information on the particle sources (Figure 11). For an easier attribution to potential sources, typical $\delta^{13}C$ and C/N ranges of organic inputs to streams according to Lamb et al. (2006) were added to the figure. Most mountain streams showed lower C/N ratios (< 20) along a wider range of $\delta^{13}C$ values (-27‰ to -31‰) compared to agricultural streams where the range of C/N values was larger (6 to 33) but most $\delta^{13}C$ values varied from -28‰ to -30‰. In mountain streams, the $\delta^{13}C$ values seemed to be dependent on the stream with more enriched values in the streams Oberer Seebach and Steinbach, more depleted

values in the streams Salza and Hinterwildalpenbach, and variable values in the stream Ois. Outliers were detected in the particle size class 100 µm - 50 µm in the mountain stream Steinbach with a C/N ratio of 67.1 (not displayed in Figure 11) and the size class 2.7 µm - 0.7 µm in the agricultural stream Ofenbach with a low C/N ratio of 7.7 and the most depleted $\delta^{13}C$ value of -33‰. Values of both stream types were predominantly located in the range of values from freshwater DOC which partly overlapped with values from freshwater POC and algae (Figure 11). One data point could be assigned to bacteria as a potential particle source because of a comparatively low C/N ratio of 6 (agricultural stream Sierning, 2.7 µm - 0.7 µm) and another was only located in the range of C_3 terrestrial plants due to a high C/N ratio of 33 (agricultural stream Schweinzbach, 500 µm - 100 µm). None of the values were overlapping with the range of C_4 terrestrial plants.

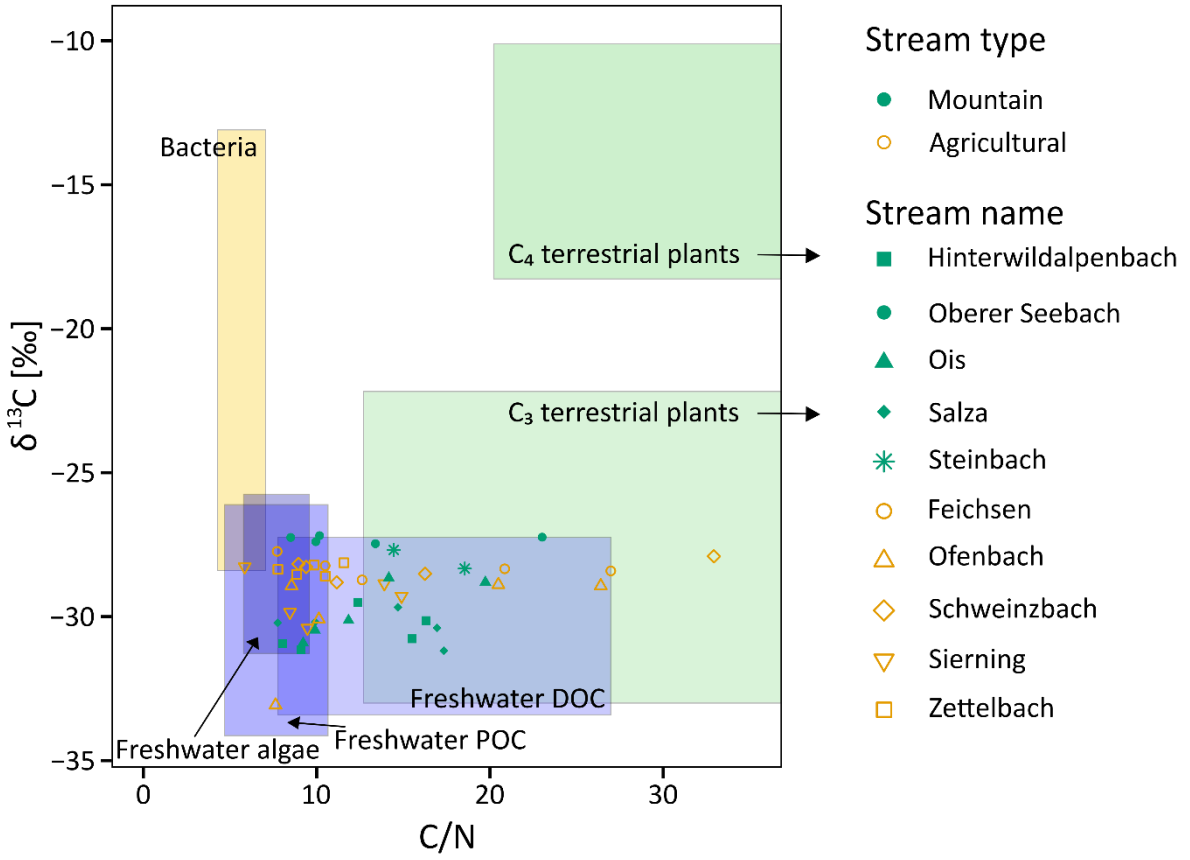

Figure 11: Median values of the $\delta^{13}C$ values of all size classes in all streams plotted against their corresponding median C/N ratio (N= 48). One exceptionally high C/N ratio of 67.1 is excluded from the figure (size class 100 µm - 50 µm of the mountain stream Steinbach) by restricting the x-axis limit to 35. In addition, typical $\delta^{13}C$ and C/N ranges of organic inputs to streams are included (adapted from Lamb et al. (2006)).

3.4.3) Fatty acid composition

Fatty acids were analysed as another indicator of particle quality. **Comparing stream types, total lipid** concentrations summed across all particle size classes were on average more than three times higher in agricultural than in mountain streams (Mann-Whitney U test, $p = 0.007937$, $W = 0$; Figure 12A). They ranged from 18.0 µg/L to 43.3 µg/L in mountain and from 53.1 µg/L to 163.6 µg/L in agricultural streams. Divided into size classes, the total lipid concentrations were < 10 µg/L in the three largest size classes except in the agricultural stream Ofenbach (44 µg/L in the size class 50 µm - 15 µm). The largest fraction of the total lipids occurred in the two finest size classes. Concentrations ranged up to 20 µg/L for mountain streams and were on average almost four times lower than in agricultural streams in the size class 15 µm - 2.7 µm (Mann-Whitney U test, $p = 0.007937$, $W = 0$). In agricultural streams, total lipid concentrations ranged from 29.6 µg/L to 132.4 µg/L in the size class 15 µm - 2.7 µm and from 15.1 µg/L and 27.4 µg/L in the size class 2.7 µm - 0.7 µm (Table 9, Figure 12B).

Comparing total lipid concentrations **between size classes** (Appendix 6), no significant differences were detected between the two small size classes in either of the stream types. Nevertheless, total lipid concentrations were on average more than twice as high in the size class 15 µm - 2.7 µm compared to the finest size class in agricultural streams (Wilcoxon signed-rank test, $p = 0.0625$, $V = 10$). Also, no significant differences were revealed among the three larger size classes although the Friedman test showed a significant difference between some size classes in agricultural streams. This was, however, not confirmed by post hoc tests (see Appendix 6 for sample sizes, *p*- and *Friedman Chi*^{2}-values).

A fraction of the total lipids was converted to fatty acid methyl esters (FAMEs) which were analysed by GC. The proportion of FAMEs, expressed as a percentage of total lipids, ranged from 8.7% to 53.5% with a median value of 22.0%. When the concentrations and proportions of fatty acids (FAs) are examined below, this refers to the concentrations and proportions of their FAMEs.

Concentrations of the sum of bacterial fatty acids (**BFA**) as a proxy for the bacterial biomass were compared **between stream types** (Figure 12C, D, Table 9). The total BFA concentration summed across all particle size classes ranged from 0.44 µg/L to 1.01 µg/L in mountain streams. In agricultural streams, it ranged from 1.74 µg/L to 4.17 µg/L and was on average four times higher than in mountain streams (one-sided Mann-Whitney U test, $p = 0.003968$, $W = 0$). The highest concentrations of BFA were found in the two smaller size classes and in agricultural streams, especially in the size class 15 µm - 2.7 µm (Figure 12D). In this size class, median BFA concentrations were 1.94 µg/L while they were 0.99 µg/L in the size class 2.7 µm -0.7 µg/L. In mountain streams, the median BFA concentrations in the two small size classes were 0.38 µg/L and 0.33 µg/L, respectively (Table 9). Thus, they were five times and three times lower than in agricultural streams (one-sided Mann-Whitney U test, $p = 0.003968$, $W = 0$ for both size classes). Much lower concentrations of < 0.1 µg/L occurred in the three larger size classes in mountain streams while they were ≤ 0.12 µg/L in agricultural streams in the two largest size classes. The BFA concentrations in the size class 50 µm - 15 µm showed intermediate values of up to 1.04 µg/L in agricultural streams and were on average two times higher than in mountain streams (one-sided Mann-Whitney U test, $p = 0.007937$, $W = 1$). No differences between stream types were found in the two larger size classes with low BFA concentrations in both stream types (Table 9).

Finally, BFA concentrations were compared **between size classes** within each stream type (Appendix 6) No significant difference between the BFA concentrations in the two small size classes in either stream type was found although they were twice as high in the size class 15 µm - 2.7 µm compared to the finest size class in agricultural streams. Comparing the three large size classes, the Friedman test

revealed significant differences among some size classes in both stream types which were not confirmed by post hoc tests. As pointed out before, the main difference occurred between the two small and the three large size classes which were not statistically compared due to the different methods of sample collection.

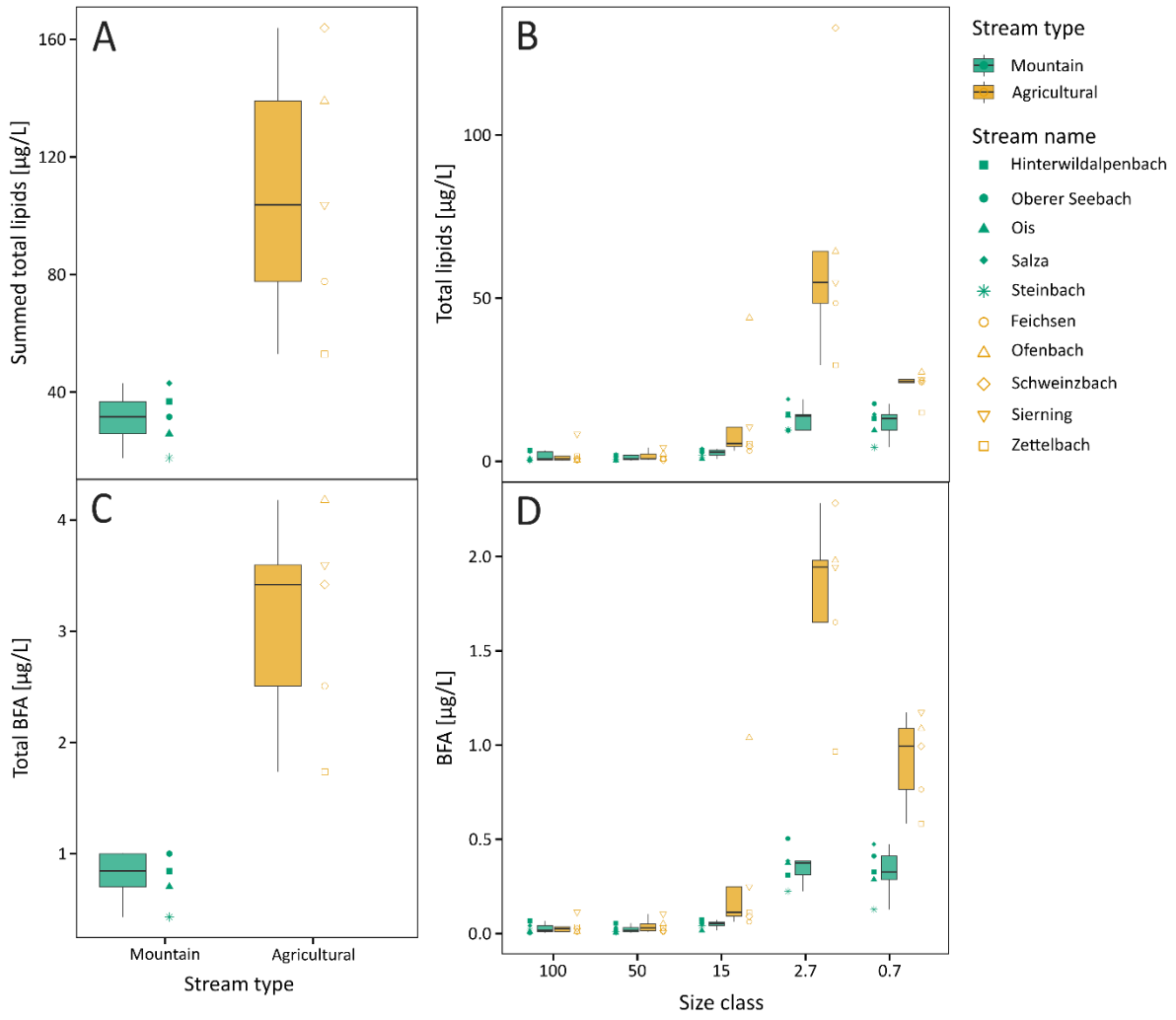

Figure 12: Summed (A, C) and size-class specific (B, D) median concentration of total lipids (A, B) and bacterial fatty acids (BFA, sum of concentrations of: iso-15:0, anteiso-15:0, 15:0, iso-16:0, iso-17:0, 16Δ9,10, 17:0, 17:1n-7, 18Δ9,10, 18:1n-6, and 18:1n-7; C, D) of each stream divided by stream type. The boxplots visualise the median total lipid or BFA concentration by stream type or by stream type and size class (horizontal line), the boxes encompass the first to third quartile and the whiskers extend to a maximum of 1.5 times the interquartile range. Outliers are only shown with the individual data points. The x-axis labels refer to the lowest size of each particle size class (e.g. 100 stands for the size class 500 µm - 100 µm).

Table 9: Summed total lipid and BFA concentration (size class 'all') and total lipid and BFA concentration in each particle size class divided by stream type. Median, mean, interquartile range (IQR), and sample size (N) are shown. Additionally, *p*- and *W*-values from comparisons between the stream types using two-sided (for total lipids) and one-sided (for BFA) Mann-Whitney U tests are given in the rows of the mountain streams and printed in bold if a significant difference was detected with $p < 0.05$ or $p < 0.01$ after Bonferroni correction. The size class refers to the lowest size of each particle size class (e.g. 100 stands for the size class 500 µm - 100 µm).

Parameter	Stream type	Size class	Median [µg/L]	Mean [µg/L]	IQR [µg/L]	N	*p*	*W*
Total lipids	Mountain	all	31.9	31.3	11.0	5	**0.003968**	**0**
	Agricultural	all	103.7	107.4	61.1	5		
	Mountain	100	0.9	1.8	2.6	5	1	13
		50	0.9	1.3	1.4	5	0.4206	8
		15	3.1	2.7	1.6	5	0.03175	2
		2.7	14.1	13.5	4.7	5	**0.007937**	**0**
		0.7	13.3	12.0	4.9	5	0.01587	1
	Agricultural	100	1.0	2.5	1.2	5		
		50	1.0	1.9	1.5	5		
		15	5.6	13.7	5.8	5		
		2.7	54.8	65.9	15.8	5		
		0.7	24.7	23.3	1.0	5		
BFA	Mountain	all	0.85	0.80	0.30	5	**0.007937**	**0**
	Agricultural	all	3.42	3.08	1.08	5		
	Mountain	100	0.02	0.03	0.03	5	0.5	12
		50	0.02	0.03	0.02	5	0.2738	9
		15	0.06	0.05	0.02	5	**0.007937**	**1**
		2.7	0.38	0.36	0.07	5	**0.003968**	**0**
		0.7	0.33	0.33	0.12	5	**0.003968**	**0**
	Agricultural	100	0.03	0.04	0.03	5		
		50	0.03	0.05	0.04	5		
		15	0.12	0.31	0.16	5		
		2.7	1.94	1.76	0.33	5		
		0.7	0.99	0.92	0.32	5		

In total, 43 single FAs were detected across all samples. After calculating median concentrations for each size class in each stream, 42 FAs were present (neuronic acid, 24:1n-9, was only present in one sample) of which 11 occurred in all samples. 14 FAs had mean concentrations of > 0.05 µg/L and were defined as major components, ten of these were present in all samples. The SFA palmitic acid (16:0) and stearic acid (18:0) as well as the MUFA palmitoleic acid (16:1n-7) had the highest mean concentrations of 0.67 µg/L, 0.346 µg/L, and 0.324 µg/L, respectively (Appendix 7). From the most abundant fatty acids (maximum ≥ 5%, expressed as percentage of total FAME), again palmitic, stearic, and palmitoleic acid were the most abundant FAs (Appendix 7). 15 FAs had a maximum proportion of ≥ 5%, including all FAs defined as major components above and arachidonic acid (ARA, 20:4n-6).

A PCA of the relative proportions [% of total FAME] of the 15 most abundant single FAs showed a separation according to size class but not between stream types (Figure 13A). The differences in fatty acid profiles between size classes could, however, not be explicitly linked to biomarkers for certain groups of organisms. PC1 accounted for 50.9% of the variation and separated the three large particle size classes from the size class 15 µm - 2.7 µm. The finest particle size class showed a large scatter and an overlap with the other size classes. The large particles displayed negative values along PC1, which was negatively correlated with the FAs 16:0 (correlation coefficient = -0.35), 18:0 (-0.33) and 20:3n-6 (-0.31). Palmitic and stearic acid (16:0 and 18:0) are fungal biomarkers but LIN (18:2n-6, 0.27) as another fungal biomarker was positively correlated with PC1. The diatom biomarker 16:1n-7 (palmitoleic acid) was also positively correlated with PC1 (0.23). PC2 explained 15.5% of the total variation and was mainly negatively correlated with DHA (22:6n-3, -0.44). Also, ALA (18:3n-3, -0.36), ARA (20:4n-6, -0.33), EPA (20:5n-3, -0.31), and stearidonic acid (18:4n-3, -0.29) showed negative correlations while oleic acid (18:1n-9; 0.40) was positively correlated with PC2. All n-3 PUFA, which are algal biomarkers, were negatively correlated with PC2, and they were mainly present in some agricultural streams in the size classes 50 µm - 15 µm and 15 µm - 2.7 µm and in this size class also in some mountain streams.

In the PCA of the relative proportions of FA groups (SFA, MUFA, n-3 PUFA, n-6 PUFA, and BFA), systematic differences between size classes were observed as well (Figure 13B). PC1 explained 54.9% of the variation and was positively associated with the proportion of SFA (correlation coefficient = 0.53) while it was negatively associated with MUFA (-0.54) and BFA proportions (-0.52). The two largest size classes showed positive values of PC1 while the two finest size classes predominantly displayed negative values of PC1. The size class 50 µm - 15 µm showed an overlap with the larger size classes along PC1 for mountain streams whereas it rather overlapped with the smaller particles in agricultural streams. PC2 explained 24.9% of the variation and was mainly affected by the proportion of n-3 PUFA (0.84). The highest values along PC2 were found in the size classes 50 µm - 15 µm and 15 µm - 2.7 µm of agricultural streams.

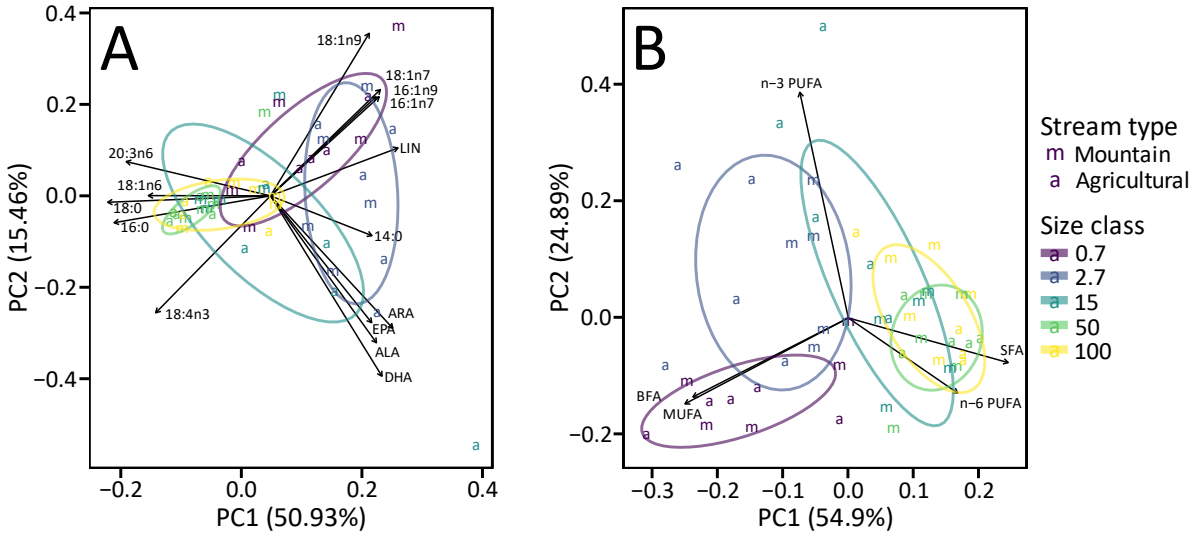

Figure 13: PCAs based on relative proportions of FAs of total FAME, showing a separation by the most abundant single FAs (≥ 5% of total FAME; A) and by FA groups (SFA, MUFA, n-3 PUFA, n-6 PUFA, and BFA; B). The letters m and a represent mountain and agricultural streams and colours indicate the different size classes.

SFA accounted for the largest proportion of total FAME in both stream types in all size classes, followed by MUFA and then n-6 PUFA, n-3 PUFA, and BFA with slight variations depending on the size class (Figure 14). The proportion of SFA was generally lower in the two finest size classes, about 50% in mountain and about 45% in agricultural streams, while it increased to 60% in the larger size classes. The MUFA showed an opposite pattern with higher proportions in the finest size classes (around 30%) and lower proportions (< 20%) in the larger size classes. The proportion of n-6 PUFA was slightly lower in the two finest size classes (around 10%) than in the larger size classes. The n-3 PUFA content was lowest in the finest size class and the two largest size classes (< 9%). A difference between the two stream types was evident, as the highest proportion of n-3 PUFA was found in the size class 15 µm - 2.7 µm in mountain (16%) and in the size class 50 µm - 15 µm (16%) in agricultural streams. The BFA showed a pattern comparable to the MUFA, with the lowest proportions (< 9%) in the three larger size classes and higher proportions of around 15% in the finest size class in both stream types and in the size class 15 µm - 2.7 µm in agricultural streams. In mountain streams, this size class had an intermediate BFA content of 10% (Figure 14A).

Another difference between stream types was the FA proportions in the size class 50 µm - 15 µm, which differed from the two largest size classes in agricultural streams, while they were similar to the larger size classes in mountain streams. In agricultural streams, this size class showed a higher proportion of MUFA and n-3 PUFA and a lower proportion of SFA and n-6 PUFA compared to the two large size classes (Figure 14B).

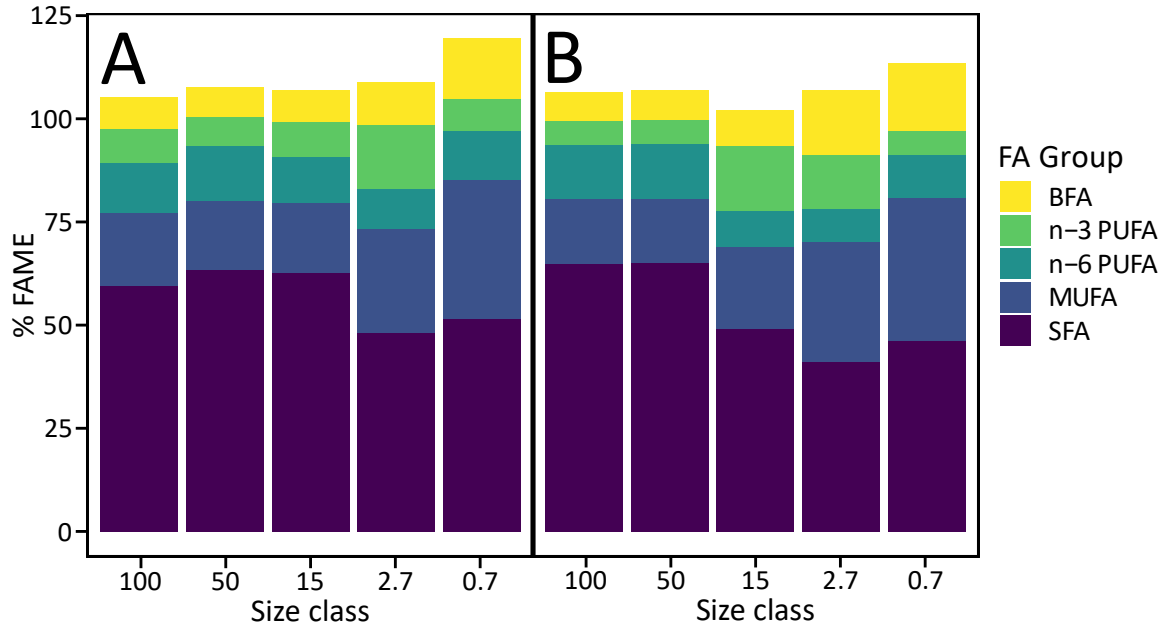

Figure 14: Stacked bar charts showing the median proportions of FA groups per size class for mountain (A) and agricultural streams (B), expressed as percentage of total FAME. The FA groups shown include SFA, MUFA, n-3 and n-6 PUFA, and BFA. As the median proportions of the different FA groups do not necessarily originate from the same sample, the proportions of SFA, MUFA, and PUFA do not add up to 100%. The x-axis labels refer to the lowest size of each particle size class (e.g. 100 stands for the size class 500 µm - 100 µm).

4) Discussion

This study revealed differences in microbial activities on FPM from 500 µm to 0.7 µm size between stream types with higher activities measured in agricultural compared to mountain streams. However, the biochemical particle composition did not generally differ between the stream types across all size classes. Furthermore, the finest particles (< 15 µm) of the investigated FPM size continuum showed the highest microbial activities independent of the stream type. The differences in particle composition were more pronounced between size classes than between stream types, lower C/N ratios and higher proportions of BFA indicated an increased microbial biomass on finer particles. This implies that irrespective of stream type, the cycling of FPM-attached organic matter predominantly takes place on the finest particles, stressing their relevance for C cycling in streams.

4.1) Differences between stream types

4.1.1) Higher FPM-attached microbial activities in agricultural streams.

The total bacterial production per volume measured on FPM from 0.8 µm to 500 µm size was 20 times higher in agricultural than in mountain streams, corresponding to the expectation of a higher FPM-attached prokaryotic productivity in agricultural streams.

The amount of FPM was in total almost four times higher in agricultural streams than in mountain streams and mainly composed of FPM from 2.7 µm to 15 µm size. It relativises differences between stream types when relating the analysed parameters such as bacterial production and POC and PN contents to FPM dry weight instead of water volume. Therefore, no significant differences between stream types were detected when assessing bacterial production per particle dry weight. Nevertheless, median values of total and size-specific bacterial production rates per particle dry weight were still higher in agricultural streams. This difference persists because the total FPM concentrations in agricultural streams were only four times higher than in mountain streams, while the total volumetric BPP was 20 times higher. In this study, agricultural streams are therefore assumed to show a higher microbial activity per unit FPM, suggesting that other factors than the FPM amount are driving FPM-attached microbial activities.

In FPM of stream sediments, POC, PN, and protein content showed a strong positive correlation with bacterial production rates and bacterial abundance (Fischer et al., 2002). On differently sized POM originating from terrestrial plants and green algae, total phosphorus and cellulose content were positively correlated to microbial respiration rates (Yoshimura et al., 2010). However, in this study median relative POC and PN contents [mg/mg] were higher in mountain than in agricultural streams for most size classes although they differed not significantly from each other. FPM in mountain streams contained 21.0% ± 17.1% OC and 1.8% ± 1.6% N (median ± IQR) compared to 15.8% ± 22.8% OC and 1.4% ± 1.4% N (median ± IQR) in FPM of agricultural streams. In contrast, volumetric POC and PN contents were two and three times higher in agricultural compared to mountain streams, respectively. Due to the four times larger amount of FPM found in the agricultural streams, the POC and PN contents overall indicate a higher proportion of OM in the studied mountain streams compared to the agricultural streams. A higher proportion of OM in FPM in forested streams has been attributed to its origin from CPOM processing while a higher inorganic content in FPM of agricultural streams was related to high mineral contents and increased soil erosion in agriculturally used soils (Gurtz et al., 1980; Kirkels et al., 2014; Wild et al., 2019).

In addition to the nutritional quality and biochemical composition of the substrate, environmental characteristics can affect the FPM-attached microbial activity (Kothawala et al., 2021) and can be a

reason for the higher microbial activity observed in agricultural streams compared to mountain streams. Elevated dissolved nutrient levels increased microbial respiration rates on leaves and wood (Stelzer et al., 2003) as well as on benthic CPOM and FPOM from North American headwater streams (Tant et al., 2013). In addition, POM-associated microbes were found to rely on dissolved nutrients rather than on nutrients associated with their substrate in nutrient-rich environments (Yoshimura et al., 2010). Higher nutrient availability in agricultural streams is generally associated with increased microbial activity and biomass on FPOM and CPOM (Lu, Canuel, et al., 2014; Tant et al., 2013) as well as on DOC (Reche et al., 1998). Indeed, nitrate, ammonium, and SRP concentrations in the studied agricultural streams were on average 2.7, 1.8, and more than 100 times higher than in the mountain streams. Enhanced microbial activity can further be linked to higher water temperatures, which are an important driver of bacterial community structure and metabolic activity in streams (e.g. Adams et al., 2015) and measured water temperatures were on average more than 5 °C higher in agricultural than in mountain streams.

The differences in heterotrophic microbial activity between stream types could also be due to differences in the total number or biomass of bacteria. Here, BFA were assessed as a proxy for the bacterial biomass. However, the total BFA concentrations were only four times higher in agricultural streams than in mountain streams, which corresponds to the difference in FPM concentration and implies that the number of bacteria per particle dry weight was similar in the different stream types. This in turn indicates a higher cell-specific activity of the bacteria on FPM in agricultural streams, which could be stimulated by higher external nutrient levels or temperatures in these streams as discussed above.

When relating the total bacterial carbon production (BCP) per day to the amount of OC on FPM, a higher relative C turnover in the studied agricultural streams is confirmed. About 0.4% of the fine POC pool in mountain streams was utilised by bacteria per day while in agricultural streams it was almost nine times as much (3.9%), resulting in a total POC turnover time of about 227 days and 25 days, respectively. In North America, about 10 days turnover time were estimated for suspended POC in a 3rd order stream dominated by agricultural land use (Richardson et al., 2013). In addition, POC half-lives of 17 ± 3 days (mean ± SE) were reported in boreal inland waters (Attermeyer et al., 2018), which corresponds to the POC turnover in the studied agricultural streams. The total POC turnover time of 227 days calculated for the mountain streams is still faster than the half-life of 202 ± 261 days estimated for OC in rivers based on 46 field studies and laboratory experiments (Catalán et al., 2016), which emphasises the relevance of fine FPM turnover for C cycling in streams.

4.1.2) No general differences in FPM composition between stream types.

Regarding the biochemical particle composition, a higher biomass of autotrophic algae and heterotrophic bacteria in FPM in agricultural streams was hypothesised. Using the combination of C/N ratios, bulk stable isotopes, and fatty acid composition, the contributions of different OM sources to the FPM pool can be assessed.

Lower C/N ratios can indicate a higher proportion of algal-derived FPM since algae have C/N ratios between 4 and 10 whereas terrestrially derived OM has C/N ratios greater than 20 (Meyers, 1994). Higher C/N ratios indicating higher contributions of terrestrial OM have been shown in a study comparing first-order streams with forested catchments to streams affected by human land use in the USA (Lu, Bauer, et al., 2014). However, the C/N ratios in this study did not significantly differ between the two stream types in any of the size classes. Lower median C/N ratios in agricultural streams were

detected in four of the five size classes but the slight differences between stream types did neither suggest that C/N ratios reflect a higher contribution of algae to FPM in the agricultural streams nor a higher contribution of terrestrial OM to FPM in the mountain streams.
Similar to the results presented here, the study by Lu, Bauer, et al. (2014) found a range of $\delta^{13}C$ values between -33.3‰ and -27.6‰ and no differences in $\delta^{13}C$ values between streams with different land uses in their catchment area. The most depleted $\delta^{13}C$ value of -33‰ was measured in the agricultural stream Ofenbach in the size class 50 µm - 15 µm and indicates predominantly phytoplankton-derived FPM since only phytoplankton as one of the potential sources of POM in streams shows $\delta^{13}C$ values more depleted than -32‰ (Ogrinc et al., 2008). Due to largely overlapping $\delta^{13}C$ values of OM derived from soils, terrestrial plants, phytoplankton, and heterotrophic bacteria (Ogrinc et al., 2008; Schidlowski et al., 1983), no further conclusions can be drawn about the FPM composition based on $\delta^{13}C$ values. Similarly, there is a wide range and overlap of $\delta^{15}N$ values of different POM sources in streams (Ogrinc et al., 2008).
In addition, higher relative proportions of n-3 PUFA in the FA composition of FPM imply a greater proportion of algae (Guo et al., 2016). Nevertheless, a higher relative proportion of n-3 PUFA in FPM from agricultural compared to mountain streams was only found in the size class 50 µm - 15 µm, and proportions were similar between stream types for the other size classes. An overall higher contribution of algal-derived FPM in agricultural streams can be linked to the differences in stream water chemistry and morphology since increased water temperature and elevated nutrient concentrations (Lu, Canuel, et al., 2014), as well as reduced flow velocities (Ghosh & Gaur, 1998), can enhance autotrophic production in streams. In this study, both higher water temperatures and on average four times lower mean flow velocities were measured in the agricultural streams. In addition, on average two times higher chlorophyll *a* concentrations were measured in the agricultural streams, which indicate a higher abundance of algae compared to the mountain streams. Therefore, the environmental characteristics would explain and indicate a larger contribution of algal material to the FPM in agricultural compared to mountain streams, but the assessed biomarkers did not point towards a general difference between the two stream types across all size classes.

Not only algal, but also bacterial biomass is generally enriched in N relative to bulk OM and can also explain low C/N ratios (Akamatsu et al., 2011). Since the C/N ratio did not differ significantly between stream types in this study, it does not indicate a higher contribution of bacterial biomass to FPM in agricultural compared to mountain streams as expected. Heterotrophic microbes are furthermore enriched in ^{15}N compared to bulk OM (Rowland et al., 2017) and median values of $\delta^{15}N$ were more enriched in agricultural (0.9‰ to 4.5‰) compared to mountain streams (-2.1‰ to -0.2‰) in this study. This may suggest a higher proportion of bacterial biomass in FPM of agricultural streams. However, only $\delta^{15}N$ values of the three larger size classes were considered and no reliable data was available for the two finest size classes. Implausibly high values distributed along a wide range from 5‰ to 67‰ were measured in the two finest size classes, which were likely a consequence of the treatment of the filter samples before the analysis. The filters were freeze-dried and decarbonated using HCl fumigation and this method was found to cause an alteration of the $\delta^{15}N$ value (Lorrain et al., 2003). Apart from an increase in bacterial biomass, the enriched $\delta^{15}N$ values found in the agricultural streams may also be due to the elevated nitrate concentrations. Lefebvre et al. (2007) revealed that the $\delta^{15}N$ values of nitrate in first-order streams in France were positively correlated with nitrate concentrations and both increased with increasing fertilisation intensity. Nitrate can be chemically adsorbed to fine particles, thereby also depressing the C/N ratio (Akamatsu et al., 2011) and this may further cause the slightly lower C/N ratios found in agricultural compared to mountain streams in this study. A study on second-

and third-order streams in the USA showed enriched $\delta^{15}N$ values of nitrate in agricultural sites (7.3‰) compared to forested sites (2.0‰; Harrington et al., 1998), indicating that the adsorption of ^{15}N-enriched nitrate may explain the higher $\delta^{15}N$ values of FPM in agricultural compared to mountain streams detected here.
A higher proportion of BFA in agricultural streams in the size class 15 µm - 2.7 µm indicates increased bacterial biomass in this size class compared to mountain streams. However, no pronounced difference was observed for the finest and the three largest FPM size classes. Lu, Canuel, et al. (2014) found a positive correlation between the relative abundance of bacterial lipids with stream water temperature and nitrate concentrations. In this study, agricultural streams also showed higher water temperatures and nitrate concentrations compared to mountain streams but the relative abundance of BFA was not consistently different between stream types across all size classes.
Thus, the analysis of the different biomarkers leads to inconsistent conclusions about the bacterial biomass on FPM when comparing the two stream types. A higher bacterial biomass in the three large FPM size classes in agricultural streams, as indicated by the $\delta^{15}N$ values, is not corroborated when considering the C/N ratios and the proportion of BFA. The results do not confirm the hypothesis of a generally higher bacterial biomass in agricultural compared to mountain streams.

Summarising, mixed sources of FPM occurred in both stream types and the contributions of bacterial and algal biomass cannot be quantified exactly. The combined analysis of several biomarkers indicated no general differences in FPM composition between the stream types. This is contrary to previous studies which have found a shift from terrestrial, mainly plant- and soil-derived POM in forested stream sites to more autochthonous, microbial- and algal-derived POM with increasing human disturbance and agricultural land use. These patterns were detected across different stream systems, in a Belgian lowland river (Lambert et al., 2017) as well as in first- to fourth-order streams (Hagen et al., 2010) and only first-order streams in the USA (Lu, Bauer, et al., 2014).
It appears that in this study the higher microbial activities and POC turnover times in agricultural streams compared to mountain streams are due to different environmental characteristics of the stream types rather than to the FPM composition. The relative importance of OM composition and ecosystem properties in controlling OM decomposition is an important research question across ecosystems and the results of this study contradict the common perception, mainly based on studies investigating DOM, that molecular composition drives OM decomposition processes in freshwaters (Kothawala et al., 2021). This indicates that conclusions from studying DOM cannot be transferred to the whole OM size spectrum. It furthermore highlights the need to study OM composition and its microbial turnover in different stream systems to achieve a more complete understanding of the mechanisms and magnitudes of OM turnover in streams.

4.2) Differences along the FPM size continuum

4.2.1) Highest FPM-attached microbial activities on the finest particles (<15 µm).

The microbial activity was clearly highest in the two finest FPM size classes including FPM < 15 µm, they accounted for > 98.8% of the total volumetric BPP in both stream types. This is contrary to the expectations based on the size-reactivity continuum model (Amon & Benner, 1996). The finest particles are commonly not investigated even in size-specific studies on the microbial activity on FPM, measured as bacterial production or microbial respiration rates. Atkinson et al. (2009) and Peters et al. (1989) considered particles > 10 µm size, Wurzbacher et al. (2016) analysed particles > 20 µm size, and the smallest size class of Yoshimura et al. (2010) comprised particles from 100 µm to 250 µm or from 100 µm to 500 µm (Yoshimura et al., 2008). If smaller-sized particles are included, they are usually part of a wider size class, e.g. Akamatsu et al. (2011) investigated particles from 1.2 µm to 100 µm, but did not fractionate the finest particles of the size continuum. Since volumetric production rates and the production per dry weight were remarkably higher in the two finest size classes compared to the three large size classes, at least 500 and 110 times in the size class 3 µm - 0.8 µm and at least 800 and 50 times in the size class 15 µm - 3 µm, respectively, the importance of investigating the finest particles of the fine particle size continuum is evident.

Part of the higher activity on the finest particles needs to be attributed to the larger amount of FPM present in these size classes. However, the production rates per dry weight already correct the volumetric rates for this effect of mass and they were still clearly higher in the two finest particle size classes. This contradicts the result of another study where microbial respiration on particles in a size class from 0.45 µm to 53 µm also accounted for the majority (57% to 97%) of the total respiration of suspended particles but the mass-specific microbial activity was higher on larger particles (Naiman & Sedell, 1979).

In addition to particle mass, the higher surface area to volume and surface area to mass ratio of smaller particles need to be considered and may explain high microbial activities on small particles. Corresponding to the results presented here, Peters et al. (1989) observed an increasing mass-specific microbial activity with decreasing particle size but the area-specific activity was lower in smaller compared to large particles. Since no measurements of particle surface area were conducted for each FPM size class in this study, the area-specific activity cannot be calculated. A greater surface area of smaller particles may facilitate microbial colonisation, however, the assumption of an increasing surface area to volume ratio with decreasing particle size is based on a spherical particle shape. The surface area differs not only depending on size, but also riparian characteristics of the stream, and particle proportions and shape have an effect (Atkinson et al., 1992). Large particles can be structurally more complex and provide space for microbial colonisation on the inside and not only on the surface (Bižić-Ionescu et al., 2015). Also, surface area to mass ratios were found to be higher in particles of 250 µm to 500 µm size than in smaller particles due to the frequent occurrence of non-spherical particle shapes (Peters et al., 1989). Therefore, the much greater microbial activity on the finest particles revealed in this study cannot only be attributed to the effects of the surface area, especially not without any measurements on it. Additional information on the number of bacteria and the structure of particles would be helpful to disentangle the effects of bacterial abundance due to available surface area on the measured microbial activity. Flow cytometry could be used to estimate the number of bacteria, to distinguish between living and dead cells, and to examine if particles are potentially composed of aggregated bacteria.

Further studies mentioned above also detected trends in the particle-associated microbial activity opposing the results presented here. The microbial respiration was found to generally decrease with decreasing particle size in studies on different size fractions of shredded leaves of the same age (Wurzbacher et al., 2016) and of leaves, wood, and green algae processed via gut passage in amphipods (Yoshimura et al., 2008, 2010). Wurzbacher et al. (2016) initially hypothesised an increased microbial activity and C turnover on smaller particles due to their larger surface to volume ratios. With results contrasting their hypothesis, they concluded that there is a relationship between particle size and microbial activity corresponding to the size-reactivity continuum model even without changes in the decomposition state. However, these trends cannot be confirmed in this study where microbial activities on FPM suspended in water of both mountain and agricultural streams were highest on the finest particles.

4.2.2) Biochemical particle composition and quality changes along the FPM size continuum.

The measures of particle quality and composition assessed in this study, POC and PN contents, C/N ratios, bulk stable isotope ratios, and FA composition, were not consistently different between the particle size classes. Following the size-reactivity continuum model, fine particles are assumed to originate from the breakdown of coarse material, thus being more decomposed and refractory (Amon & Benner, 1996). However, the analysis of the above-mentioned parameters combined with the microbial activity measurements revealed that the highest reactivity and microbial biomass occurred on the finest particles.

Most studies focus on the C/N ratio to infer on particle quality and less is reported about POC and PN contents. Elemental contents were found to have a variable relationship with particle size in suspended sediment samples from a headwater stream with a mainly forested catchment area in the USA (Rowland, 2016). The study found POC contents from 0.76% C to 5.68% C in particles < 250 µm size (Rowland, 2016), which are considerably lower than the POC contents of FPM measured in this study that ranged from 9.5% ± 2.2% to 52.9% ± 22.3% (median ± IQR). N contents varied between 0.02% and 0.34% in particles < 250 µm size (Rowland, 2016) while they ranged from 0.62% to 1.34% in suspended sediment samples from a lowland river with a grassland-dominated catchment area in the UK (Mena-Rivera et al., 2023). These values are also lower than the PN contents of 1.8% ± 1.6% and 1.4% ± 1.4% (median ± IQR) measured in mountain and agricultural streams in this study. Larger total POC contents and lower C/N ratios in fine compared to coarse POM were observed by Akamatsu et al. (2011), corresponding to the results presented here. Lower C/N ratios with decreasing particle size are consistently reported in the literature (Atkinson et al., 2009; Peters et al., 1989; Wurzbacher et al., 2016; Yoshimura et al., 2008, 2010). This has been attributed to the increased adsorption of nutrients, e.g. ammonium or nitrate, and the incorporation of more microbial biomass due to the increased surface area to volume ratio of smaller particles (Akamatsu et al., 2011). Both are potential explanations for the decrease in C/N ratios with decreasing size found in this study. A higher proportion of BFA in the two finest FPM size classes, as indicated by the PCA separating the FPM size classes from each other by the relative proportion of the FA groups (Figure 13B), also points towards an increase in microbial biomass with decreasing size.

In a fifth-order coastal plain stream in the USA, enriched $\delta^{13}C$ values of FPOM compared to CPOM indicated that finer particles consist of more degraded material although low C/N ratios commonly indicate more labile material (Atkinson et al., 2009). Furthermore, higher contents of lignin, a refractory structural component of plants, in FPOM compared to CPOM collected in an Italian river implied a higher degree of decomposition in FPOM (Yoshimura et al., 2008). Finally, Peters et al. (1989) reported

a decreasing content of organic material and acid-detergent-soluble materials (simple carbohydrates, proteins, and lipids) combined with an increase in lignin and cellulose content with decreasing particle size in a second-order stream in the USA, again indicating that smaller particles result from the breakdown of larger particles and are also of lower nutritional quality. These results collectively correspond to the predictions based on the size-reactivity continuum model although it was originally developed from experiments on DOM decomposition (Amon & Benner, 1996). However, many studies focused on particle quality without measuring microbial activity. Since the highest activities were measured on the finest particles here, these interpretations that fine particles are refractory are not convincing. Moreover, it seems paradoxical to still claim that fine particles are refractory although a low C/N ratio may result from increased microbial colonisation.

In contrast to the C/N ratio, the $\delta^{13}C$ and $\delta^{15}N$ stable isotope ratios did not confirm differences between particle size classes, $\delta^{13}C$ values were overlapping and $\delta^{15}N$ values only differed between stream types. An enrichment in $\delta^{13}C$ towards smaller particle sizes has been attributed to microbial degradation of larger particles and their origin from mixed sources like algal material or faecal pellets while larger particles may reflect the depleted $\delta^{13}C$ values of the riparian vegetation (Atkinson et al., 2009). Enriched $\delta^{15}N$ values in smaller particles were consistently linked to greater contributions of heterotrophic microbial biomass (Atkinson et al., 2009; Rowland et al., 2017). Fine particles are considered to be more variable than larger particles since they furthermore comprise erosional inputs, aggregations of DOM, and material released during CPOM breakdown by microbes and macroinvertebrates (Tant et al., 2013; Ward et al., 1994). Likely due to the focus of this study on only fine particles < 500 µm in contrast to previous studies, which included larger particle size classes, merged smaller particles into one overarching size class, and did not consider the finest particle sizes, no differences in stable isotope ratios between size classes were detected here.

A higher proportion of MUFA in the two finest size classes containing particles < 15 µm and a higher proportion of SFA in larger particles were revealed by the PCA of the FA groups (Figure 13B). Generally, unsaturated FA are degraded faster than saturated FA and the ratio of saturated to unsaturated FA can be used to infer on the degree of processing and decomposition of OM in rivers (Mills et al., 2003). Following this approach, the finest particles would be less decomposed than larger particles > 15 µm. In addition, the PCA indicated a higher proportion of bacterial fatty acids in the two finest particle size classes. These compositional differences between size classes were not dependent on the stream type. Proportions of different lipid classes are available for suspended particles > 0.7 µm from a lowland river in the UK with a grassland-dominated catchment area (Mena-Rivera, 2022), unfortunately not divided into size classes. In that study, SFA accounted for 49.7% to 54.7% of the total FA pool while unsaturated FA made up 28.1% to 34.1%, which is comparable to the results found here. Branched FA as a measure of microbially derived FA accounted for 15.6% to 19.4% of the total FA (Mena-Rivera, 2022), roughly corresponding to the BFA content of the smaller particle size classes in this study. Larger particles > 15 µm contained less BFA here.

Combining these insights with the C/N ratios, an increase in heterotrophic microbial biomass with decreasing particle size is likely. Overall, particle quality seems to increase with decreasing particle size, which contradicts the results of most previous studies. It does not rule out that finer particles result from the breakdown of larger particles, but they can have various origins and cannot be considered refractory. Since previous studies did neither measure microbial activities together with particle quality nor included the finest particle size classes in activity measurements, the finest particles < 15 µm seem to be an overlooked hotspot of microbial colonisation and activity. Considering that fine particles are

generally transported in the water column for longer times while larger particles settle more rapidly (Repasch et al., 2022), their importance for the total C turnover in the water column of streams is emphasised.

As discussed in the first part, the larger particle amounts in the two finest particle size classes relativise the striking contrast in microbial activity between the finest particles < 15 µm and the particles > 15 µm. However, the observed differences in quality and composition between particle size classes can partly explain the patterns of high microbial activity and abundance on the finest particles. A larger number of bacteria colonising the finest particles does not necessarily indicate a higher activity per organism since most organisms associated with suspended FPM in streams are inactive (Peters et al., 1989). In any case, the microbial activity on fine particles suggests that substantial C turnover occurs on suspended FPM in streams, particularly due to the activity on the finest particles < 15 µm. The relevance of C turnover on fine particles compared to other size fractions of organic matter and their contribution to C cycling in streams needs to be further examined.

4.3) Microbial activity and C turnover on fine particles in relation to the aquatic OM size continuum.

The microbial activities measured on the finest particles exceeded the activities on particles > 15 µm by several magnitudes. However, it is not clear how these numbers compare to other size classes along the aquatic OM size continuum from CPOM (leaf litter) to DOM. Bacterial carbon production measured in stream water samples including both DOM and POM ranged from 45 µg/(L·d) to 137 µg/(L·d) in a study on Canadian streams with mixed land use (Williams et al., 2010) and two studies along stream catchments in Germany (Kamjunke et al., 2015, 2019). By subtracting the median total BCP on fine particles of mountain and agricultural streams measured in this study from the production rates found in the literature, an estimate of the BCP associated with DOM in the studied streams was obtained. Comparing the calculated BCP on DOM to the measured BCP on the fine particles, the production rates on DOM were 2.6 to 72.3 times higher compared to the particles. In general, POC accounts for about 10% of DOC in streams (Lau, 2021) and this was also confirmed in this study where on average 9.4% and 11.2% of the total organic carbon was comprised of POC in mountain and agricultural streams, respectively. Hence, production rates on DOM and POM would be comparable if they were 10 times higher on DOM. The wide range of estimated production rates on DOM compared to POM can be narrowed down when differentiating between the investigated stream types. For the mountain streams, production rates were about 32 to 222 times higher on DOM while they were only 0.6 to 10.1 times higher on DOM in the studied agricultural streams. This implies that the microbial turnover per unit C of DOM is higher than the POM turnover in mountain streams, but POM turnover rates may exceed DOM turnover rates in agricultural streams. It furthermore stresses the necessity to study bacterial production rates on whole stream water samples and particle samples simultaneously in a stream system to draw more precise conclusions on the extent and relevance of POM turnover compared to DOM turnover since there are large variations between sites.

Leaf-litter-associated bacterial production rates in different stream types and on different leaf species were taken from a compilation by Buesing et al. (2020) and converted to µg C per g leaf litter dry mass and day to compare them to the median BCP rates measured in mountain and agricultural streams in this study. The reported production rates ranged from 5 µg C/(g·d) to 1750 µg C/(g·d) while the median

production rates were 869 µg C/(g·d) and 4439 µg C/(g·d) in the mountain and agricultural streams, respectively. Despite the wide range, the bacterial production rates on the fine particles in this study seem to exceed the rates measured on leaf litter, implying that there is a higher microbial turnover of OM on fine particles per dry mass. For a more detailed evaluation, the amount of leaf litter compared to the amount of fine particles present in streams needs to be considered. Wallace et al. (1982) reported CPOM:FPOM ratios varying between 0.05 and 0.12 along a headwater stream (separating FPOM from CPOM at 0.864 mm particle size), which results in about 8 to 20 times more FPOM than CPOM. Due to the wide range of production rates and CPOM:FPOM ratios and the fact that these values are derived from different studies and stream systems, only incomplete general conclusions can be drawn about the microbial turnover on fine compared to coarse POM. However, the comparatively high production rates measured on fine particles in this study indicate that a relevant fraction of the C turnover occurs not on coarse but on fine material.

4.4) Limitations of the study design.

This study compared the microbial activity and biochemical particle composition in mountain streams with forested catchment areas and agricultural streams located in lowland areas. Thus, assessing the effects of land use between less anthropogenically impacted mountain and agriculturally impacted streams is difficult due to the different geomorphology of the streams. A comparison of more natural and impacted lowland streams like in the studies by Lu, Bauer, et al. and Lu, Canuel, et al. (2014) would be an improved experimental design to be able to attribute differences in microbial activity and C turnover on fine particles to the changing land use. Different stream types were compared here and conclusions about the effects of agricultural land use should be treated with caution.

The filtration of large volumes of water may collect not only FPM-attached but also free-living bacteria which are increasingly retained on a filter the more volume is filtered (Lee et al., 1995). In addition, it has been argued that dislodged microbes that potentially get released by wet sieving could accumulate in the finest particle size class that is collected (Wallace et al., 1982). Since the highest microbial activities were found in the second finest particle size class and increased microbial biomass was indicated for the two finest size classes, this is not an apparent problem here. Also, fine particles and the attached bacteria can be concentrated due to clogging. Clogging can be ruled out for most of the samples in this study: for measuring BPP, only 10 mL of water were filtered, so no clogging occurred, therefore the activity measurements are reliable and the high production rates in the two small size classes cannot be the result of concentrating finer particles or free-living bacteria on the filter. Clogging can be a problem for the filtration using the peristaltic pump. For some streams, the filtration was stopped before the whole water volume was filtered due to high pressures on the GF/D filters noticed by leaking of the filter holders or the filter holders falling off. This was not the case for the GF/F filters, so measurement results in the size class 2.7 µm - 0.7 µm are credible. Clogging affected the GF/D filters (size class 15 µm -2.7 µm) of the agricultural streams which were used for FA and elemental analysis. In samples from the mountain streams, only the GF/D filters for the elemental analysis were clogged in some cases; this occurred in the samples from the Oberer Seebach and in one replicate sample each from Salza and Ois. Still, since the microbial activity measurements are reliable, and the analyses conducted with these GF/D filters yielded reasonable results, it can be argued that clogging did not affect the main messages of the study. Exchanging the filters of the peristaltic pump each time the filtration speed slows down like in studies by Bižić-Ionescu et al. (2018) and Mestre et al. (2020) or

ensuring that a certain pressure is never exceeded (Attermeyer et al., 2018) would improve the sample collection by filtration for further investigations.

This study assessed headwater streams during baseflow conditions in summer in two different stream types. However, it is still unclear if and how these results are transferable to other stream types, times of the year, or flow conditions. As an example, the origin and decomposition state of suspended PM was found to vary with season (Mills et al., 2003), and concentrations, origin, and particle sizes of suspended PM changed during storm events (Rowland et al., 2017). Heavy precipitation and flash flood events have increasingly occurred in temperate regions of Europe (Meyer et al., 2022) and studies investigating changes in PM characteristics during storm events have not considered the associated microbial activity so far. Summarising, there are many aspects of particle-associated OM processing that need to be investigated in more detail to understand their implications on C cycling in streams.

4.5) Conclusions and outlook

Confirming the expectations, higher microbial activities were observed in agricultural compared to mountain streams. However, the differences in microbial activity could not be linked to differences in FPM composition. They may result from different environmental characteristics of the stream types, contrary to the common perception that OM degradation in freshwater ecosystems is mainly driven by its molecular composition. This highlights the importance of studying FPM composition and turnover mechanisms in different stream systems and along gradients of human influence.

The clearly highest microbial activities were detected on the finest particles < 15 µm, supported by low C/N ratios and a higher proportion of BFA as indicators of increased microbial biomass in both stream types. The higher reactivity of finer particles contradicts the results of many previous studies and the expectations based on the size-reactivity continuum model by Amon & Benner (1996). Although the reactivity of suspended POC in marine ecosystems corresponds to the expectations of this model (Benner & Amon, 2015), its predictions can evidently not be translated to all size fractions of particulate material in streams. Despite noticing a potential increase in microbial biomass on finer particles while they are becoming more refractory compared to coarse material, many previous studies generally aligned with the size-reactivity continuum model, leading to the expectation of a reduced C turnover on small particles. This potentially results from not studying microbial activities simultaneously with particle composition or not considering the finest particle size classes. Thus, a better understanding of the exact drivers as well as the mechanisms of FPM turnover across different FPM size classes in streams is essential.

The finest size fractions of FPM represent an overlooked hotspot of microbial activity and C turnover in streams, and they are likely relevant in comparison to CPOM and DOM processing and turnover rates. It is therefore crucial to include the different types of OM and their interactions when investigating C turnover in streams to entirely capture the turnover and to examine the proportions associated with different fractions of the OM size continuum more precisely. Furthermore, OM cycling needs to be studied across different stream types, seasons, and flow conditions to deepen our understanding of these processes and their implications on C transport, burial, and emission.

References

Adams, H., Crump, B., & Kling, G. (2015). Isolating the effects of storm events on arctic aquatic bacteria: Temperature, nutrients, and community composition as controls on bacterial productivity. *Frontiers in Microbiology*, *6*. https://www.frontiersin.org/articles/10.3389/fmicb.2015.00250

Akamatsu, F., Kobayashi, S., Amano, K., Nakanishi, S., & Oshima, Y. (2011). Longitudinal and seasonal changes in the origin and quality of transported particulate organic matter along a gravel-bed river. *Hydrobiologia*, *669*(1), 183–197. https://doi.org/10.1007/s10750-011-0682-8

Alliance Instruments GmbH. (2007). *Products—Continuous-Flow Analysis (CFA)*. http://www.alliance-instruments.at/htm_english/products.htm#cfa2

Amon, R. M. W., & Benner, R. (1996). Bacterial Utilization of Different Size Classes of Dissolved Organic Matter. *Limnology and Oceanography*, *41*(1), 41–51.

Argerich, A., Haggerty, R., Johnson, S. L., Wondzell, S. M., Dosch, N., Corson-Rikert, H., Ashkenas, L. R., Pennington, R., & Thomas, C. K. (2016). Comprehensive multiyear carbon budget of a temperate headwater stream. *Journal of Geophysical Research: Biogeosciences*, *121*(5), 1306–1315. https://doi.org/10.1002/2015JG003050

Atkinson, C. F., Aumen, N. G., Miller, G. L., & Ward, G. M. (1992). Influence of Particle Shapes and Size Distributions on Fine Particulate Organic Matter Surface Area in Streams. *Journal of the North American Benthological Society*, *11*(3), 261–268. https://doi.org/10.2307/1467646

Atkinson, C. L., Golladay, S. W., Opsahl, S. P., & Covich, A. P. (2009). Stream discharge and floodplain connections affect seston quality and stable isotopic signatures in a coastal plain stream. *Journal of the North American Benthological Society*, *28*(2), 360–370. https://doi.org/10.1899/08-102.1

Attermeyer, K., Catalán, N., Einarsdottir, K., Freixa, A., Groeneveld, M., Hawkes, J. A., Bergquist, J., & Tranvik, L. J. (2018). Organic Carbon Processing During Transport Through Boreal Inland Waters: Particles as Important Sites. *Journal of Geophysical Research: Biogeosciences*, *123*(8), 2412–2428. https://doi.org/10.1029/2018JG004500

Beckman Coulter, Inc. (2019). *LS 13 320 XR Laser Diffraction Particle Size Analyzer. Instructions for Use.*

Benner, R., & Amon, R. M. W. (2015). The Size-Reactivity Continuum of Major Bioelements in the Ocean. *Annual Review of Marine Science*, *7*(1), 185–205. https://doi.org/10.1146/annurev-marine-010213-135126

Bižić-Ionescu, M., Ionescu, D., & Grossart, H.-P. (2018). Organic Particles: Heterogeneous Hubs for Microbial Interactions in Aquatic Ecosystems. *Frontiers in Microbiology*, *9*, 2569. https://doi.org/10.3389/fmicb.2018.02569

Bižić-Ionescu, M., Zeder, M., Ionescu, D., Orlić, S., Fuchs, B. M., Grossart, H.-P., & Amann, R. (2015). Comparison of bacterial communities on limnic versus coastal marine particles reveals profound differences in colonization: Marine and limnic particle-associated bacteria. *Environmental Microbiology*, *17*(10), 3500–3514. https://doi.org/10.1111/1462-2920.12466

Brodie, C. R., Leng, M. J., Casford, J. S. L., Kendrick, C. P., Lloyd, J. M., Yongqiang, Z., & Bird, M. I. (2011). Evidence for bias in C and N concentrations and δ13C composition of terrestrial and aquatic organic materials due to pre-analysis acid preparation methods. *Chemical Geology*, *282*(3–4), 67–83. https://doi.org/10.1016/j.chemgeo.2011.01.007

Brüggemann-Ledolter, M., Bayer, I., Ruthner, J., & Stöckl, W. (2015). *Geologische Übersichtskarte der Republik Österreich 1: 1 500 000 (ohne Quartär)* [Map]. Geologische Bundesanstalt Wien. https://www.geologie.ac.at/fileadmin/user_upload/dokumente/Rocky_Austria/Graphiken/uebersichtskarte_oesterreich.pdf

Buesing, N., Gessner, M. O., & Kuehn, K. A. (2020). Growth and Production of Litter-Associated Bacteria. In F. Bärlocher, M. O. Gessner, & M. A. S. Graça (Eds.), *Methods to Study Litter Decomposition: A Practical Guide* (pp. 275–284). Springer International Publishing. https://doi.org/10.1007/978-3-030-30515-4_30

Bundesministerium für Landwirtschaft, Regionen und Tourismus. (2020). *Nationaler Gewässerbewirtschaftungsplan 2021*.

Catalán, N., Marcé, R., Kothawala, D. N., & Tranvik, L. J. (2016). Organic carbon decomposition rates controlled by water retention time across inland waters. *Nature Geoscience*, *9*(7), Article 7. https://doi.org/10.1038/ngeo2720

Cole, J. J., Prairie, Y. T., Caraco, N. F., McDowell, W. H., Tranvik, L. J., Striegl, R. G., Duarte, C. M., Kortelainen, P., Downing, J. A., Middelburg, J. J., & Melack, J. (2007). Plumbing the Global Carbon Cycle: Integrating Inland Waters into the Terrestrial Carbon Budget. *Ecosystems*, *10*(1), 172–185. https://doi.org/10.1007/s10021-006-9013-8

Cooney, J. J., Doolittle, M. M., Grahl-Nielsen, O., Haaland, I. M., & Kirk, P. W. (1993). Comparison of fatty acids of marine fungi using multivariate statistical analysis. *Journal of Industrial Microbiology*, *12*(6), 373–378. https://doi.org/10.1007/BF01569668

Delong, M. D., & Brusven, M. A. (1992). Patterns of periphyton chlorophyll α in an agricultural nonpoint source impacted stream. *JAWRA Journal of the American Water Resources Association*, *28*(4), 731–741. https://doi.org/10.1111/j.1752-1688.1992.tb01495.x

Derrien, M., Brogi, S. R., & Gonçalves-Araujo, R. (2019). Characterization of aquatic organic matter: Assessment, perspectives and research priorities. *Water Research*, *163*, 114908. https://doi.org/10.1016/j.watres.2019.114908

Downing, J. A., Cole, J. J., Duarte, C. M., Middelburg, J. J., Melack, J. M., Prairie, Y. T., Kortelainen, P., Striegl, R. G., McDowell, W. H., & Tranvik, L. J. (2012). Global abundance and size distribution of streams and rivers. *Inland Waters*, *2*(4), 229–236. https://doi.org/10.5268/IW-2.4.502

Drake, T. W., Raymond, P. A., & Spencer, R. G. M. (2018). Terrestrial carbon inputs to inland waters: A current synthesis of estimates and uncertainty. *Limnology and Oceanography Letters*, *3*(3), 132–142. https://doi.org/10.1002/lol2.10055

Eberlein, K., & Kattner, G. (1987). Automatic method for the determination of ortho-phosphate and total dissolved phosphorus in the marine environment. *Fresenius' Zeitschrift Für Analytische Chemie*, *326*(4), 354–357. https://doi.org/10.1007/BF00469784

European Environmental Agency (EEA). (2019). *Corine Land Cover (CLC) 2018, Version 2020_20u1* [Map]. https://land.copernicus.eu/pan-european/corine-land-cover/clc2018

Fischer, H., Wanner, S. C., & Pusch, M. (2002). Bacterial abundance and production in river sediments as related to the biochemical composition of particulate organic matter (POM). *Biogeochemistry*, *61*, 37–55.

Geoland.at. (2015). *Digital Elevation Modell (DEM) Austria* [Map]. https://www.data.gv.at/katalog/dataset/land-ktn_digitales-gelandemodell-dgm-osterreich#additional-info

GeoSphere Austria, B. für G., Geophysik, Klimatologie und Meteorologie. (2023). *SPARTACUS v2.1 Jahresdaten*. https://dataset.api.hub.geosphere.at/app/frontend/raster/historical/spartacus-v2-1y-1km

Ghosh, M., & Gaur, J. P. (1998). Current velocity and the establishment of stream algal periphyton communities. *Aquatic Botany*, *60*(1), 1–10. https://doi.org/10.1016/S0304-3770(97)00073-9

Guo, F., Kainz, M. J., Valdez, D., Sheldon, F., & Bunn, S. E. (2016). High-quality algae attached to leaf litter boost invertebrate shredder growth. *Freshwater Science*, *35*(4), 1213–1221. https://doi.org/10.1086/688667

Gurtz, M. E., Webster, J. R., & Wallace, J. B. (1980). Seston Dynamics in Southern Appalachian Streams: Effects of Clear-cutting. *Canadian Journal of Fisheries and Aquatic Sciences*, *37*(4), 624–631. https://doi.org/10.1139/f80-078

Hagen, E. M., McTammany, M. E., Webster, J. R., & Benfield, E. F. (2010). Shifts in allochthonous input and autochthonous production in streams along an agricultural land-use gradient. *Hydrobiologia*, *655*(1), 61–77. https://doi.org/10.1007/s10750-010-0404-7

Harrington, R. R., Kennedy, B. P., Chamberlain, C. P., Blum, J. D., & Folt, C. L. (1998). 15N enrichment in agricultural catchments: Field patterns and applications to tracking Atlantic salmon (Salmo salar). *Chemical Geology*, *147*(3), 281–294. https://doi.org/10.1016/S0009-2541(98)00018-7

Ivančič, I., & Degobbis, D. (1984). An optimal manual procedure for ammonia analysis in natural waters by the indophenol blue method. *Water Research*, *18*(9), 1143–1147. https://doi.org/10.1016/0043-1354(84)90230-6

Kamjunke, N., Hertkorn, N., Harir, M., Schmitt-Kopplin, P., Griebler, C., Brauns, M., von Tümpling, W., Weitere, M., & Herzsprung, P. (2019). Molecular change of dissolved organic matter and patterns of bacterial activity in a stream along a land-use gradient. *Water Research*, *164*, 114919. https://doi.org/10.1016/j.watres.2019.114919

Kamjunke, N., Herzsprung, P., & Neu, T. R. (2015). Quality of dissolved organic matter affects planktonic but not biofilm bacterial production in streams. *Science of The Total Environment*, *506–507*, 353–360. https://doi.org/10.1016/j.scitotenv.2014.11.043

Kempers, A. J., & Luft, A. G. (1988). Re-examination of the determination of environmental nitrate as nitrite by reduction with hydrazine. *The Analyst*, *113*(7), 1117. https://doi.org/10.1039/an9881301117

Kirchman, D. (2001). Measuring bacterial biomass production and growth rates from leucine incorporation in natural aquatic environments. In *Methods in Microbiology* (Vol. 30, pp. 227–237). Elsevier. https://doi.org/10.1016/S0580-9517(01)30047-8

Kirchman, D., K'Nees, E., & Hodson, R. (1985). Leucine Incorporation and Its Potential as a Measure of Protein Synthesis by Bacteria in Natural Aquatic Systemst. *APPL. ENVIRON. MICROBIOL.*, *49*.

Kirkels, F. M. S. A., Cammeraat, L. H., & Kuhn, N. J. (2014). The fate of soil organic carbon upon erosion, transport and deposition in agricultural landscapes—A review of different concepts. *Geomorphology*, *226*, 94–105. https://doi.org/10.1016/j.geomorph.2014.07.023

Kothawala, D. N., Kellerman, A. M., Catalán, N., & Tranvik, L. J. (2021). Organic Matter Degradation across Ecosystem Boundaries: The Need for a Unified Conceptualization. *Trends in Ecology & Evolution*, *36*(2), 113–122. https://doi.org/10.1016/j.tree.2020.10.006

Lamb, A. L., Wilson, G. P., & Leng, M. J. (2006). A review of coastal palaeoclimate and relative sea-level reconstructions using δ13C and C/N ratios in organic material. *Earth-Science Reviews*, *75*(1), 29–57. https://doi.org/10.1016/j.earscirev.2005.10.003

Lambert, T., Bouillon, S., Darchambeau, F., Morana, C., Roland, F. A. E., Descy, J.-P., & Borges, A. V. (2017). Effects of human land use on the terrestrial and aquatic sources of fluvial organic matter in a temperate river basin (The Meuse River, Belgium). *Biogeochemistry*, *136*(2), 191–211. https://doi.org/10.1007/s10533-017-0387-9

Lau, M. P. (2021). Linking the Dissolved and Particulate Domain of Organic Carbon in Inland Waters. *Journal of Geophysical Research: Biogeosciences*, *126*(5). https://doi.org/10.1029/2021JG006266

Lee, S., Kang, Y.-C., & Fuhrman, J. A. (1995). Imperfect retention of natural bacterioplankton cells by glass fiber filters. *Marine Ecology Progress Series*, *119*(1/3), 285–290.

Lefebvre, S., Clément, J.-C., Pinay, G., Thenail, C., Durand, P., & Marmonier, P. (2007). N-Nitrate signature in low-order streams: Effects of land cover and agricultural practices. *Ecological Applications*, *17*(8), 2333–2346. https://doi.org/10.1890/06-1496.1

Lorrain, A., Savoye, N., Chauvaud, L., Paulet, Y.-M., & Naulet, N. (2003). Decarbonation and preservation method for the analysis of organic C and N contents and stable isotope ratios of low-carbonated suspended particulate material. *Analytica Chimica Acta*, *491*(2), 125–133. https://doi.org/10.1016/S0003-2670(03)00815-8

Lu, Y. H., Bauer, J. E., Canuel, E. A., Chambers, R. M., Yamashita, Y., Jaffé, R., & Barrett, A. (2014). Effects of land use on sources and ages of inorganic and organic carbon in temperate headwater streams. *Biogeochemistry*, *119*(1), 275–292. https://doi.org/10.1007/s10533-014-9965-2

Lu, Y. H., Canuel, E. A., Bauer, J. E., & Chambers, R. M. (2014). Effects of watershed land use on sources and nutritional value of particulate organic matter in temperate headwater streams. *Aquatic Sciences*, *76*(3), 419–436. https://doi.org/10.1007/s00027-014-0344-9

Marshall, A., Iskin, E., & Wohl, E. (2021). Seasonal and diurnal fluctuations of coarse particulate organic matter transport in a SNOWMELT-DOMINATED stream. *River Research and Applications*, *37*(6), 815–825. https://doi.org/10.1002/rra.3802

Mena-Rivera, L. A. (2022). *Molecular insights into the role of particulate organic matter in biogeochemical cycling in freshwater ecosystems*.

Mena-Rivera, L., Lloyd, C. E. M., Reay, M. K., Goodall, T., Read, D. S., Johnes, P. J., & Evershed, R. P. (2023). Tracing carbon and nitrogen microbial assimilation in suspended particles in freshwaters. *Biogeochemistry*, *164*(1), 277–293. https://doi.org/10.1007/s10533-022-00915-x

Mestre, M., Höfer, J., Sala, M. M., & Gasol, J. M. (2020). Seasonal Variation of Bacterial Diversity Along the Marine Particulate Matter Continuum. *Frontiers in Microbiology*, *11*, 1590. https://doi.org/10.3389/fmicb.2020.01590

Meybeck, M. (1982). Carbon, nitrogen, and phosphorus transport by world rivers. *American Journal of Science*, *282*(4), 401–450. https://doi.org/10.2475/ajs.282.4.401

Meyer, J., Neuper, M., Mathias, L., Zehe, E., & Pfister, L. (2022). Atmospheric conditions favouring extreme precipitation and flash floods in temperate regions of Europe. *Hydrology and Earth System Sciences*, *26*(23), 6163–6183. https://doi.org/10.5194/hess-26-6163-2022

Meyers, P. A. (1994). Preservation of elemental and isotopic source identification of sedimentary organic matter. *Chemical Geology*, *114*(3), 289–302. https://doi.org/10.1016/0009-2541(94)90059-0

Mills, G. L., McArthur, J. V., & Wolfe, C. P. (2003). Lipid composition of suspended particulate matter (SPM) in a southeastern blackwater stream. *Water Research*, *37*(8), 1783–1793. https://doi.org/10.1016/S0043-1354(02)00048-9

Naiman, R. J., & Sedell, J. R. (1979). Characterization of Particulate Organic Matter Transported by Some Cascade Mountain Streams. *Journal of the Fisheries Research Board of Canada*, *36*(1), 17–31. https://doi.org/10.1139/f79-003

Ogrinc, N., Markovics, R., Kanduč, T., Walter, L. M., & Hamilton, S. K. (2008). Sources and transport of carbon and nitrogen in the River Sava watershed, a major tributary of the River Danube. *Applied Geochemistry*, *23*(12), 3685–3698. https://doi.org/10.1016/j.apgeochem.2008.09.003

Oki, T., & Kanae, S. (2006). Global Hydrological Cycles and World Water Resources. *Science*, *313*(5790), 1068–1072. https://doi.org/10.1126/science.1128845

OTT HydroMet GmbH. (2023). *Technical Data. OTT MF pro—Water Flow Meter.* https://www.ott.com/en-uk/products/water-flow-3/ott-mf-pro-water-flow-meter-968/productAction/outputAsPdf/

Paul, D., Skrzypek, G., & Fórizs, I. (2007). Normalization of measured stable isotopic compositions to isotope reference scales – a review. *Rapid Communications in Mass Spectrometry*, *21*(18), 3006–3014. https://doi.org/10.1002/rcm.3185

Peters, G. T., Benfield, E. F., & Webster, J. R. (1989). Chemical Composition and Microbial Activity of Seston in a Southern Appalachian Headwater Stream. *Journal of the North American Benthological Society*, *8*(1), 74–84. https://doi.org/10.2307/1467403

Pohlert, T. (2022). *PMCMRplus: Calculate Pairwise Multiple Comparisons of Mean Rank Sums Extended* (1.9.6) [Computer software]. https://CRAN.R-project.org/package=PMCMRplus

Potapov, A. M., Tiunov, A. V., & Scheu, S. (2019). Uncovering trophic positions and food resources of soil animals using bulk natural stable isotope composition: Stable isotopes in soil food web studies. *Biological Reviews*, *94*(1), 37–59. https://doi.org/10.1111/brv.12434

QGIS.org. (2022). *QGIS Geographic Information System* [Computer software]. QGIS Association. http://www.qgis.org

R Core Team. (2022). *R: A language and environment for statistical computing* [Computer software]. R Foundation for Statistical Computing. https://www.R-project.org/

Reche, I., Pace, M. L., & Cole, J. J. (1998). Interactions of Photobleaching and Inorganic Nutrients in Determining Bacterial Growth on Colored Dissolved Organic Carbon. *Microbial Ecology*, *36*(3), 270–280. https://doi.org/10.1007/s002489900114

Regnier, P., Friedlingstein, P., Ciais, P., Mackenzie, F. T., Gruber, N., Janssens, I. A., Laruelle, G. G., Lauerwald, R., Luyssaert, S., Andersson, A. J., Arndt, S., Arnosti, C., Borges, A. V., Dale, A. W., Gallego-Sala, A., Goddéris, Y., Goossens, N., Hartmann, J., Heinze, C., … Thullner, M. (2013). Anthropogenic perturbation of the carbon fluxes from land to ocean. *Nature Geoscience*, *6*(8), 597–607. https://doi.org/10.1038/ngeo1830

Repasch, M., Scheingross, J. S., Hovius, N., Vieth-Hillebrand, A., Mueller, C. W., Höschen, C., Szupiany, R. N., & Sachse, D. (2022). River Organic Carbon Fluxes Modulated by Hydrodynamic Sorting of Particulate Organic Matter. *Geophysical Research Letters*, *49*(3). https://doi.org/10.1029/2021GL096343

Richardson, D. C., Newbold, J. D., Aufdenkampe, A. K., Taylor, P. G., & Kaplan, L. A. (2013). Measuring heterotrophic respiration rates of suspended particulate organic carbon from stream ecosystems: Measuring respiration rates of POC. *Limnology and Oceanography: Methods*, *11*(5), 247–261. https://doi.org/10.4319/lom.2013.11.247

Rowland, R. (2016). *Particulate Organic Matter (POM) Export From Catchments: Role of Particle Size, Sources, Headwater Drainage Area and Storm Event Magnitude*. Pro Quest LLC. https://udspace.udel.edu/server/api/core/bitstreams/9273a5f1-ca9d-4ec3-84b9-96a7089b5bb9/content

Rowland, R., Inamdar, S., & Parr, T. (2017). Evolution of particulate organic matter (POM) along a headwater drainage: Role of sources, particle size class, and storm magnitude. *Biogeochemistry*, *133*(2), 181–200. https://doi.org/10.1007/s10533-017-0325-x

Schidlowski, M., Hayes, J., & Kaplan, I. (1983). *Isotopic inferences of ancient biochemistries—Carbon, sulfur, hydrogen, and nitrogen*. https://www.semanticscholar.org/paper/Isotopic-inferences-of-ancient-biochemistries-and-Schidlowski-Hayes/127098a5dbc52791965709cab3702cba1aa8a02f

Shimadzu Europa GmbH. (2023). *TOC Application Handbook*. https://www.shimadzu.de/sites/shimadzu.seg/files/TOC_application_handbook_12K_Low.pdf

Simon, M., & Azam, F. (1989). Protein content and protein synthesis rates of planktonic marine bacteria. *Marine Ecology Progress Series*, *51*, 201–213. https://doi.org/10.3354/meps051201

Stahl, P. D., & Klug, M. J. (1996). Characterization and differentiation of filamentous fungi based on Fatty Acid composition. *Applied and Environmental Microbiology*, *62*(11), 4136–4146. https://doi.org/10.1128/aem.62.11.4136-4146.1996

Stelzer, R. S., Heffernan, J., & Likens, G. E. (2003). The influence of dissolved nutrients and particulate organic matter quality on microbial respiration and biomass in a forest stream: *Nutrients and microbes*. *Freshwater Biology*, *48*(11), 1925–1937. https://doi.org/10.1046/j.1365-2427.2003.01141.x

Strauss, E. A., & Lamberti, G. A. (2002). Effect of dissolved organic carbon quality on microbial decomposition and nitrification rates in stream sediments. *Freshwater Biology*, *47*(1), 65–74. https://doi.org/10.1046/j.1365-2427.2002.00776.x

Tant, C. J., Rosemond, A. D., & First, M. R. (2013). Stream nutrient enrichment has a greater effect on coarse than on fine benthic organic matter. *Freshwater Science*, *32*(4), 1111–1121. https://doi.org/10.1899/12-049.1

Torres-Ruiz, M., Wehr, J. D., & Perrone, A. A. (2007). Trophic relations in a stream food web: Importance of fatty acids for macroinvertebrate consumers. *Journal of the North American Benthological Society*, *26*(3), 509–522. https://doi.org/10.1899/06-070.1

Tranvik, L. J., Downing, J. A., Cotner, J. B., Loiselle, S. A., Striegl, R. G., Ballatore, T. J., Dillon, P., Finlay, K., Fortino, K., Knoll, L. B., Kortelainen, P. L., Kutser, T., Larsen, Soren., Laurion, I., Leech, D. M., McCallister, S. L., McKnight, D. M., Melack, J. M., Overholt, E., … Weyhenmeyer, G. A. (2009). Lakes and reservoirs as regulators of carbon cycling and climate. *Limnology and Oceanography*, *54*(6part2), 2298–2314. https://doi.org/10.4319/lo.2009.54.6_part_2.2298

Umweltbundesamt GmbH. (2020). *Fließgewässer des Gesamtgewässernetz Österreich (GGN)* [Map]. https://www.data.gv.at/katalog/dataset/c2287ccb-f44c-48cd-bf7c-ac107b771246

Wallace, J. B., Ross, D. H., & Meyer, J. L. (1982). Seston and Dissolved Organic Carbon Dynamics in a Southern Appalachian Stream. *Ecology*, *63*(3), 824–838. https://doi.org/10.2307/1936802

Wallace, J. B., Whiles, M. R., Eggert, S., Cuffney, T. F., Lugthart, G. J., & Chung, K. (1995). Long-Term Dynamics of Coarse Particulate Organic Matter in Three Appalachian Mountain Streams. *Journal of the North American Benthological Society*, *14*(2), 217–232. https://doi.org/10.2307/1467775

Ward, G. M., Ward, A. M., Dahm, C. N., & Aumen, N. G. (1994). Origin and Formation of Organic and Inorganic Particles in Aquatic Systems. In *The Biology of Particles in Aquatic Systems, Second Edition* (2nd ed.). CRC Press.

Wickham, H. (2016). *Ggplot2: Elegant graphics for data analysis* (2nd ed.). Springer International Publishing.

Wild, R., Gücker, B., & Brauns, M. (2019). Agricultural land use alters temporal dynamics and the composition of organic matter in temperate headwater streams. *Freshwater Science*, *38*(3), 566–581. https://doi.org/10.1086/704828

Williams, C. J., Yamashita, Y., Wilson, H. F., Jaffé, R., & Xenopoulos, M. A. (2010). Unraveling the role of land use and microbial activity in shaping dissolved organic matter characteristics in stream ecosystems. *Limnology and Oceanography*, *55*(3), 1159–1171. https://doi.org/10.4319/lo.2010.55.3.1159

Wotton, R. S. (1994). *The Biology of Particles in Aquatic Systems, Second Edition*. CRC Press.

Wurzbacher, C., Wannicke, N., Grimmett, I. J., & Bärlocher, F. (2016). Effects of FPOM size and quality on aquatic heterotrophic bacteria. *Limnologica*, *59*, 109–115. https://doi.org/10.1016/j.limno.2016.04.001

Yang, Q., Zhang, X., Xu, X., Asrar, G. R., Smith, R. A., Shih, J.-S., & Duan, S. (2016). Spatial patterns and environmental controls of particulate organic carbon in surface waters in the conterminous United States. *Science of The Total Environment*, *554–555*, 266–275. https://doi.org/10.1016/j.scitotenv.2016.02.164

Yoshimura, C., Fujii, M., Omura, T., & Tockner, K. (2010). Instream release of dissolved organic matter from coarse and fine particulate organic matter of different origins. *Biogeochemistry*, *100*(1), 151–165. https://doi.org/10.1007/s10533-010-9412-y

Yoshimura, C., Gessner, M. O., Tockner, K., & Furumai, H. (2008). Chemical properties, microbial respiration, and decomposition of coarse and fine particulate organic matter. *Journal of the North American Benthological Society*, *27*(3), 664–673. https://doi.org/10.1899/07-106.1

Appendix

Zusammenfassung

Die Umsetzung von organischem Material ist eine Schlüsselkomponente des Kohlenstoffkreislaufs in Fließgewässerökosystemen und hat Auswirkungen auf den Transport und die Mineralisierung von Kohlenstoff sowie die Funktion der Gewässer als Kohlenstoffsenke. Obwohl suspendierte Partikel zunehmend als aktive Orte der Umsetzung von organischem Material anerkannt werden, ist die Forschung bislang auf den Kreislauf von gelöstem organischem Material konzentriert. Die Eigenschaften und der Umsatz von feinen Partikeln (< 1000 µm) sind hingegen kaum verstanden, insbesondere die feinsten Partikel (< 100 µm) werden üblicherweise nicht untersucht. In dieser Studie wurden die mikrobielle Aktivität und die biochemische Zusammensetzung von Partikeln in fünf verschiedenen Größenklassen von 500 µm bis 0,7 µm analysiert. Fünf Gebirgsbäche, die durch bewaldete Einzugsgebiete gekennzeichnet sind, und fünf landwirtschaftlich genutzte Flachlandbäche wurden untersucht. Die bakteriellen Produktionsraten in landwirtschaftlichen Bächen waren zwanzigmal höher als in Gebirgsbächen, wodurch es 25 bzw. 227 Tage dauert, bis der Kohlenstoff auf den Partikeln vollständig umgesetzt ist. Es wurden keine generellen Unterschiede in der Partikelzusammensetzung zwischen den Fließgewässertypen festgestellt, was darauf hindeutet, dass Umweltmerkmale zur Steuerung des Umsatzes der feinen Partikel beitragen. Im Vergleich der Größenklassen waren die bakteriellen Produktionsraten auf den feinsten Partikeln < 15 µm am höchsten, mehr als 98,8 % der Gesamtaktivität trat in beiden Fließgewässertypen in diesen Partikeln auf. Die Fettsäurenzusammensetzung und das C/N-Verhältnis zeigten zudem eine erhöhte mikrobielle Biomasse auf den feinsten Partikeln an. Somit stellen feine Partikel < 15 µm übersehene Hotspots des mikrobiellen Umsatzes von organischem Material in Fließgewässern dar. Welche Mechanismen ihren Umsatz bestimmen, ist von wesentlicher Bedeutung für unser Verständnis des fluvialen Kohlenstoffkreislaufs.

Schlagwörter: suspendierte Partikel, FPOM, Seston, mikrobielle Aktivität, Partikelgröße, Partikelzusammensetzung, Fettsäuren, Kohlenstoffumsatz, Fließgewässer, Landnutzung

Appendix 1: Median FPM concentration [mg/L] ± IQR [mg/L] in each particle size class in each stream. The values were calculated using all available sample dry weights for elemental and fatty acid analysis divided by the volume filtered for the respective sample. N represents the number of available samples used for the calculation.

Stream type	Stream name	Size class	Median FPM concentration [mg/L] ± IQR [mg/L]	N
Mountain	Hinterwildalpenbach	100	0.184 ± 0.090	6
		50	0.180 ± 0.071	6
		15	0.248 ± 0.051	6
		2.7	0.264 ± 0.090	6
		0.7	0.045 ± 0.023	6
	Oberer Seebach	100	0.007 ± 0.005	5
		50	0.007 ± 0.003	5
		15	0.065 ± 0.017	6
		2.7	0.585 ± 0.150	6
		0.7	0.108 ± 0.077	6
	Ois	100	0.015 ± 0.008	6
		50	0.007 ± 0.004	6
		15	0.025 ± 0.011	6
		2.7	0.132 ± 0.103	5
		0.7	0.022 ± 0.005	6
	Salza	100	0.039 ± 0.009	6
		50	0.037 ± 0.013	6
		15	0.111 ± 0.025	6
		2.7	0.432 ± 0.072	6
		0.7	0.089 ± 0.029	6
	Steinbach	100	0.010 ± 0.010	6
		50	0.011 ± 0.009	6
		15	0.092 ± 0.005	6
		2.7	0.357 ± 0.037	3
		0.7	0.036 ± 0.001	3
Agricultural	Feichsen	100	0.006 ± 0.004	6
		50	0.012 ± 0.012	6
		15	0.158 ± 0.029	6
		2.7	1.912 ± 0.069	6
		0.7	0.206 ± 0.116	5
	Ofenbach	100	0.007 ± 0.005	6
		50	0.038 ± 0.010	6
		15	0.795 ± 0.061	6
		2.7	3.758 ± 1.778	6
		0.7	0.377 ± 0.144	6
	Schweinzbach	100	0.007 ± 0.002	4
		50	0.004 ± 0.010	5
		15	0.180 ± 0.036	6
		2.7	3.585 ± 0.492	6
		0.7	0.217 ± 0.091	6

	Siernin g	100	0.030 ± 0.002	6
		50	0.041 ± 0.003	6
		15	0.316 ± 0.054	6
		2.7	2.189 ± 0.326	6
		0.7	0.207 ± 0.024	6
	Zettelbach	100	0.023 ± 0.019	6
		50	0.027 ± 0.015	6
		15	0.292 ± 0.090	6
		2.7	1.374 ± 0.259	6
		0.7	0.140 ± 0.054	6

Appendix 2: Medians and sample sizes (N) of the FPM concentrations divided by size class and summary of the results of the statistical comparison between the size classes. The size class refers to the lowest size of each particle size class (e.g. 100 stands for the size class 500 µm - 100 µm).
The size classes 15 µm - 2.7 µm and 2.7 µm - 0.7 µm were compared using a two-sided Wilcoxon signed-rank test, the *p*-value is shown in the column *p* Wilcoxon test (0.7) and the *V*-value in the column *V*.
The three large size classes were compared using the Friedman test (*p*-value, *Friedman Chi*^{2}, and degrees of freedom (*df*) given in the column *p* Friedman test). If this test was significant, the Conover's all-pairs test with application of the Bonferroni-method to adjust *p*-values was used as a post hoc test. The *p*-values are shown in the column *p* (50) for comparison of the size class 100 µm - 50 µm with the size class 500 µm - 100 µm and in the column *p* (15) for comparison of the size class 15 µm - 2.7 µm with the size classes 500 µm - 100 µm and 100 µm - 50 µm.
Significant *p*-values are printed in bold. The Friedman test was conducted for all streams irrespective of stream type (stream type 'both') and for mountain and agricultural streams separately, the Wilcoxon signed-rank test was only calculated separated by stream type.

Stream type	**Size class**	**Median FPM concentration [mg/L]**	**N**	***p* Friedman test**	***p* (50)**	***p* (15)**	***p* Wilcoxon test (0.7)**	***V***
Both	100	0.01	10	**0.0005531** ***Chi*^{2} = 15, *df* = 2**	1.000	**0.011**		
	50	0.02	10			**0.011**		
	15	0.17	10					
Mountain	100	0.01	5	**0.015** ***Chi*^{2} = 8.4, *df* = 2**	1.000	0.283		
	50	0.01	5			0.065		
	15	0.09	5					
	2.7	0.36	5				0.0625	15
	0.7	0.04	5					
Agricultural	100	0.02	5	**0.015** ***Chi*^{2} = 8.4, *df* = 2**	1.000	0.065		
	50	0.03	5			0.283		
	15	0.29	5					
	2.7	2.19	5				0.0625	15
	0.7	0.21	5					

Appendix 3: Medians and sample sizes (N) of the BPP and summary of the results of the statistical comparison between the size classes using medians of the three replicates per stream. The size class refers to the lowest size of each particle size class (e.g. 100 stands for the size class 500 µm - 100 µm).

The size classes 15 µm - 3 µm and 3 µm - 0.8 µm were compared using a two-sided Wilcoxon signed-rank test, the *p*-value is shown in the column *p* Wilcoxon test (0.8) and the *V*-value in the column *V*.

The three large size classes were compared using the Friedman test (*p*-value, *Friedman Chi*^{2}, and degrees of freedom (*df*) given in the column *p* Friedman test). If this test was significant, the Conover's all-pairs test with application of the Bonferroni-method to adjust *p*-values was used as a post hoc test. The *p*-values are shown in the column *p* (50) for comparison of the size class 100 µm - 50 µm with the size class 500 µm - 100 µm and in the column *p* (15) for comparison of the size class 15 µm - 3 µm with the size classes 500 µm - 100 µm and 100 µm - 50 µm.

Significant *p*-values are printed in bold. All calculations were conducted for all streams irrespective of stream type (stream type 'both') and for mountain and agricultural streams separately, for the BPP related to volume [ng/(L·h)] and the BPP related to dry weight [ng/(mg·h)].

Parameter	Stream type	Size class	Median	N	*p* Friedman test	*p* (50)	*p* (15)	*p* Wilcoxon test (0.8)	*V*
BPP [ng/(L·h)]	Both	100	0.04	10	**0.001148, Chi^2 = 6.2, *df* = 2**	0.405	0.073		
		50	0.05	10			0.405		
		15	0.09	10					
		3	157.83	9				0.07813	25
		0.8	48.34	8					
	Mountain	100	0.02	5	0.5488 Chi^2 = 1.2, *df* = 2	-	-		
		50	0.03	5			-		
		15	0.04	5					
		3	33.01	4				1	3
		0.8	20.15	4					
	Agricultural	100	0.05	5	**0.02237 Chi^2 = 7.2, *df* = 2**	0.17	0.11		
		50	0.11	5			1.000		
		15	0.18	5					
		3	448.08	5				0.125	10
		0.8	124.65	4					
BPP [ng/(mg·h)]	Both	100	1.92	10	**0.001836 Chi^2 = 12.6, *df* = 2**	1.000	**0.046**		
		50	2.79	10			**0.0111**		
		15	0.45	10					
		3	135.56	9				**0.01563**	**0**
		0.8	468.44	8					

	Mountain	100	1.06	5	0.07427 Chi^2 = 5.2, df = 2	-	-		
		50	1.60	5			-		
		15	0.40	5					
		3	123.54	4				0.25	0
		0.8	468.44	4					
	Agricultural	100	4.09	5	**0.02237 Chi^2 = 7.6, df = 2**	1.000	0.17		
		50	2.99	5			0.11		
		15	0.49	5					
		3	204.68	5				0.125	0
		0.8	455.09	4					

Appendix 4: Medians and sample sizes (N) of volumetric POC and PN content [µg/L], POC and PN content related to dry weight [mg/mg] and C/N ratio and summary of the results of the statistical comparison between the size classes using medians of the three replicates per size class in each stream. The size class refers to the lowest size of each particle size class (e.g. 100 stands for the size class 500 µm - 100 µm).
The size classes 15 µm - 2.7 µm and 2.7 µm - 0.7 µm were compared using a two-sided Wilcoxon signed-rank test, the *p*-value is shown in the column *p* Wilcoxon test (0.7) and the *V*-value in the column *V*.
The three large size classes were compared using the Friedman test (*p*-value, *Friedman Chi²*, and degrees of freedom (*df*) given in the column *p* Friedman test). If this test was significant, the Conover's all-pairs test with application of the Bonferroni-method to adjust *p*-values was used as a post hoc test. The *p*-values are shown in the column *p* (50) for comparison of the size class 100 µm - 50 µm with the size class 500 µm - 100 µm and in the column *p* (15) for comparison of the size class 15 µm - 2.7 µm with the size classes 500 µm - 100 µm and 100 µm - 50 µm.
Significant *p*-values are printed in bold. All calculations were conducted for all streams irrespective of stream type (stream type 'both') and for mountain and agricultural streams separately.

Parameter	Stream type	Size class	Median	N	*p* Friedman test	*p* (50)	*p* (15)	*p* Wilcoxon test (0.7)	*V*
POC [µg/L]	Both	100	4.1	10	**0.00823 Chi^2 = 9.6, *df* = 2**	1.000	**0.046**		
		50	4.6	10			**0.046**		
		15	14.3	10					
		2.7	161.6	10				**0.003906**	**45**
		0.7	52.1	9					
	Mountain	100	4.2	5	0.2466 Chi^2 = 2.8, *df* = 2	-	-		
		50	6.4	5			-		
		15	13.3	5					
		2.7	93.6	5				0.125	10
		0.7	26.8	4					
	Agricultural	100	2.5	5	**0.02237 Chi^2 = 7.6, *df* = 2**	1.000	0.11		
		50	4.2	5			0.17		
		15	27.5	5					
		2.7	231.0	5				0.0625	15
		0.7	101.5	5					
PN [µg/L]	Both	100	0.33	10	**0.0006755 Chi^2 = 14.6, *df* = 2**	0.4048	0.1147		
		50	0.25	10			**0.0039**		
		15	1.42	10					
		2.7	18.80	10				**0.003906**	**45**
		0.7	9.06	9					

	Mountain	100	0.42	5	**0.015** Chi^2 **= 8.4,** ***df*** **= 2**	0.283	1.00		
		50	0.12	5			0.065		
		15	1.09	5					
		2.7	10.60	5				0.125	10
		0.7	4.15	4					
	Agricultural	100	0.12	5	**0.02237** Chi^2 **= 7.6,** ***df*** **= 2**	1.000	0.17		
		50	0.38	5			0.11		
		15	3.09	5					
		2.7	31.64	5				0.0625	15
		0.7	13.18	5					
POC [mg/mg]	Both	100	0.287	10	**0.0002249** Chi^2 **= 16.8,** ***df*** **= 2**	1.000	**0.0024**		
		50	0.212	10			**0.0455**		
		15	0.111	10					
		2.7	0.118	10				**0.01953**	**3**
		0.7	0.459	9					
	Mountain	100	0.284	5	**0.02237** Chi^2 **= 7.6,** ***df*** **= 2**	1.000	0.11		
		50	0.289	5			0.17		
		15	0.124	5					
		2.7	0.229	5				0.125	2
		0.7	0.529	4					
	Agricultural	100	0.346	5	**0.006738** Chi^2 **= 10,** ***df*** **= 2**	0.46	**0.04**		
		50	0.158	5			0.46		
		15	0.095	5					
		2.7	0.106	5				0.0625	0
		0.7	0.371	5					
PN [mg/mg]	Both	100	0.018	10	**0.002243** Chi^2 **= 12.2,** ***df*** **= 2**	**0.028**	**0.017**		
		50	0.011	10			1.000		
		15	0.010	10					
		2.7	0.015	10				**0.003906**	**0**
		0.7	0.061	9					
	Mountain	100	0.024	5	**0.02237**	0.17	0.11		

					***Chi²* = 7.6, *df* = 2**				
		50	0.012	5			1.000		
		15	0.010	5					
		2.7	0.025	5				0.125	0
		0.7	0.080	4					
	Agricultural	100	0.016	5	0.09072 *Chi²* = 4.8, *df* = 2	-	-		
		50	0.011	5			-		
		15	0.011	5					
		2.7	0.013	5				0.0625	0
		0.7	0.056	5					
C/N	Both	100	16.4	10	**0.01357 *Chi²* = 8.6, *df* = 2**	0.835	0.271		
		50	18.3	10			**0.028**		
		15	12.5	10					
		2.7	9.9	10				**0.03906**	**45**
		0.7	8.1	9					
	Mountain	100	15.5	5	0.07427 *Chi²* = 5.2, *df* = 2	-	-		
		50	19.7	5			-		
		15	14.2	5					
		2.7	9.9	5				0.125	10
		0.7	8.3	4					
	Agricultural	100	20.8	5	0.09072 *Chi²* = 4.8, *df* = 2	-	-		
		50	16.2	5			-		
		15	10.5	5					
		2.7	9.4	5				0.0625	15
		0.7	7.8	5					

Appendix 5: Medians and sample sizes (N) of $\delta^{13}C$ and $\delta^{15}N$ values and summary of the results of the statistical comparison between the size classes using medians of the three replicates per size class in each stream. The size class refers to the lowest size of each particle size class (e.g. 100 stands for the size class 500 µm - 100 µm). The size classes 15 µm - 2.7 µm and 2.7 µm - 0.7 µm were compared using a two-sided Wilcoxon signed-rank test, the *p*-value is shown in the column *p* Wilcoxon test (0.7) and the *V*-value in the column *V*.
The three large size classes were compared using the Friedman test (*p*-value, *Friedman Chi*^{2}, and degrees of freedom (*df*) given in the column *p* Friedman test). If this test was significant, the Conover's all-pairs test with application of the Bonferroni-method to adjust *p*-values was used as a post hoc test. The *p*-values are shown in the column *p* (50) for comparison of the size class 100 µm - 50 µm with the size class 500 µm - 100 µm and in the column *p* (15) for comparison of the size class 15 µm - 2.7 µm with the size classes 500 µm - 100 µm and 100 µm - 50 µm. Significant *p*-values are printed in bold. For $\delta^{13}C$, the calculations were conducted for all streams irrespective of stream type (stream type 'both') and for mountain and agricultural streams separately and for $\delta^{15}N$ only separated by stream type.

Parameter	Stream type	Size class	Median	N	*p* Friedman test	*p* (50)	*p* (15)	*p* Wilcoxon test (0.7)	*V*
$\delta^{13}C$ [‰]	Both	100	-28.6	10	0.3012 *Chi*^{2} = 2.4, *df* = 2	-	-		
		50	-28.6	10			-		
		15	-28.7	10					
		2.7	-29.2	10				0.2754	16
		0.7	-28.3	10					
	Mountain	100	-30.1	5	0.07427 *Chi*^{2} = 5.2, *df* = 2	-	-		
		50	-28.8	5			-		
		15	-28.6	5					
		2.7	-30.2	5				0.3125	12
		0.7	-30.2	5					
	Agricultural	100	-28.3	5	**0.02237 *Chi*^{2} = 7.6, *df* = 2**	1.000	0.17		
		50	-28.5	5			0.11		
		15	-28.8	5					
		2.7	-28.5	5				0.0625	0
		0.7	-28.3	5					
$\delta^{15}N$ [‰]	Mountain	100	-2.1	5	0.07427 *Chi*^{2} = 5.2, *df* = 2	-	-		
		50	-1.9	5			-		
		15	-0.2	5					
	Agricultural	100	0.9	5	0.4493 *Chi*^{2} = 1.6, *df* = 2	-	-		
		50	3.8	5			-		
		15	4.5	5					

Appendix 6: Medians and sample sizes (N) of the total lipid and bacterial fatty acid (BFA) concentration [µg/L] and summary of the results of the statistical comparison between the size classes using medians of the three replicates per size class in each stream. The size class refers to the lowest size of each particle size class (e.g. 100 stands for the size class 500 µm - 100 µm).
The size classes 15 µm - 2.7 µm and 2.7 µm - 0.7 µm were compared using a two-sided Wilcoxon signed-rank test, the *p*-value is shown in the column *p* Wilcoxon test (0.7) and the *V*-value in the column *V*.
The three large size classes were compared using the Friedman test (*p*-value, *Friedman Chi²*, and degrees of freedom (*df*) given in the column *p* Friedman test). If this test was significant, the Conover's all-pairs test with application of the Bonferroni-method to adjust *p*-values was used as a post hoc test. The *p*-values are shown in the column *p* (50) for comparison of the size class 100 µm - 50 µm with the size class 500 µm - 100 µm and in the column *p* (15) for comparison of the size class 15 µm - 2.7 µm with the size classes 500 µm - 100 µm and 100 µm - 50 µm.
Significant *p*-values are printed in bold. All calculations were conducted for mountain and agricultural streams separately since statistically significant differences between stream types were detected in some of the size classes.

Parameter	Stream type	Size class	Median	N	*p* Friedman test	*p* (50)	*p* (15)	*p* Wilcoxon test (0.7)	*V*
Total lipids [µg/L]	Mountain	100	0.9	5	0.07425 $Chi^2 = 5.2$, $df = 2$	-	-		
		50	0.9	5			-		
		15	3.1	5					
		2.7	14.1	5				0.625	10
		0.7	13.3	5					
	Agricultural	100	1.0	5	**0.02237** $\mathbf{Chi^2 = 7.6}$, $\mathbf{df = 2}$	1.000	0.17		
		50	1.0	5			0.11		
		15	5.6	5					
		2.7	54.8	5				0.0625	15
		0.7	24.7	5					
BFA [µg/L]	Mountain	100	0.02	5	**0.015** $\mathbf{Chi^2 = 8.4}$, $\mathbf{df = 2}$	1.000	0.283		
		50	0.02	5			0.065		
		15	0.06	5					
		2.7	0.38	5				0.4375	11
		0.7	0.33	5					
	Agricultural	100	0.03	5	**0.02237** $\mathbf{Chi^2 = 7.6}$, $\mathbf{df = 2}$	1.00	0.17		
		50	0.03	5			0.11		
		15	0.12	5					
		2.7	1.94	5				0.0625	15
		0.7	0.99	5					

Appendix 7: Single fatty acids defined as major components (mean concentration > 0.05 µg/L), sorted by mean concentration [µg/L]. All major components had maximum proportions of ≥ 5%. Also, arachidonic acid (20:4n-6) had a maximum proportion of > 5% and was added to the table although it was not defined as a major component. Minimum, maximum (Min. and Max.), mean and median concentrations [µg/L], and minimum and maximum proportions of total FAME [%] are shown.

FA trivial name	Abbreviation	Min. [µg/L]	Max. [µg/L]	Mean [µg/L]	Median [µg/L]	Min. [%]	Max. [%]
Palmitic acid	16:0	0.040	3.143	0.647	0.277	17.9	35.6
Stearic acid	18:0	0.031	2.014	0.346	0.193	2.9	29.6
Palmitoleic acid	16:1n-7	0.002	2.141	0.324	0.054	0.4	30.9
Eicosapentaenoic acid (EPA)	20:5n-3	0	1.828	0.153	0.031	0	15.4
Vaccenic acid	18:1n-7	0.001	1.113	0.144	0.012	0.2	10.6
Oleic acid	18:1n-9	0.003	1.184	0.143	0.039	0.8	11.2
α-linolenic acid (ALA)	18:3n-3	0	3.115	0.131	0.012	0	21.5
Dihomo-g-linolenic acid	20:3n-6	0.010	0.465	0.116	0.062	0.6	13.9
Linoleic acid (LIN)	18:2n-6	0.002	1.026	0.108	0.020	0.5	8.1
6-Octadecaenoic acid	18:1n-6	0.002	0.333	0.074	0.036	0.6	9.7
Stearidonic acid	18:4n-3	0	0.621	0.069	0.031	0	7.1
Myristic acid	14:0	0.001	0.393	0.067	0.019	1.0	5.0
7-Hexadecaenoic acid	16:1n-9	0.000	0.434	0.054	0.009	0.2	5.5
Docosahexaenoic acid (DHA)	22:6n-3	0	0.911	0.054	0	0	6.4
Arachidonic acid (ARA)	20:4n-6	0	0.760	0.042	0	0	5.4